Characteristics of adsorptive removal of 2-methylisoborneol by micro-milled activated carbon

Dissertation Prepared for the Degree of
Doctor of Philosophy

The Environmental Risk Engineering Laboratory
Division of Environmental Engineering
Graduate School of Engineering
Hokkaido University
Japan

February 2017

Long Pan

Acknowledgement

For the achievements of my research and the past three years of my doctoral course, I would like to express my sincere gratitude to my supervisor, Prof. Yoshihiko MATSUI, for his motivation, patience and immense knowledge. His guidance helped me in all the time of research including writing of this dissertation. Without his help and guidance, I could not have imagined having such outcomes of my Ph.D. study. Besides my supervisor, I would like to thank Associate Prof. Taku MATSUSHITA and Assistant Prof. Nobutaka SHIRASAKI who helped me a lot by their insightful comments, practical guide and considerate encouragement throughout my Ph.D. study. I also want to thank Prof. Toshifumi IGARASHI who attended the academic progress evaluation in my Ph.D. study and gave me many useful ideas and comments. What's more, I want to express my acknowledgement towards Prof. Masahiro TAGAHASHI and the rest of my thesis committee not only for their advices, time and patience, but also for questions which incented me to widen my research from various perspectives.

I thank my fellow team member, such as Ms. Asuka SAKAMOTO, Mr. Yuichi TAKAGI, Mr. Yuki NISHIMURA, and Mr. Hideki TAKAESU and all the rest of my labmates, in for their hard work together in the sleepless nights, for the valuable discussion we had, for all the fun we have had in the last three years. Also I thank the teachers, instructors and engineers who instructed and cooperated with me when I used their machines and facilities for experiments.

In particular, I am grateful to the financial support from Scholarship (201306460006) of China Scholarship Council (CSC) for my doctoral program and the spiritual support from my family and friends for their always understanding and tolerance. They have become the base to support my research and daily life, and helped me to overcome my weakness and the problems I met.

(This papge is set to be blank.)

CONTENT

Acknowledgement ..... **i**

Chapter 1. Introduction **1**

1.1. Background 1

1.2. Objectives and originalities 3

Chapter 2. Superiority of Wet-milled over Dry-milled Superfine Powdered Activated Carbon for Adsorptive 2-methylisoborneol Removal **7**

2.1 Chapter introduction 7

2.2 Objectives and approaches 9

2.3 Experimental 10

2.3.1 Activated carbons (adsorbents) 10

2.3.2 Adsorbate and working solution 11

2.3.3 Batch adsorption tests 12

2.3.4 Pore diffusion model for batch adsorption process 12

2.3.5 Mass balance equation for an adsorbate in a batch reactor 13

2.4 Results and discussion 15

2.4.1 Comparison of MIB removal between wet-milled and dry-milled SPAC 15

2.4.2 Comparison of particle sizes between wet-milled and dry-milled SPAC 16

2.4.3 Verifying the reasons for lower MIB removal by dry-milled SPAC 18

2.4.4 Quantifying the impacts of aggregation and adsorption capacity on adsorptive MIB removal 20

2.4.5 Stability after disaggregation 25

2.5 Chapter conclusions 28

2.6 Reference 29

Chapter 3. Change of Equilibrium Adsorption Capacity with Decreasing Activated Carbon Particle Diameter from 30 μm to 140 nm **33**

3.1 Chapter introduction 33

3.2 Objectives and approaches 35

3.3 Experimental 36

3.3.1 Activated carbons (adsorbents) 36

3.3.2 Production of SPAC and SSPAC 36

3.3.3 Characterizations of carbons 40

3.3.4 Adsorbates and working solution 40

3.3.5 Batch adsorption tests 41

3.4 Results and discussion 42

3.4.1 SSPAC production by normal micro-milling 42

3.4.2 Carbon particle size effect on adsorption capacity of MIB. 44

3.4.3 Oxygen contents of carbons 47

3.4.4 Controlling oxidation during the productions of SPAC and SSPAC 49

3.4.5 Correlation between oxygen content and MIB adsorption capacity. 52
3.4.6 Carbon particle size effects on adsorption capacities of various adsorbates. ... 53
3.5 Chapter conclusions 60
3.6 Reference 61

Chapter 4. Micro-milling of Spent Granular Activated Carbon for Its Possible Reuse as Adsorbent: Remaining Capacity and Characteristics 65
4.1 Chapter introduction 65
4.2 Objectives and approaches 67
4.3 Experimental 68
4.3.1 Activated carbons (adsorbents) 68
4.3.2 Production of PAC, SPAC, and SSPAC from GAC 69
4.3.3 AC samples used in preliminary tests 75
4.3.4 Adsorbates 78
4.3.5 Working solutions and batch adsorption tests 78
4.3.6 Absorbability Indices 80
4.4 Results and discussion 82
4.4.1 Preliminary tests for used activated carbons 82
4.4.2 MIB adsorption kinetics. 85
4.4.3 MIB adsorption capacities. 88
4.4.4 Pore size distributions 91
4.4.5 Iodine, phenol, methylene and ABS numbers 93
4.4.6 Influence of adsorbates properties on the adsorption capacity 99
4.5 Chapter conclusions 106
4.6 Reference 107

Chapter 5. Conclusions 113

Chapter 1. Introduction

1.1. Background

The quality of drinking water, which tightly relates to people's daily life, has been paid attention as always. The conventional purification treatments on drinking water, including sedimentation, coagulation, oxidation, and filtration and so on, have been generalized in the worldwide (Stackelberg et al., 2004; Stackelberg et al., 2007). Among the water purification technologies, the adsorption process with activated carbon (AC) always plays an important role due to the consistent removal effect towards various kinds of contaminants (Snyder et al., 2007; Sontheimer et al., 1988). Adsorption by AC shows its advantage at relatively low cost, convenient operation and wide scope of application. Therefore, there are countless studies relating to adsorption by ACs about the adsorption performance on different target adsorbates, about the properties of AC which relates to their adsorption ability, and so on.

It is known that normal AC was activated from the carbonaceous materials, such as wood, nutshells and fruit stones, peat, charcoal, soft coal, lignite, bituminous coal, petroleum coke, etc. (Dąbrowski et al., 2005). Granular activated carbon (GAC), which is the direct product after activation process, is composed of large AC particles with median particle diameter (D_{50}) around few millimeters and has already been widely used as the adsorbents in filter beds or columns in water purification processes (Aygün et al., 2003; Collivignarelli et al., 2006; Corwin et al., 2010; Matsui et al., 2002a; Matsui et al., 2002b; Zietzschmann et al., 2016). Previous researchers found that powdered activated carbon (PAC), which is produced by grinding GAC to smaller powders with D_{50} around tens micrometers, exhibited higher removal rate of pollutants than its parent GAC (Dunn et al., 2013; Kim et al., 2010; Tancredi et al., 2004; Zoschke et al., 2011). This point is meaningful for improving the efficiency of water treatment and the flexibility towards occasional environmental problems. What's more, researchers found that the adsorption capacity was also increased when GAC was ground to PAC (Basar et al., 2004; Kim et al., 2010; Tancredi et al., 2004). Recent years, thanks to the development of pulverization technology, much finer activated carbon than PAC can be produced. The merits of improving adsorption kinetics and capacity by grinding GAC to PAC continued when the PAC was milled to superfine PAC, termed as

SPAC, whose D_{50} is only few micrometers (Matsui et al., 2007; Matsui et al., 2009; Matsui et al., 2011; Wang et al., 2011). This doctoral dissertation is one of the works which pay attention on the adsorption performance of SPAC and the submicron-sized SPAC (termed as SSPAC) produced by milling SPAC to particles of the smallest size possible with a cutting-edge pulverization technology. We focused on the change of characteristics, such as the chemical and geometrical heterogeneities which contribute to the unique sorption properties of ACs (László et al., 2003; Podkościelny et al., 2003), when SPAC and SSPAC were produced by micro-milling and the related effects on adsorption mechanism.

To evaluate the adsorption performance of SSPAC, SPAC and related ACs, we chose 2-methylisoborneol (MIB) as the main representative target adsorbate and also numbers of other environmental relevant compounds as target adsorbates. MIB, which is produced by the metabolism and biodegradation of actinomycetes and cyanobacteria (Watson et al., 2000; Westerhoff et al., 2005), is one of the main contaminants causing earthy-musty odors. The odors of water make people uncomfortable and hypersensitive to the environments. With the increased awareness of water quality, more and more serious requirements from consumers make the limitation of remaining concentration of MIB and other similar off-flavors causing compounds to < 10 ng/L (Hattori, 2008). The problem is that MIB is extremely refractory to be removed by conventional water treatment processes (Srinivasan et al., 2011). However, it is a conventional target compound of activated carbon adsorption processes during water treatment (Cook et al., 2001; Gillogly et al., 1998; Matsui et al., 2008; Newcombe et al., 1997; Pendleton et al., 1997). Therefore, the adsorption performance of activated carbon on MIB is regarded as an important indicator of evaluating the activated carbons in drinking water treatments.

1.2. Objectives and originalities

Based on the background information, this doctoral dissertation focused on the MIB adsorption performance of micro-milled activated carbon, i.e. SSPAC and SPAC, from following 3 perspectives.

(1). It is originative to evaluate the MIB adsorption performance of dry-milled SPAC by comparing with that of wet-milled SPAC. The difference between the adsorption performance of dry-milled SPAC and that of same sized wet-milled SPAC produced from the same parent PAC revealed the effects of milling methods of SPAC on the MIB removal ability. The reasons leading to different adsorption performance were verified not only qualitatively but also quantitatively by modeling-simulation.

(2). It is novel to clarify the MIB adsorption capacity change with carbon particle size reduction in the range of SPAC to SSPAC. Efforts were payed to find out the carbon property which was modified during the micro-milling and impacted the MIB adsorption capacity. Except MIB, several other environmental related compounds with variety of properties were also tested to check the effect of carbon particle size reduction on their adsorption capacity.

(3). It is the first attempt to reuse the spent GAC to adsorb MIB in the forms of PAC, SPAC and SSPAC which were produced by milling GAC to small size. After discussing the possibility of utilizing used SPAC and used SSPAC produced from used GAC to adsorb MIB, 4 common absorbability indices of activated carbon were tested on used carbons to see their relativity with the remaining MIB adsorption capacities. The explanations of the different adsorption capacities towards different adsorbates showed by used carbons with various age have been put forward in the perspectives of physiochemical properties of both adsorbates and adsorbents, i.e. carbons.

With the results of the above 3 perspectives, the vacancies of SPAC study relating to the SPAC production methods, particle size of SPAC, SPAC physiochemical properties and reuse of spent carbons by milling them to SPAC have been filled. Especially for MIB, the main target adsorbate throughout this dissertation, the adsorption performance showed by various SPACs with different properties have been studied a lot. Several related conclusions have been made after discussion.

Reference

Aygün, A., Yenisoy-Karakaş, S. and Duman, I., 2003. Production of granular activated carbon from fruit stones and nutshells and evaluation of their physical, chemical and adsorption properties. Microporous and Mesoporous Materials 66(2–3), 189-195.

Basar, C.A., Karagunduz, A., Cakici, A. and Keskinler, B., 2004. Removal of surfactants by powdered activated carbon and microfiltration. Water Research 38(8), 2117-2124.

Collivignarelli, C., Sorlini, S. and Belluati, M., 2006. Chlorite removal with GAC. Journal (American Water Works Association) 98(12), 74-81.

Cook, D., Newcombe, G. and Sztajnbok, P., 2001. The application of powdered activated carbon for mib and geosmin removal: predicting pac doses in four raw waters. Water Research 35(5), 1325-1333.

Corwin, C.J. and Summers, R.S., 2010. Scaling Trace Organic Contaminant Adsorption Capacity by Granular Activated Carbon. Environmental Science & Technology 44(14), 5403-5408.

Dąbrowski, A., Podkościelny, P., Hubicki, Z. and Barczak, M., 2005. Adsorption of phenolic compounds by activated carbon—a critical review. Chemosphere 58(8), 1049-1070.

Dunn, S.E. and Knappe, D.R., 2013. DBP Precursor and Micropollutant Removal by Powdered Activated Carbon [Project# 4294].

Gillogly, T.E., Snoeyink, V.L., Elarde, J.R., Wilson, C.M. and Royal, E.P., 1998. 14C-MIB adsorption on PAC in natural water. American Water Works Association 90(1), 98-108.

Hattori, M., 2008. The Drinking Water Quality Standards (DWQSs) and problems of odor and taste in water supply. Journal of Japan Association on Odor Environment 39(2), 94-101.

Kim, S.H., Shon, H.K. and Ngo, H.H., 2010. Adsorption characteristics of antibiotics trimethoprim on powdered and granular activated carbon. Journal of Industrial and Engineering Chemistry 16(3), 344-349.

László, K., Podkościelny, P. and Dąbrowski, A., 2003. Heterogeneity of Polymer-Based Active Carbons in Adsorption of Aqueous Solutions of Phenol and 2,3,4-Trichlorophenol. Langmuir 19(13), 5287-5294.

Matsui, Y., Aizawa, T., Kanda, F., Nigorikawa, N., Mima, S. and Kawase, Y., 2007. Adsorptive removal of geosmin by ceramic membrane filtration with super-powdered activated carbon. Journal of Water Supply: Research & Technology-AQUA 56.

Matsui, Y., Ando, N., Sasaki, H., Matsushita, T. and Ohno, K., 2009. Branched pore kinetic model analysis of geosmin adsorption on super-powdered activated carbon. Water Research 43(12), 3095-3103.

Matsui, Y., Ando, N., Yoshida, T., Kurotobi, R., Matsushita, T. and Ohno, K., 2011. Modeling high adsorption capacity and kinetics of organic macromolecules on super-powdered activated carbon. Water research 45(4), 1720-1728.

Matsui, Y., Knappe, D.R.U., Iwaki, K. and Ohira, H., 2002a. Pesticide Adsorption by Granular Activated Carbon Adsorbers. 2. Effects of Pesticide and Natural Organic Matter Characteristics on Pesticide Breakthrough Curves. Environmental Science & Technology 36(15), 3432-3438.

Matsui, Y., Knappe, D.R.U. and Takagi, R., 2002b. Pesticide Adsorption by Granular Activated Carbon Adsorbers. 1. Effect of Natural Organic Matter Preloading on Removal Rates and Model Simplification. Environmental Science & Technology 36(15), 3426-3431.

Matsui, Y., Murai, K., Sasaki, H., Ohno, K. and Matsushita, T., 2008. Submicron-sized activated carbon particles for the rapid removal of chlorinous and earthy-musty compounds. Journal of Water Supply: Research and Technology - Aqua 57(8), 577-583.

Newcombe, G., Drikas, M. and Hayes, R., 1997. Influence of characterised natural organic material on activated carbon adsorption: II. Effect on pore volume distribution and adsorption of 2-methylisoborneol. Water Research 31(5), 1065-1073.

Pendleton, P., Wong, S.H., Schumann, R., Levay, G., Denoyel, R. and Rouquero, J., 1997. Properties of activated carbon controlling 2-Methylisoborneol adsorption. Carbon 35(8), 1141-1149.

Podkościelny, P., Dbrowski, A. and Marijuk, O.V., 2003. Heterogeneity of active carbons in adsorption of phenol aqueous solutions. Applied Surface Science 205(1–4), 297-303.

Snyder, S.A., Adham, S., Redding, A.M., Cannon, F.S., DeCarolis, J., Oppenheimer, J., Wert, E.C. and Yoon, Y., 2007. Role of membranes and activated carbon in the removal of endocrine disruptors and pharmaceuticals. Desalination 202(1-3), 156-181.

Sontheimer, H., Crittenden, J.C., Summers, R.S., Hubele, C., Roberts, C. and Snoeyink, V.L., 1988. Activated carbon for water treatment, Universitaet Karlsruhe, Karlsruhe.

Srinivasan, R. and Sorial, G.A., 2011. Treatment of taste and odor causing compounds 2-methyl isoborneol and geosmin in drinking water: A critical review. Journal of Environmental Sciences 23(1), 1-13.

Stackelberg, P.E., Furlong, E.T., Meyer, M.T., Zaugg, S.D., Henderson, A.K. and Reissman, D.B., 2004. Persistence of pharmaceutical compounds and other organic wastewater contaminants in a conventional drinking-water-treatment plant. Science of The Total Environment 329(1–3), 99-113.

Stackelberg, P.E., Gibs, J., Furlong, E.T., Meyer, M.T., Zaugg, S.D. and Lippincott, R.L., 2007. Efficiency of conventional drinking-water-treatment processes in removal of pharmaceuticals and other organic compounds. Science of The Total Environment 377(2–3), 255-272.

Tancredi, N., Medero, N., Möller, F., Píriz, J., Plada, C. and Cordero, T., 2004. Phenol adsorption onto powdered and granular activated carbon, prepared from Eucalyptus wood. Journal of Colloid and Interface Science 279(2), 357-363.

Wang, Y., Rao, G.Y. and Hu, J.Y., 2011. Adsorption of EDCs/PPCPs from drinking water by submicron-sized powdered activated carbon. Water Science and Technology: Water Supply 11(6), 711-718.

Watson, S.B., Brownlee, B., Satchwill, T. and Hargesheimer, E.E., 2000. Quantitative analysis of trace levels of geosmin and MIB in source and drinking water using headspace SPME. Water Research 34(10), 2818-2828.

Westerhoff, P., Rodriguez-Hernandez, M., Baker, L. and Sommerfeld, M., 2005. Seasonal occurrence and degradation of 2-methylisoborneol in water supply reservoirs. Water Research 39(20), 4899-4912.

Zietzschmann, F., Stützer, C. and Jekel, M., 2016. Granular activated carbon adsorption of organic micro-pollutants in drinking water and treated wastewater – Aligning breakthrough curves and capacities. Water Research 92, 180-187.

Zoschke, K., Engel, C., Börnick, H. and Worch, E., 2011. Adsorption of geosmin and 2-methylisoborneol onto powdered activated carbon at non-equilibrium conditions: Influence of NOM and process modelling. Water Research 45(15), 4544-4550.

Chapter 2. Superiority of Wet-milled over Dry-milled Superfine Powdered Activated Carbon for Adsorptive 2-methylisoborneol Removal

2.1 Chapter introduction

Compared with PAC, SPAC, which consists of particles with diameters of no more than a few micrometers, has advantages regarding both adsorption capacity and kinetics. These merits of SPAC belongs to the one more step of larger specific external surface area per unit of mass from PAC to SPAC which is based on the increase from GAC to PAC mentioned in Chapter 1, and the shortened diffusion distance within each carbon particle (Ando et al., 2010; Matsui et al., 2009; Matsui et al., 2015; Matsui et al., 2013b; Sontheimer et al., 1988). The SPAC is produced from PAC by milling processes which are classified into the wet-milling method and the dry-milling method.

In all scientific studies and actual field applications to date, wet-milling systems have been used to produce SPAC. In wet-milling systems, the PAC is suspended in carrier water to make a slurry, and then the slurry is introduced into a bead mill to produce SPAC (Partlan et al., 2016). However, the production efficiency of such small-sized particles by this wet-milling system is limited because the viscosity of the carrier fluid, and thus the slurry concentration, must be low (Knieke et al., 2010; Schmidt et al., 2012). The low concentration of the slurry also increases the bulk volume of the SPAC and thus the cost of its transport after production. Even if SPAC is produced onsite in water treatment plants, the SPAC slurry has a large storage footprint.

In addition to wet-milling systems, dry-milling systems have recently become available that can successfully produce submicrometer-sized particles of various materials, such as intermetallics (Suryanarayana, 2001), boron (Jung et al., 2015), and boron carbides (Ramos et al., 2006). Unlike wet-milling systems, dry-milling systems utilize gas or steam, rather than a liquid, as the carrier of the particles during comminution by the milling medium. Compared with wet milling, dry milling mitigates the high production volume problem, reducing both the size of the storage footprint and the transport volume. In addition to these advantages, the dry-milling process can reduce the size of the milled particles

at a higher rate and the particles may be less likely to become contaminated by milling medium residues, compared with the wet-milling process (Jung et al., 2015).

Despite these merits of dry milling compared with wet milling to produce finely milled particles, adsorption by dry-milled SPAC has not yet been investigated. Therefore, in this study, the adsorption performance of dry-milled SPAC was compared with that of wet-milled SPAC. As mentioned in chapter 1, we chose MIB as a representative target compound for adsorptive removal to evaluate the adsorption ability of the SPACs. The results of the comparison showed that the adsorption performance of the dry-milled SPAC was inferior to that of the wet- milled SPAC, so we further investigated the reasons for the different performances. Overall, an attempt was made to simulate the adsorption performance with a kind of universal model which was proposed under our understanding.

2.2 Objectives and approaches

The main objective of this chapter is to 1st compare the adsorption performance of the SPAC with similar size produced by the dry-milling method and wet-milling method respectively. Considering that the diameter reduction of products without dispersant by current dry-milling is limited to around 1 μm (Yokoyama et al., 2005), the comparision of MIB adsorptive removal is between the SPAC with D_{50} of 1 μm which are intendedly produced by dry-milling and the SPAC produced by wet-milling respectively from the same parent PAC. Then the 2nd objective is to find out the reasons causing the difference between the MIB adsorption performance of dry-milled SPAC and that of wet-milled SPAC. The final objective (3rd) is to quantify the effects of reasons found in 2nd objective by modeling-simulation.

2.3 Experimental

2.3.1 Activated carbons (adsorbents)

Table 2-1. SPACs and PACs classified by size and milling method

Designation	Original carbon	Production method	Median diameter D_{50} (μm)	
			True size (measured after the addition of dispersant and ultrasonication)	Apparent size (measured with no pretreatment)
PAC-S	PAC-S	Non-milled	11.8	13.8
SPAC-S-W		Wet milling	1.28	3.80
SPAC-S-D		Dry milling	1.24	14.2
SPAC-S-DS		Dry milling followed by ultrasonication	1.24	2.42
PAC-F	PAC-F	Non-milled	27.5	36.5
SPAC-F-W		Wet milling	1.21	3.42
SPAC-F-D		Dry milling	1.22	10.3
SPAC-F-DS		Dry milling followed by ultrasonication	1.22	1.99

Two commercial wood-based PACs were obtained and designated PAC-S (Shirasagi, Osaka Chemical Co., Osaka, Japan) and PAC-F (Futamura Chemical Co., Tokyo, Japan). Dry-milled SPACs for use in the experiments were produced by milling each PAC to the target size in a dry-milling system (SDA5, Ashizawa Finetech Ltd., Chiba, Japan; bead diameter, 1.5 mm; carrier, air), and wet-milled SPACs were separately produced in a wet-milling system (LMZ015, Ashizawa Finetech Ltd., Chiba, Japan; bead diameter, 0.1 mm; carrier, pure water). All activated carbons, including non-milled PACs, wet-milled SPACs, and dry-milled SPACs, were stored in a slurry (1%–5% w/v) made with pure water at 4 °C after vacuum conditioning to remove any air from the activated carbon pores. Aliquots of the dry-milled SPACs slurry were ultrasonicated (150 W, 19.5 kHz, 1 min for 50 mL carbon slurry) for dispersion. The SPACs were labeled according to the milling process used and the PAC (-S or -F) from which they were produced; for example, SPAC-S-D was produced by dry milling from PAC-S, and ultrasonicated dry-milled SPAC that was produced from SPAC-S-D was designated SPAC-S-DS (Table 2-1).

Particle size distributions of the SPACs and PACs were determined by using a laser-light scattering instrument (Microtrac MT3300EXII, Nikkiso Co., Tokyo, Japan). To measure the true particle size of the carbon samples, the samples were taken from the stock slurries and then pretreated by the addition

of a dispersant (Triton X-100, Kanto Chemical Co., Tokyo, Japan; final concentration, 0.08% w/v) and subsequent ultrasonic dispersion before measurement with the Microtrac instrument. The apparent particle sizes were measured without this pretreatment. The graphs of particle size distributions are the Fig.2-1, Fig.2-2 and Fig.2-4.

Elemental analysis was performed on the SPACs with regard to oxygen by an elemental analyzer (Vario EL Cube, Elementar Japan K.K., Yokohama, Japan) with thermal conductivity and infra-red detectors.

The BET (Brunauer-Emmett-Teller) surface areas of the activated carbon particles were obtained by using the nitrogen gas adsorption-desorption method (Autosorb-iQ, Quantachrome Instruments, Kanagawa, Japan). The isotherm data for nitrogen gas desorption at 77.4 K were analyzed with the BET equation (ASiQwin, ver.3.01, Quantachrome Instruments).

Zeta potentials of the SPACs measured in suspension at various pHs. Organic-free water was prepared by amending ultrapure water with inorganic ions such that conductivity was 77−89 μS/cm and the ionic composition was similar to that used in the study by Matsui et al., 2015.. SPAC suspension samples were prepared by diluting the stock slurry of each SPAC to a concentration of 20 mg/L and adjusting the pH to values ranging from 2 to 11 by adding HCl or NaOH. After stirring each sample suspension for 8 h, a portion of the suspension was withdrawn and injected into the cell of an electrophoretic light-scattering spectrophotometer (Zetasizer Nano ZS; 532-nm green laser, Malvern Instruments, Malvern, Worcestershire, UK). The zeta potential of each sample was measured at 25 ˚C three times, and the average was calculated.

2.3.2 Adsorbate and working solution

A stock solution of MIB (~900 μg/L) was prepared by dissolving pure MIB (Wako Pure Chemical Industries, Ltd., Osaka, Japan) in ultrapure water and then filtering the solution through a 0.2-μm pore size membrane filter (DISMIC-25HP; Toyo Roshi Kaisha, Ltd., Tokyo, Japan). Organic-free water containing ions same as previous researches (Matsui et al., 2015) was spiked with the MIB stock solution to obtain working solutions with MIB concentrations of around 1 and 4 μg/L, because MIB usually occurs naturally at concentrations lower than these concentrations. The working solutions were adjusted to pH 7.0 ± 0.1 with HCl or NaOH as required. The MIB concentration was detected by using deuterium-labeled geosmin (Wako Pure Chemical Industries, Ltd., Osaka, Japan) as an internal standard in a purge and trap concentrator (Aqua PT 5000 J; GL Sciences, Inc., Tokyo, Japan) coupled to a gas

chromatograph−mass spectrometer (GCMS-QP2010 Plus; Shimadzu Co., Kyoto, Japan), where the *m/z* 95 and *m/z* 115 peaks were interpreted as corresponding to MIB and deuterium-labeled geosmin, respectively.

2.3.3 Batch adsorption tests

The adsorption kinetics was investigated by means of batch tests with efficient mixing. A working solution of water and MIB was placed in a beaker (1 L or 3 L), and an aliquot was withdrawn from the beaker to determine the initial MIB concentration. After the addition of a specified amount of SPAC or PAC slurry, aliquots were withdrawn at intervals and filtered immediately through 0.2-μm membrane filters (DISMIC-25HP, Toyo Roshi Kaisha, Tokyo, Japan) for analysis of the MIB concentration.

For the adsorption equilibrium tests, aliquots (110 mL) of the working solutions (hereafter, water samples) containing MIB (1 ± 0.2 μg/L) were transferred to 120-mL vials. Specified amounts of SPAC or PAC were immediately added (0.3−1.8 mg/L), and the vials were manually shaken and then agitated on a mechanical shaker for 1 week at a constant temperature of 20 °C. Preliminary experiments confirmed that the adsorption equilibrium of MIB was reached after 1 week of contact (Matsui et al., 2013a; Matsui et al., 2012). Control tests of water samples that did not contain carbon (i.e., blanks) were also conducted to confirm that changes in the blank MIB concentration during long-term mixing were negligible. After 1 week of shaking, the water samples were filtered through 0.2-μm pore size membrane filters, and then MIB concentrations in the aqueous phase were measured. Solid-phase concentrations of MIB were calculated from the mass balance.

2.3.4 Pore diffusion model for batch adsorption process

These experimental data of adsorption kinetics were simulated by applying pore diffusion model (PDM), modified by incorporating adsorbent particle aggregation.

$$\frac{\partial q(t,r,R)}{\partial t} = \frac{\varepsilon D_P}{\rho r^2}\frac{\partial}{\partial r}\left(r^2\frac{\partial c(t,r,R)}{\partial r}\right) \quad (2\text{-}1)$$

where t is adsorption time in a batch system (s); R is the radius of an aggregate (cm), r is the radial distance from the center of an aggregate to its outer edge (cm); ρ is the apparent particle density of an aggregate (g/L), ε is porosity (dimensionless), D_P is the diffusion coefficient in a pore (cm^2/s); $q(t, r, R)$ is the solid-phase concentration of the adsorbate (i.e., MIB) in the pore of an aggregate with radius R at radial distance r and time t (ng/g); and $c(t, r, R)$ is the liquid-phase concentration of the adsorbate in a pore of an aggregate having radius R at radial distance r and time t (ng/g).

In the model, each adsorbent particle aggregate is treated as a single adsorbent unit; thus, for simplicity, diffusion in interparticle pores between the adsorbent particles composing the aggregate and diffusion in the pores of the individual adsorbent particles are merged. Mass transfer resistance across a liquid film external to the aggregates is neglected because it should not be a rate-determining step in a well-mixed reactor (Sontheimer et al., 1988). The conservation of adsorbent particle size during the adsorption process is assumed, consistent with the evidence presented in section 2.4.2. Although the Shell Adsorption Model (SAM) is used to simulate the different isotherms of PAC and wet-milled SPAC (Matsui et al., 2013a; Matsui et al., 2014), it is not yet possible to use this model to simulate the different isotherms of wet-milled and dry-milled SPACs, which have a similar particle size. Therefore, because of its wide application and simplicity, we decided to use the Freundlich model.

The apparent density (ρ) and porosity (ε) of an aggregate in PDM equation can be estimated by using fractal theory (Elimelech et al., 2013) as follows:

$$\frac{\rho}{\rho_{\mathrm{P}}} = \frac{1-\varepsilon}{1-\varepsilon_{\mathrm{P}}} = \left(\frac{d_{\mathrm{P}}}{d}\right)^{3-\beta} \tag{2-2}$$

where ρ is the apparent density of an aggregate (g/L), ρ_{P} is the apparent density of the adsorbent particles composing the aggregate (g/L), ε_{P} is the porosity of the adsorbent particles composing the aggregate (cm), ε is the porosity of the aggregate (cm), d_{P} is the diameter of the adsorbent particles composing the aggregate (cm), d is the diameter of the aggregate (cm), and β is the fractal dimension (dimensionless).

2.3.5 Mass balance equation for an adsorbate in a batch reactor

To determine the size distribution of aggregates, we used the following mass balance equation for an adsorbate in a batch reactor:

$$\frac{\mathrm{d}C(t)}{\mathrm{d}t} = -3C_{\mathrm{C}} \int_0^{\infty} \frac{f_{\mathrm{R}}(R)}{R^3} \left[\int_0^{\mathrm{R}} r^2 \frac{dq(t,r,R)}{dt} \mathrm{d}r \right] \mathrm{d}R \tag{2-3}$$

where $C(t)$ is the adsorbate concentration in the bulk water phase as a function of time (mg/L), C_{C} is the carbon dosage (g/L), and $f_{\mathrm{R}}(R)$ is the size (radius) distribution function of aggregates.

Particle size (radius) distribution of adsorbent was approximated by a discrete density function consisting of 11 size classes, as the example shown in Fig. 2-1. The conservation of adsorbent particle size during the adsorption process was assumed, consistent with the evidence presented in section 2.4.2.

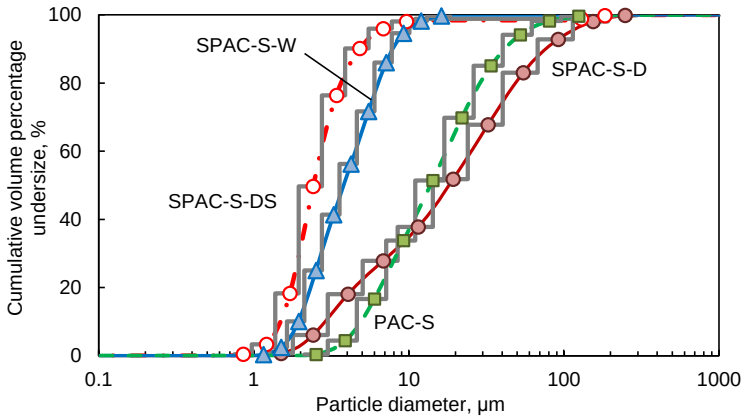

Fig. 2-1. Measured particle size distributions and their discrete approximations

The PDM equation and the mass balance equation for an adsorbate in a batch reactor were converted into a set of ordinary differential equations with respect to time, *t*, using the method of orthogonal collocation (Matsui et al., 2009). The resultant equations were solved as a system of ordinary differential equations by Gear's stiff method (IMSL® Math Library) after deriving the analytical Jacobian of the equations.

2.4 Results and discussion

2.4.1 Comparison of MIB removal between wet-milled and dry-milled SPAC

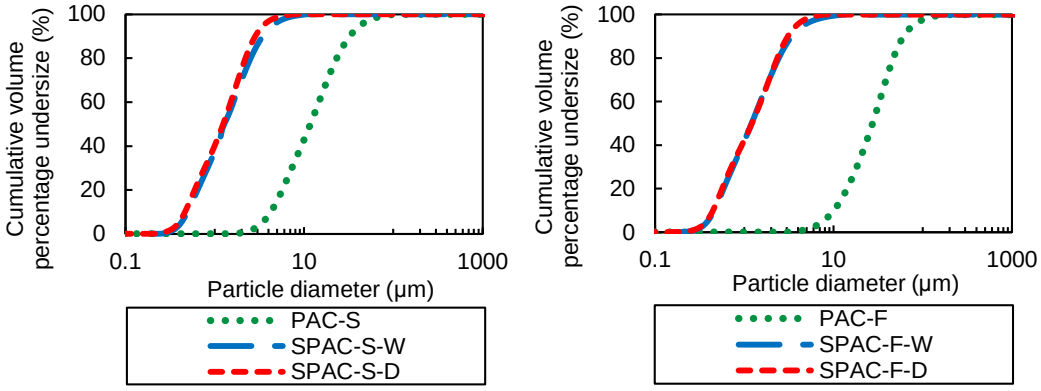

Fig. 2-2. True size distributions of SPACs and PACs

Wet-milled and dry-milled SPACs were intentionally produced with similar true particle size distributions (Fig. 2-2). For example, the median true diameter (D_{50}) of SPAC-S-D was 1.24 μm, whereas that of SPAC-S-W was 1.28 μm (Table 2-1). However, the MIB adsorption kinetics of SPAC-S-D and SPAC-S-W differed (Fig. 2-3); the MIB removal rate of SPAC-S-D was obviously lower than that of SPAC-S-W. Wet milling of PAC-S improved MIB removal (Fig. 2-3, SPAC-S-W vs. PAC-S), consistent with results reported previously (Matsui et al., 2009; Matsui et al., 2013a), whereas dry milling did not result in any improvement in MIB removal (SPAC-S-D vs. PAC-S). Compared to the MIB removal rate of PAC-F, the rates of both SPAC-F-D and SPAC-F-W were higher. However, the adsorption kinetics of SPAC-F-D was inferior to that of SPAC-F-W, despite their similar true particle size distributions (Table 2-1).

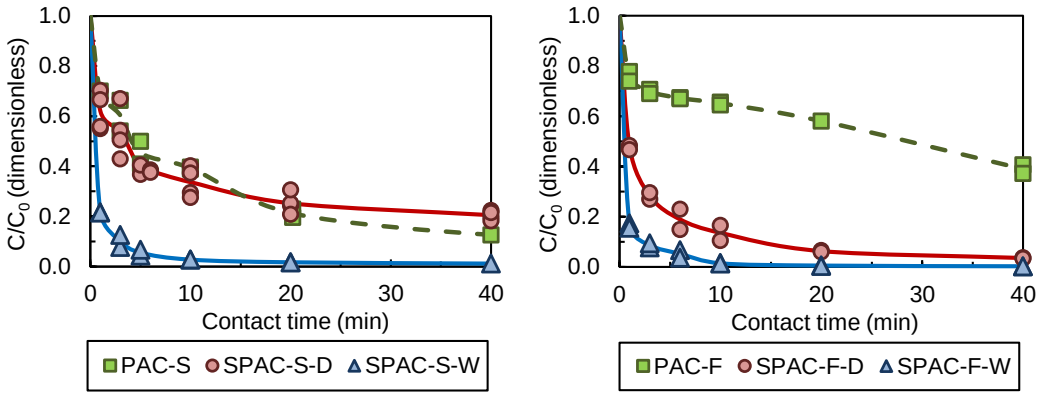

Fig. 2-3. Adsorption kinetics of MIB by PACs and dry-milled and wet-milled SPACs (MIB initial concentration C_0 = 1.25 ± 0.15 μg/L; carbon dosage, 3 mg/L, except 3.7 mg/L for SPAC-S-W. C = MIB concentration at each measurement time).

2.4.2 Comparison of particle sizes between wet-milled and dry-milled SPAC

According to the theory of adsorption kinetics, the adsorptive removal by carbon particles is enhanced by a reduction of the carbon particle size because (1) the specific outer surface area of the particles is increased, leading to a higher rate of adsorbate uptake from the bulk phase into pores; and (2) the internal radial diffusion distance within a carbon particle is shortened, thus increasing the mass flux rate. Therefore, to identify the reasons for the different MIB removal rates by wet-milled and dry-milled SPACs, we focused on the carbon particle size.

The results presented in section 2.4.1 are those based on the true carbon particle diameters of each SPAC, determined after the addition of dispersant and ultrasonication. However, carbon particles in a suspension may exist as aggregates rather than as discrete particles (Bonvin et al., 2016). Thus, although the wet-milled and dry-milled SPACs had the same true particle size distribution, the apparent particle size distributions in the suspensions used for the experiments were not necessarily the same because the degree of aggregation might have differed between wet- and dry-milled SPACs.

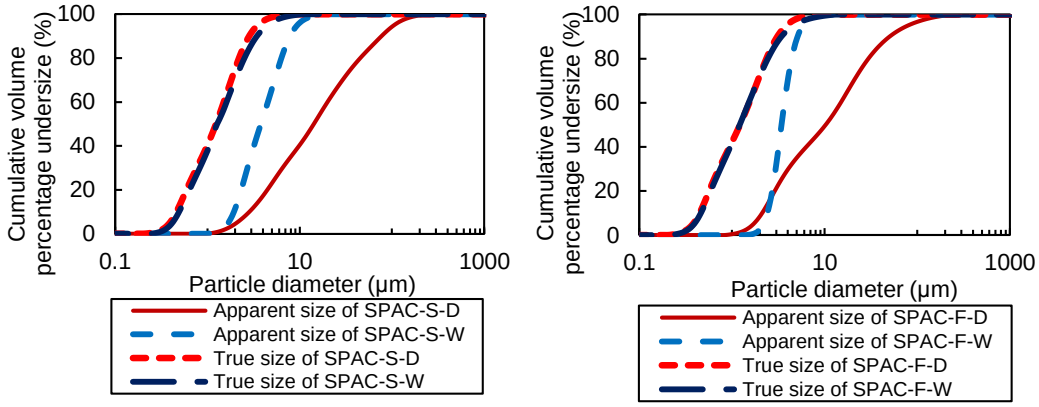

Fig. 2-4. True and apparent SPAC size distributions

Research on SPAC adsorption in membrane filtration systems has reported aggregated forms of SPAC on the membrane surface (Ellerie et al., 2013). During the adsorption kinetic experiments, however, direct observation of the particles in the suspension for particle size measurement was not possible because of the very low carbon concentration, the small particle sizes, and the high-speed movement of the particles in the stirred vessel. Therefore, we used non-pretreated samples to evaluate apparent SPAC particle diameters. In addition, the sonicator attached to the Microtrac instrument was switched off during the measurements. To minimize as much as possible any flow or mixing effect from the instrument on the particle size measurement, each measurement was conducted soon after signal stabilization, which took place around 30 to 40 s after the carbon sample was transferred from the stock bottle to the instrument. The resulting apparent particle diameter distributions (Fig. 2-4) clearly revealed the presence of aggregates in the SPAC slurry. The extent of aggregation differed between dry- and wet-

milled SPACS; SPAC-S-D and SPAC-F-D were aggregated to a higher degree than SPAC-S-W and SPAC-F-W.

Moreover, the apparent particle size distribution of the dry-milled carbons did not change in relation to the mixing time during the adsorption experiment (Fig. 2-5). Although the same mixing conditions were used as in the adsorption tests, the carbon concentration of the suspension used for the particle size measurement was 30 times the concentration used in the absorption experiment because of the detection limit of the Microtrac instrument. Higher concentrations of particles lead to more frequent particle–particle collisions, and the collision frequency determines the aggregation rate (Baalousha, 2009; Christian et al., 2008; Phenrat et al., 2007). Therefore, the fact that the particle size distribution was not changed by the mixing even at the higher concentration suggests that during the adsorption experiments the apparent carbon particle size probably remained unchanged by the mixing as well.

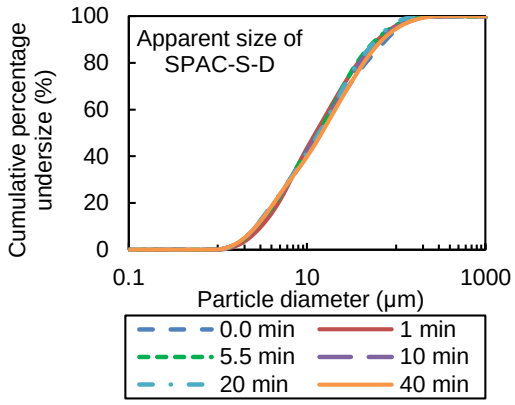

Fig. 2-5. Apparent size distributions of SPAC-S-D sampled after various mixing times

Aliquots for apparent particle size measurement were collected from a beaker containing 100 mg/L of SPAC-S-D under the same mixing conditions and at the same times as in the adsorption kinetics experiment. Immediately after each sampling, the aliquots were transferred to the Microtrac instrument, and their particle size distributions were measured without any pretreatment.

The mass transfer process in the activated carbon adsorption consists of two general mechanisms: (i) external mass transfer across the liquid film surrounding the carbon particle, and (ii) radial intraparticle diffusion through pores (Sontheimer et al., 1988). When carbon particles are aggregated, the interparticle space acts as pseudopores through which molecules must diffuse to reach the external surfaces of the individual particles. Thus, when the particles are aggregated, the total diffusive pass length is lengthened and the available external surface area and number of particles are both smaller, all of which reduce the adsorption rate. Therefore, the slower MIB removal rate by the dry-milled SPAC compared with that by the wet-milled SPAC should be related to the different degree of aggregation between the SPACs.

2.4.3 Verifying the reasons for lower MIB removal by dry-milled SPAC

To verify the effects of aggregation on the adsorption kinetics, the dry-milled carbons were ultrasonicated for disaggregation and decrease their apparent particle size. The apparent particle size of the ultrasonicated dry-milled SPACs (SPAC-S-DS and SPAC-F-DS) became smaller; in fact, the apparent particle size of SPAC-S-DS and SPAC-F-DS were even smaller than those of the wet-milled carbons SPAC-S-W and SPAC-F-W (Fig. 2-6). SPAC-S-DS and SPAC-F-DS showed higher MIB removal rates than SPAC-S-D and SPAC-F-D, respectively (Fig. 2-7). The adsorption kinetics of the dry-milled SPACs was thus clearly improved after they were pretreated by ultrasonication. Therefore, aggregation can explain in part the low MIB removal rates of the (non-sonicated) dry-milled SPACs.

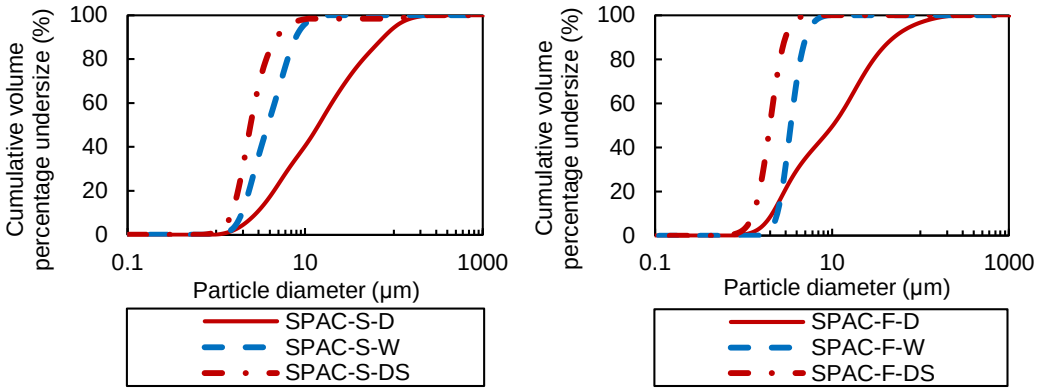

Fig. 2-6. Apparent particle size distributions of the dry-milled SPACs, the ultrasonicated dry-milled SPACs, and the wet-milled SPACs

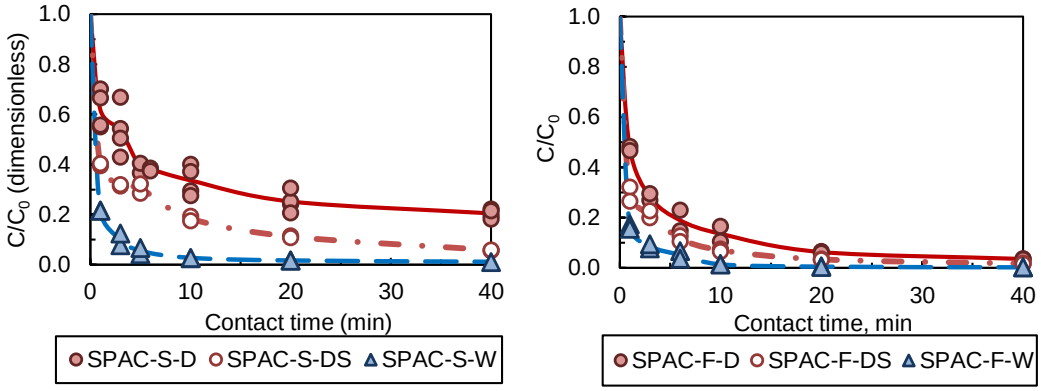

Fig. 2-7. Adsorption kinetics of the dry-milled SPACs, the ultrasonicated dry-milled SPACs, and the wet-milled SPACs (MIB initial concentration, 1.25 ± 0.15 μg/L; carbon dosage, 3 mg/L, except 3.7 mg/L for SPAC-S-W)

However, the MIB removal attained by the ultrasonicated dry-milled SPACs was still lower than the removal attained by the corresponding wet-milled SPACs, even though the ultrasonicated dry-milled SPACs were less aggregated and their true particle size distributions were similar to those of the wet-milled SPACs. The difference in MIB removal between the ultrasonicated dry-milled SPACs and the wet-milled SPACs suggests that there is another reason, in addition to aggregation, for the lower MIB removal ability of the dry-milled SPACs.

In addition to adsorption kinetics, adsorption capacity affects adsorptive removal. Therefore, we examined the MIB adsorption isotherms of the carbons (Fig. 2-8). SPAC-S-W and SPAC-F-W both had higher capacities than their parent carbons (PAC-S and PAC-F, respectively). This result is in agreement with previous findings that adsorption capacity is increased when the carbon particle diameter is decreased from a few tens of micrometers to a few micrometers (Ando et al., 2010; Ando et al., 2011; Matsui et al., 2012). Dry milling, however, did not increase the adsorption capacity: the adsorption capacities of SPAC-S-D and SPAC-F-D were nearly the same as those of their parent carbons (PAC-S and PAC-F, respectively). The contact time between the carbon and water was sufficient for even the PACs to reach adsorption equilibrium; therefore, the adsorption capacities of the dry-milled SPACs were not influenced by particle aggregation. Dunn et al., 2013.) have suggested that interparticle pseudopores formed as a result of SPAC particle aggregation might act as additional mesopores and thus increase the adsorption capacity relative to that of the corresponding PAC. However, we observed an opposite effect: the dry-milled SPACs, which were more severely aggregated, had lower adsorption capacities than the wet-milled SPACs.

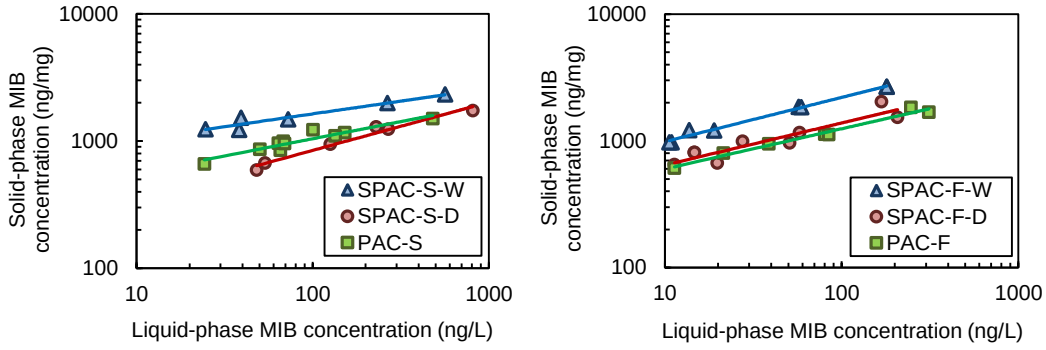

Fig. 2-8. Adsorption isotherms of the PACs, the wet-milled SPACs, and the dry-milled SPACs.

Internal pore areas before and after wet milling are previously investigated. These report that the change in carbon particle size by the wet milling did not result in any substantial change in internal pore areas, and therefore the dependency of the adsorption capacity on carbon particle size is not related to internal pore. In the present study, the internal pores, which were measures as BET surface areas, did not explain the adsorption capacity differences: SPAC-S-W and SPAC-F-W both had higher capacities than

their parent carbons, even after the solid-phase concentrations in the isotherms were normalized by using the mass of adsorbed MIB divided by BET (Brunauer-Emmett-Teller) surface area (Fig. 2-9).

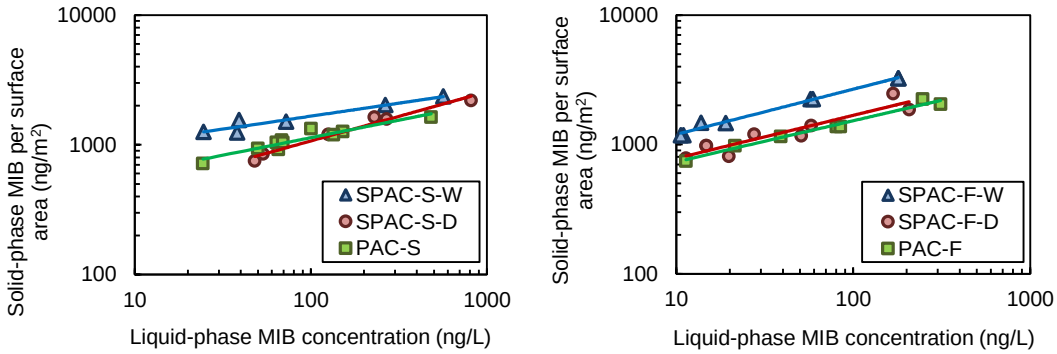

Fig. 2-9. Adsorption isotherms normalized by BET surface area of the PACs, the wet-milled SPACs, and the dry-milled SPACs (solid-phase concentrations are the amounts of adsorbed MIB divided by BET surface area of activated carbons).

The increased adsorption capacity of smaller sized carbon particles can be explained by SAM. According to this model, the adsorbate molecule penetrates the carbon particles only a certain distance (Matsui et al., 2011). If the carbon particle radius is substantially larger than this penetration distance, adsorption sites in the interior region of the carbon particle are not utilized (Matsui et al., 2015). As a result, the equilibrium adsorption capacity increases as the carbon particle size decreases until the particle radius becomes much smaller than the penetration distance. Once the particle radius is much smaller than the adsorbate penetration distance, as in the case of the SPACs, the adsorption capacity becomes independent of particle size and is then mainly determined by the pore surface chemistry (Li et al., 2002; Matsui et al., 2015; Quinlivan et al., 2005). Therefore, the different adsorption capacities of the wet-milled and dry-milled SPACs might reflect differences in the chemical characteristics of the pore surfaces due to the different milling methods. One possible cause of different pore surface chemical characteristics might be oxidation occurring during milling by which the carbon became more hydrophilic (Partlan et al., 2016); the carbon might become more oxidized during dry milling than during wet milling. Actually, dry-milled SPACs were higher in oxygen content than the wet-milled SPACs (SPAC-S-D: 10.2% vs. SPAC-S-W: 6.3%; SPAC-F-D: 6.4% vs. SPAC-F-W: 4.4%), which suggests the dry-milled SPACs had more oxygen-containing functional groups and more hydrophilic. Therefore the adsorption capacity of the dry-milled SPACs would be lower than that of the wet-milled SPACs.

2.4.4 Quantifying the impacts of aggregation and adsorption capacity on adsorptive MIB removal

I. Model simulations describing experimental data

To evaluate separately and quantitatively the impacts of adsorption capacity and particle

aggregation on adsorption kinetics, we conducted PDM simulations. The PDM parameter values were determined for each carbon by independent experiments (Table 2-2). The unknown model parameters were the pore diffusion coefficient (D_P) and the fractal dimension (β). We searched for a single set of values for these unknowns that best described all the experimental adsorption kinetics data of the four differently sized carbons (PAC and SPACs). Because markedly different adsorption kinetics were exhibited by PAC-S and the SPACs produced from it (see Fig. 2-3 and Fig. 2-7), we focused on this series of carbon samples. The final objective of the modeling was to evaluate quantitatively the effect of particle aggregation and adsorption capacity on adsorptive MIB removal for a given carbon–water contact time and carbon dosage. Therefore, we searched for a single set of model parameters, including the pore diffusion coefficient, which could successfully describe the experimentally determined adsorption kinetics of PAC-S, SPAC-S-W, SPAC-S-D, and SPAC-S-DS.

Table 2-2 Model input parameter values.

	Particles composing aggregates				Aggregates	
	Median diameter (d) (μm)	True density (g/L)	Porosity (dimensionless)	Apparent particle density (g/L)	Median diameter, d_A (μm)	Size distribution
PAC-S	11.5	1795	0.53	850	13.8	Fig. 2-5
SPAC-S-W	1.28				3.80	
SPAC-S-D	1.24				14.2	
SPAC-S-DS	1.24				2.42	

We found that a pore diffusion coefficient of 1.55×10^{-6} cm/s and a fractal dimension of 2.75 yielded the best fit the experimental data (Fig. 2-10 and Table 2-3). The diffusivity of a MIB molecule in water, estimated by the Hayduk–Laudie correlation method (Lyman et al., 1990), was 5.39×10^{-6} cm/s.

$$D_M = \frac{13.26\times10^{-5}}{\eta_W{}^{1.14}\times V_B{}^{0.589}} \quad (2\text{-}4)$$

where D_M is the diffusivity in water (cm^2/s), η_W is the viscosity of the water at a given temperature (cP), and V_B is the LeBas molar volume of the adsorbate (cm^3/mol). η_W = 1.002 cP and V_B = 229.2 cm^3/mol were used in the calculation.

By applying pore diffusion coefficient equation (2-5) (Sontheimer et al., 1988), therefore, the tortuosity was calculated to be 3.5 from the pore diffusion coefficient (1.55×10^{-6} cm/s) and the diffusivity. This value is plausible for tortuosity in activated carbon (Sontheimer et al., 1988).

$$D_P = \frac{D_M}{\chi} \quad (2\text{-}5)$$

where D_M is diffusivity in water (cm^2/s) and χ is tortuosity (dimensionless).

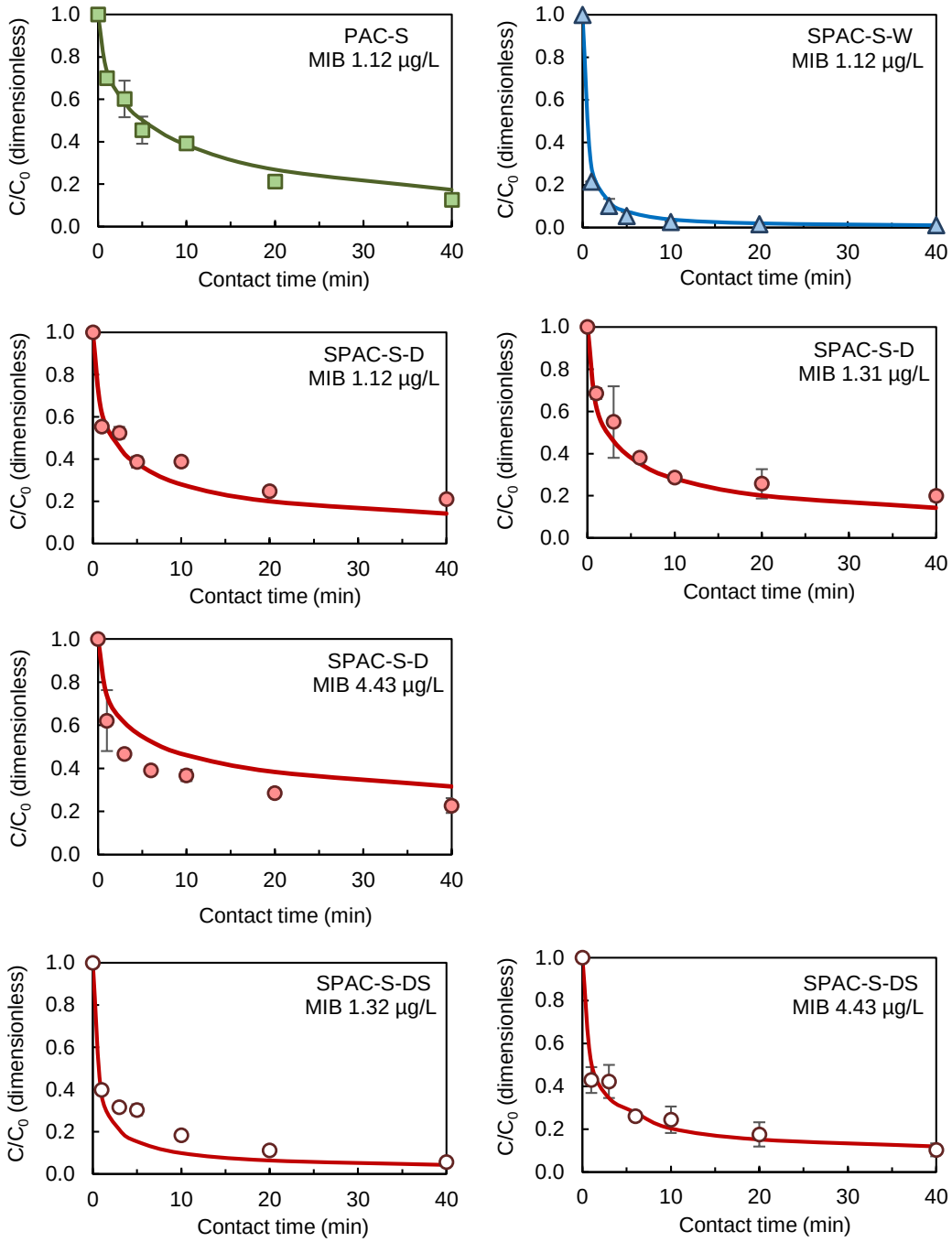

Fig. 2-10. Simulated (lines) and experimentally observed (symbols) adsorption kinetics of PAC-S and the SPACs produced from it (carbon dosage, 3 mg/L, except 3.7 mg/L for SPAC-S-W).

Table 2-3 Optimum values of the model parameters.

	Adsorbate		Aggregates		
	Pore diffusion coefficient (cm/s)	Tortuosity (dimensionless)	Fractal dimension	Apparent aggregate density (g/L)	Aggregate porosity (dimensionless)
PAC-S	1.55×10^{-6}	3.5	2.75	812	0.55
SPAC-S-W				647	0.64
SPAC-S-D				462	0.74
SPAC-S-DS				719	0.60

The fractal dimension of aggregates should be between 1.5 and 3 (Avnir et al., 1984; Elimelech et al., 2013; Logan, 1999). Therefore, the best-fit value of 2.75 is also reasonable and not inconsistent with the abovementioned range. The fractal dimension of 2.75 suggests tightly aggregated particles, which is consistent with observations by scanning electron microscope (SEM, Fig. 2-11). Thus, the PDM modified to consider adsorbent aggregation by incorporating fractal theory successfully described the adsorption kinetics of SPACs with different degrees of aggregation.

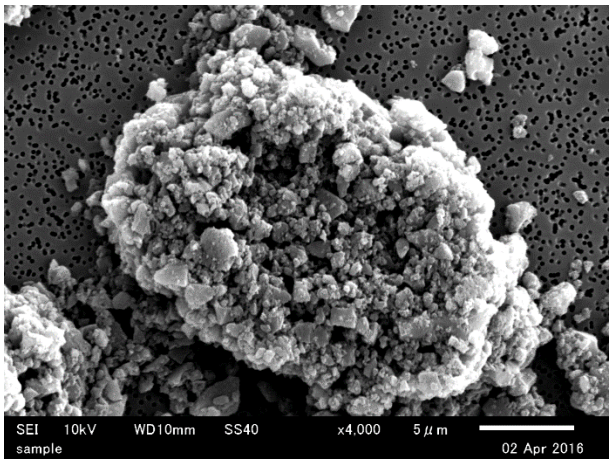

Fig. 2-11. Scanning electron microscope photo of SPAC-S-D

II. Effects of adsorbent aggregation and adsorption capacity

To quantify separately the impacts of adsorbent aggregation and adsorption capacity on adsorption kinetics, we conducted a series of four model simulations (cases I–IV). As the point of departure, we used the case of MIB removal by the dry-milled carbon, SPAC-S-D, which had a low adsorption capacity and a large apparent carbon particle size owing to severe aggregation, compared with that of the wet-milled carbon SPAC-S-W. Model simulations were conducted in which the apparent particle size of SPAC-S-D (case I, median diameter, 14.2 μm) was replaced with smaller sizes (case II, median diameter,

2.42 μm; case III, median diameter, 1.24 μm) to see how a particle size reduction due to disaggregation would enhance MIB removal. In addition, a simulation was conducted by replacing the SPAC-S-D isotherm with that of SPAC-S-W, which had a higher adsorption capacity (case IV). The particle size distribution of case II was based on the apparent size distribution of SPAC-S-DS (ultrasonicated carbon), and the distribution of case III was based on the apparent size distribution measured after both the addition of dispersant and ultrasonication (completely dispersed carbon). We then compared the simulated MIB removal rates among the cases (Fig. 2-12). Compared with case I, MIB removal was improved in case II, and further improved in case III, and these improvements were obtained within a short contact time. However, by about 30 min of contact time, the MIB removal curves of cases II and III merged. Therefore, even if the carbon particles are aggregated so that the apparent particle size is twice the true particle size, the effect of that aggregation on MIB removal is small after a contact time of 10 min or longer.

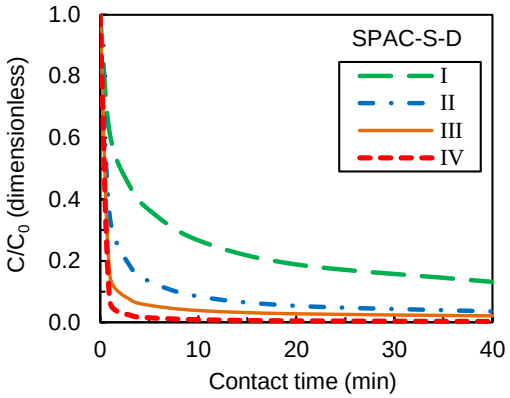

	Aggregation degree	Median diameter (μm)	Adsorption isotherm
I	Original aggregation	14.24	SPAC-S-D
II	After ultrasonication	2.42	
III	Complete dispersion	1.24	
IV	Complete dispersion	1.24	SPAC-S-W

Fig. 2-12. Model simulations of four cases of MIB removal by SPAC-S-D (MIB initial concentration, 1 μg/L; carbon dosage, 3 mg/L).

Moreover, only a small effect of particle aggregation was seen in wet-milled carbon, SPAC-S-W, when moderately aggregated carbon particles (case V, apparent particle size 3 times that of case VI, the true size). The MIB removal of these two cases became similar after 30 min of carbon–water contact (Fig. 2-13). Therefore, when SPAC is used for water treatment, its particle size should be measured, and its degree of aggregation should be determined. If, for example, the SPAC particles are aggregated such that the aggregate size is much more than twice the true particle size, disaggregation, for example by ultrasonication, should be considered as an easy way to improve the adsorptive removal performance.

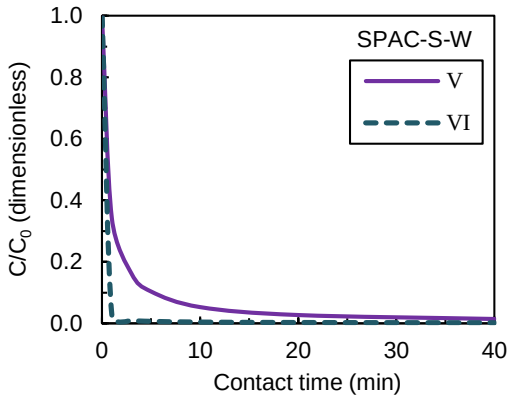

	Aggregation degree	Median diameter (μm)	Adsorption isotherm
V	Original aggregation	3.80	SPAC-S-W
VI	Complete dispersion	1.28	

Fig. 2-13. Simulated MIB removal by SPAC-S-W (MIB initial concentration, 1 μg/L; carbon dosage, 3 mg/L)**.**

In addition to carbon particle aggregation, the dry-milled SPAC (SPAC-S-D) had the disadvantage of low adsorption capacity. When the SPAC-S-D isotherm was replaced with the SPAC-S-W isotherm (case IV), MIB removal was further improved (Fig. 2-12). The improvement resulting from the increased adsorption capacity achieved by changing the isotherm was moderate compared with that achieved by disaggregation. However, the gap between the case III and case IV curves was almost constant, regardless of the contact time. Thus, an increase in adsorption capacity is necessary to improve MIB removal for carbon–water contact times longer than about 20 min.

2.4.5 Stability after disaggregation

As discussed in part *II* of section 2.4.4, for more efficient MIB removal, the disaggregation of SPAC particles, for example by ultrasonication, is recommended. To investigate the effectiveness of disaggregation, we conducted an experiment to see how long a time the dispersed state of the ultrasonicated SPAC would be maintained and whether re-aggregation would occur after disaggregation by ultrasonication. The stocks of wet-milled and dry-milled SPAC were stored in a slurry after ultrasonication, and samples were withdrawn at intervals and their apparent size distributions were measured to determine whether the median diameters (D_{50}) of the ultrasonicated SPACs changed with storage time after ultrasonication (Fig. 2-14). The results showed little change in D_{50} after storage for up to 20 days; thus, the ultrasonicated SPACs maintained their initial dispersed state for at least that long. These results indicate that the aggregations of dry-milled and wet-milled SPAC is a temporary state that can be reversed by ultrasonication.

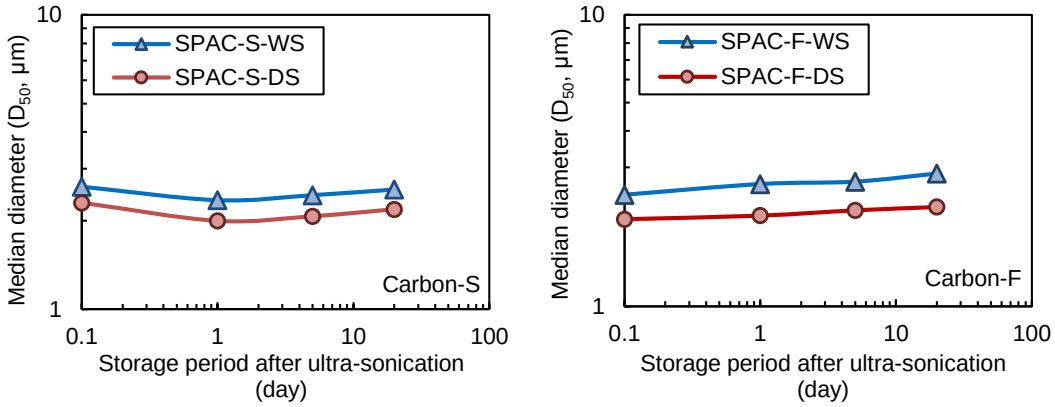

Fig. 2-14. Median diameters of SPAC samples taken from the stock slurries after storage for various periods.

Table 2-4 Effect of ultrasonication on SPAC size

Designation	Original carbon	True diameter (μm)	Apparent diameter (μm)		D_{50a}/D_{50t}
			Before ultrasonication	After ultrasonication	
		D_{50t}	D_{50b}	D_{50a}	
SPAC-S-D	PAC-S	1.24	14.2	2.42	1.95
SPAC-S-W		1.28	3.80	2.61	2.04
SPAC-F-D	PAC-F	1.22	10.3	1.99	1.63
SPAC-F-W		1.21	3.42	2.41	2.00

In addition, ultrasonication was more effective toward dry-milled SPACs than wet-milled SPACs, because after ultrasonication the apparent size of the dry-milled SPAC (SPAC-F-DS) was smaller than that of the wet-milled SPAC (SPAC-F-WS) (Table 2-4), even though (1) the true size distribution of the dry-milled SPAC was similar to that of the wet-milled SPAC and (2) the apparent size of the dry-milled SPAC was larger before ultrasonication. Therefore, the dry-milled SPAC may be more amenable to dispersion by ultrasonication, and its size may become closer to the true size after ultrasonication. The ratio of the median apparent diameter after ultrasonication to true diameter (D_{50a}/D_{50t}; Table 2-4) was smaller for SPAC-F-D than for SPAC-F-W, and D_{50a}/D_{50t} was slightly smaller for SPAC-S-D than for SPAC-S-W.

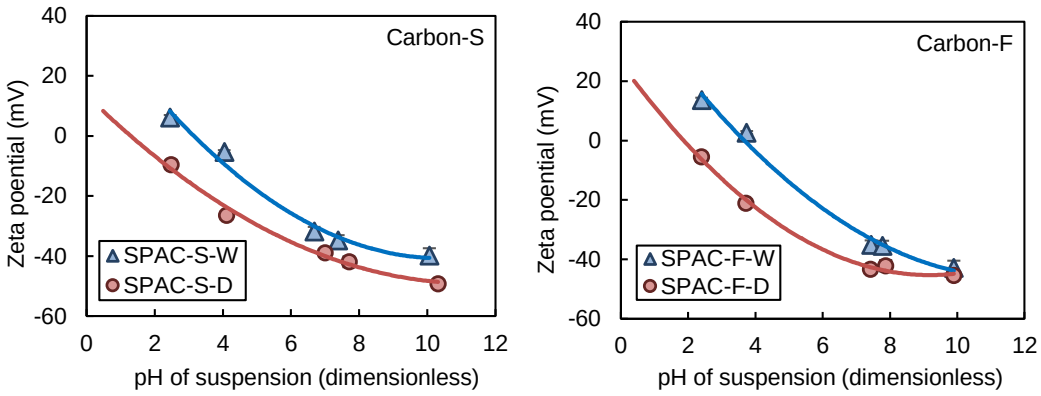

Fig. 2-15. Zeta potential of SPACs in relation to pH

Fig. 2-15 shows that the values of the zeta potential, and thus the relative charge, of the dry-milled SPACs were lower than those of the wet-milled SPACs in suspensions with a wide range of pH values. More negative charge of dry-milled SPACs than of the wet-milled SPACs is in accordance with the result of the higher oxygen content, which suggests that the dry-milled SPACs have more oxygen-containing functional groups, producing negative charge. Thus, there may be stronger repulsion between dry-milled SPAC than between wet-milled SPAC particles, with the result that the dry-milled SPAC particles are more easily dispersed by ultrasonication. The higher degree of aggregation for the dry-milled SPAC compared with the wet-milled SPAC when it was initially produced might be related to the production condition. Moisture in the air as the carrier of the particles might induced aggregation of dry-milled SPACs by the liquid bridge force. Also inter-particle forces such as van der Waals' force might also act as a bridge force. The aggregation of dry-milled SPACs would be held if external dispersion forces such as ultrasonication was not introduced.

2.5 Chapter conclusions

(1). Dry-milled SPAC removes MIB at a lower rate than wet-milled SPAC. There are two reasons for this: compared with wet-milled SPAC, (i) dry-milled SPAC is more severely aggregated and (ii) its adsorption capacity is lower.

(2). Wet-milled SPAC is only moderately aggregated, so the effect of the aggregation on its adsorptive removal of MIB is small. Dry-milled SPAC is severely aggregated, and this aggregation lowers its adsorptive removal of MIB, in particular when the carbon–water contact time is short (< 20 min).

(3). Dry-milled SPAC is more easily disaggregated by ultrasonication than wet-milled SPAC, although it aggregates more severely after production. The high disaggregation tendency of dry-milled SPAC is due to the high negative surface charge of the carbon particles. SPACs do not become re-aggregated once after they are disaggregated.

(4). The low adsorption capacity of dry-milled SPAC compared with wet-milled SPAC would be due to the oxidation during milling.

(5). The pore diffusion model modified to consider adsorbent aggregation by incorporating fractal theory could successfully describe the adsorption kinetics of SPACs with different degrees of aggregation with a single set of parameter values.

2.6 Reference

Ando, N., Matsui, Y., Kurotobi, R., Nakano, Y., Matsushita, T. and Ohno, K., 2010. Comparison of natural organic matter adsorption capacities of super-powdered activated carbon and powdered activated carbon. Water research 44(14), 4127-4136.

Ando, N., Matsui, Y., Matsushita, T. and Ohno, K., 2011. Direct observation of solid-phase adsorbate concentration profile in powdered activated carbon particle to elucidate mechanism of high adsorption capacity on super-powdered activated carbon. Water research 45(2), 761-767.

Avnir, D., Farin, D. and Pfeifer, P., 1984. Molecular fractal surfaces. Nature 308(5956), 261-263.

Baalousha, M., 2009. Aggregation and disaggregation of iron oxide nanoparticles: Influence of particle concentration, pH and natural organic matter. Science of The Total Environment 407(6), 2093-2101.

Bonvin, F., Jost, L., Randin, L., Bonvin, E. and Kohn, T., 2016. Super-fine powdered activated carbon (SPAC) for efficient removal of micropollutants from wastewater treatment plant effluent. Water Research 90, 90-99.

Christian, P., Kammer, F., Baalousha, M. and Hofmann, T., 2008. Nanoparticles: structure, properties, preparation and behaviour in environmental media. Ecotoxicology 17(5), 326-343.

Dunn, S.E. and Knappe, D.R.U., 2013. DBP precursor and micropollutant removal by powdered activated carbon, Water Research Foundation, Denver, CO, USA.

Elimelech, M., Gregory, J., Jia, X. and Richard, A.W., 2013. Particle deposition and aggregation: measurement, modelling and simulation, Butterworth-Heinemann.

Ellerie, J.R., Apul, O.G., Karanfil, T. and Ladner, D.A., 2013. Comparing graphene, carbon nanotubes, and superfine powdered activated carbon as adsorptive coating materials for microfiltration membranes. Journal of Hazardous Materials 261, 91-98.

Jung, H.J., Sohn, Y., Sung, H.G., Hyun, H.S. and Shin, W.G., 2015. Physicochemical properties of ball milled boron particles: Dry vs. wet ball milling process. Powder Technology 269, 548-553.

Knieke, C., Steinborn, C., Romeis, S., Peukert, W., Breitung‐Faes, S. and Kwade, A., 2010. Nanoparticle Production with Stirred‐Media Mills: opportunities and Limits. Chemical Engineering & Technology 33(9), 1401-1411.

Li, L., Quinlivan, P.A. and Knappe, D.R.U., 2002. Effects of activated carbon surface chemistry and pore structure on the adsorption of organic contaminants from aqueous solution. Carbon 40(12), 2085-2100.

Logan, B.E., 1999. Environmental transport processes, John Wiley & Sons, Inc., Canada.

Lyman, W.J., Reehl, W.F. and Rosenblatt, D.H., 1990. Handbook of chemical property estimation methods: environmental behavior of organic compounds, American Chemical Society.

Matsui, Y., Ando, N., Sasaki, H., Matsushita, T. and Ohno, K., 2009. Branched pore kinetic model analysis of geosmin adsorption on super-powdered activated carbon. Water Research 43(12), 3095-3103.

Matsui, Y., Ando, N., Yoshida, T., Kurotobi, R., Matsushita, T. and Ohno, K., 2011. Modeling high adsorption capacity and kinetics of organic macromolecules on super-powdered activated carbon. Water research 45(4), 1720-1728.

Matsui, Y., Nakao, S., Sakamoto, A., Taniguchi, T., Pan, L., Matsushita, T. and Shirasaki, N., 2015. Adsorption capacities of activated carbons for geosmin and 2-methylisoborneol vary with activated carbon particle size: Effects of adsorbent and adsorbate characteristics. Water Research 85, 95-102.

Matsui, Y., Nakao, S., Taniguchi, T. and Matsushita, T., 2013a. Geosmin and 2-methylisoborneol removal using superfine powdered activated carbon: Shell adsorption and branched-pore kinetic model analysis and optimal particle size. Water research 47(8), 2873-2880.

Matsui, Y., Nakao, S., Yoshida, T., Taniguchi, T. and Matsushita, T., 2013b. Natural organic matter that penetrates or does not penetrate activated carbon and competes or does not compete with geosmin. Separation And Purification Technology 113, 75-82.

Matsui, Y., Sakamoto, A., Nakao, S., Taniguchi, T., Matsushita, T., Shirasaki, N., Sakamoto, N. and Yurimoto, H., 2014. Isotope Microscopy Visualization of the Adsorption Profile of 2-Methylisoborneol and Geosmin in Powdered Activated Carbon. Environmental Science & Technology 48(18), 10897-10903.

Matsui, Y., Yoshida, T., Nakao, S., Knappe, D.R.U. and Matsushita, T., 2012. Characteristics of competitive adsorption between 2-methylisoborneol and natural organic matter on superfine and conventionally sized powdered activated carbons. Water Research 46(15), 4741-4749.

Partlan, E., Davis, K., Ren, Y., Apul, O.G., Mefford, O.T., Karanfil, T. and Ladner, D.A., 2016. Effect of bead milling on chemical and physical characteristics of activated carbons pulverized to superfine sizes. Water Research 89, 161-170.

Phenrat, T., Saleh, N., Sirk, K., Tilton, R.D. and Lowry, G.V., 2007. Aggregation and Sedimentation of Aqueous Nanoscale Zerovalent Iron Dispersions. Environmental Science & Technology 41(1), 284-290.

Quinlivan, P.A., Li, L. and Knappe, D.R.U., 2005. Effects of activated carbon characteristics on the simultaneous adsorption of aqueous organic micropollutants and natural organic matter. Water Research 39(8), 1663-1673.

Ramos, A.S., Taguchi, S.P., Ramos, E.C.T., Arantes, V.L. and Ribeiro, S., 2006. High-energy ball milling of powder B–C mixtures. Materials Science and Engineering: A 422(1–2), 184-188.

Schmidt, J., Plata, M., Tröger, S. and Peukert, W., 2012. Production of polymer particles below 5 μm by wet grinding. Powder Technology 228, 84-90.

Sontheimer, H., Crittenden, J.C., Summers, R.S., Hubele, C., Roberts, C. and Snoeyink, V.L., 1988. Activated carbon for water treatment, Universitaet Karlsruhe, Karlsruhe.

Suryanarayana, C., 2001. Mechanical alloying and milling. Progress in Materials Science 46(1–2), 1-184.

Yokoyama, T. and Huang, C.C., 2005. Nanoparticle Technology for the Production of Functional Materials. KONA Powder and Particle Journal 23, 7-17.

(This page is set to be blank.)

Chapter 3. Change of Equilibrium Adsorption Capacity with Decreasing Activated Carbon Particle Diameter from 30 μm to 140 nm

3.1 Chapter introduction

Superfine powdered activated carbon (SPAC), which is produced from normal powdered activated carbon (PAC) by micro-milling, offers a new treatment option to efficiently remove natural organic materials, disinfection byproduct precursors, organic micro pollutants, and taste & odor compounds (Bonvin et al., 2016; Dunn et al., 2013; Heijman et al., 2009; Matsui et al., 2007; Matsui et al., 2004; Matsui et al., 2005; Wang et al., 2011).

Compared with the parent PAC with larger particle size, many merits are presented for SPAC such as higher adsorption capacity (Ando et al., 2010; Ando et al., 2011; Bonvin et al., 2016; Matsui et al., 2010), rapider adsorption kinetics (Dudley, 2012; Matsui et al., 2009a; Matsui et al., 2011; Wang et al., 2011), and ability to attenuate transmembrane pressure buildup when SPAC is injected before microfiltration (Ellerie et al., 2013; Li, 2014; Matsui et al., 2007; Matsui et al., 2009b). Among these merits, the higher adsorption capacity of SPAC than that of PAC scientifically as well as practically attracts attentions because it had been implicitly believed that the adsorption occur in internal pores of activated carbon particles and the equilibrium adsorption capacity is unchanged independent from carbon particle size (Letterman et al., 1974; Najm et al., 1990; Peel et al., 1980).

The higher adsorption capacity of SPAC than that of PAC is explained by the shell adsorption model (SAM) in which the adsorbates are principally adsorbed in the exterior (shell) region of carbon particles due to the limited diffusive penetration depth (Ando et al., 2011; Matsui et al., 2011; Matsui et al., 2013; Matsui et al., 2014). Therefore, by micro-milling, the carbon particle size becomes smaller, which leads to increase exterior region thus enhancing the adsorption capacity, as far as the carbon particle radius is larger than the limited penetration depth. The penetration depth varies with target adsorbates and ACs. For example, the penetration depth of 2-methylisoborneol (MIB), one of the conventional target taste & odor compounds that should be treated in water treatments, is around a few micron meters (Matsui et al., 2015; Matsui et al., 2014). In this case, SPAC with the particles radius of 0.5-1 μm has higher MIB adsorption capacity than PAC with the particles radius of 5-10 μm.

On the other hand, SAM suggests that the adsorption capacity, if the penetration depth is a few micron meters, may not be increased with decreasing AC radius from a few μm to submicron meter or less. However, the change of the adsorption capacity and carbon characteristics in this particle size range have not been fully investigated. The newest nano-technology of micro-grinding (wet-milling) enables production of particles with median diameter (D_{50}) of the submicron ranging up to hundreds nm or even smaller (Mende et al., 2003; 2004), for example, corundum (α-Al_2O_3) (Stenger et al., 2005); aluminum nitride (Jia et al., 2015; Qiu et al., 2006), $Li_4Ti_5O_{12}$ (Han et al., 2012); Barium sulfate ($BaSO_4$) (Patel et al., 2014); Silica (SiO_2) (Patel et al., 2015); and crystalline organic model compound pyrene (Flach et al., 2016, in press). For activated carbon (AC), our research group (Pan et al., 2015) and other research

groups have successfully (Amaral et al., 2016; Partlan et al., 2016) produced carbon particles with submicron D_{50} (200 nm ~ 150 nm).

Several full-scale SPAC-microfiltration plants are also already designed and implemented for drinking water production (Kanaya et al., 2015). SPACs are produced onsites in treatment plants and added prior to membrane filtrations. However, these plants only apply for the SPAC of D_{50} from 1 to 2 μm. The success of carbon adsorbent with smaller particle size, such as 150 nm diameter, might further enhance the adsorptive removal efficiency.

In this paper, the AC particles with the dimaters from 30 μm to 140 nm were produced, and plenty of adsorption experiments have been conducted to see and discuss the changes the adsorption capacities and adsorbate chracteristics in these particle sizes.

3.2 Objectives and approaches

The objective is to investigate the MIB adsorption capacity change of AC when carbon size is reduced from SPAC to SSPAC and the reasons related to the change. What's more, we also want to know whether the trends of MIB adsorption capacity change from SPAC to SSPAC are similar with or different from that of other adsorbates.

The approaches of the research in this chapter are 1) test the MIB adsorption capacity of PAC, SPAC, and SSPAC which are produced from the same PAC; 2) detect the chemical properties of all the samples to summary the apparent property change; 3) check the relativities between the MIB adsorption capacity and the modified properties found in 2); test the adsorption capacities of various environmental related compounds which have different physiochemical properties.

3.3 Experimental

3.3.1 Activated carbons (adsorbents)

Five commercially-available wood-based PACs (Table 3-1) were obtained and milled to SPACs and submicron-sized SPACs (SSPACs) separately. These PACs, SPACs and SSPACs were given unique three-term designations as follows. The first term indicates the particle size category of the carbon: PAC (12.0 – 28.0 μm), SPACa (3.80 – 8.10 μm), SPACb (0.83 – 1.64 μm), and SSPAC (0.14 -0.24 μm). The second term indicates the parent PAC. The third term in the name of SPAC and SSPAC indicates production method: "N" indicates "normal milling", "OI" indicates "oxygen-inhibitory milling", and "R" indicates "rinsing with pure water" (see the section 3.2.2 and Tables 3-2 and 3-3). When multiple samples were produced by the same condition in different batches, they are distinguished and given a number in the fourth term. For example, SSPAC-C-N-2 is a SSPAC produced from PAC-N under the normal condition in the second batch.

Table 3-1. Information of obtained PACs

Designation	Series	Brand name	Production	Raw material	Producer
PAC-A-N	Carbon-A	Taiko W	2008	wood	Futamura Chemical Co., Tokyo, Japan
PAC-B-N	Carbon-B	Taiko W	2015		
PAC-C-N	Carbon-C	Taiko W	2016		
PAC-D-N	Carbon-D	Shirasagi	2016		Shirasagi, Osaka Chemical Co., Osaka, Japan
PAC-E-N	Carbon-E	6MD	2016	coal	Calgon Carbon Japan KK

3.3.2 Production of SPAC and SSPAC

The production of SPACa was conducted by a ball-mill (a closed chamber; Nikkato Ltd., Osaka, Japan) with balls of two sizes (5 and 10 mm diameter). The production of SPACb and SSPAC was conducted by a beads-mill (a circulation milling system; LMZ015, Ashizawa Finetech Ltd., Chiba, Japan) with ZrO_2 beads (0.3 mm or 0.1 mm diameter). Other procedures are described below.

(1) Normal milling

As-received PACs were added into pure water (Milli-Q Advantage; Millipore Co., Bedford, MA, USA) to get PAC slurries with concentration about 15 % (w/w) (e.g., designated as PAC-A-N) and then was milled by the ball mill under 45 rpm for 4 to 5 hours to become particles with D_{50} around 4 μm (e.g., designated as SPACa-A-N). After collecting the slurry with pure water from a pot of ball mill, the slurry was diluted to around 1 % (w/w).

The diluted carbon slurries of 400-mL were then milled by the beads mill with 0.3-mm beads under 2,590-rpm rotational speed in the circulation mode for 20 to 30 min to become smaller particle whose D_{50} is < 1.5 μm but > 0.5 μm (e.g., designated as SPACb-A-N). Carbon particles with D_{50} of around 200 nm was produced from the SPACa or SPACb by the beads mill with 0.1-mm beads under 3,884-rpm rotational speed in the circulation mode for 1.5 to 2 hours.

Table 3-2 Designation of normal PAC/SPAC/SSPAC

Designation	Median diameter D_{50} (μm)	Mill	Source carbon	Median diameter D_{50} (μm)
SPACa-A-N	no measured	Ball mill	PAC-A-N	12.0
SPACb-A-N	1.47	Bead mill	SPACa-A-N	no measured
SPACc-A-N	0.528		SPACb-A-N	1.47
SSPAC-A-N	0.198		SPACb-A-N	1.47
SPACa-B-N	3.85	Ball mill	PAC-B-N	27.5
SPACb-B-N	1.21	Bead mill	SPACa-B-N	3.85
SSPAC-B-N	0.194		SPACb-B-N	1.21
SPACa-C-N-1	no measured	Ball mill	PAC-C-N	23.1
SPACa-C-N-2	4.00			
SPACa-C-N-3	3.87			
SPACa-C-N-4	4.04			
SPACa-C-N-5	3.79			
SPACb-C-N-1	1.12	Bead mill	SPACa-C-N-1	no measured
SPACb-C-N-2	0.949		SPACa-C-N-2	4.00
SPACb-C-N-3	1.64		SPACa-C-N-3	3.87
SPACb-C-N-4	1.30		SPACa-C-N-4	4.04
SPACb-C-N-5	no measured		SPACa-C-N-5	3.79
SPACb-C-N-6	1.45		SPACa-C-N-6	4.44
SSPAC-C-N-1	0.176		SPACa-C-N-1	no measured
SSPAC-C-N-2	0.137		SPACa-C-N-2	4.00
SSPAC-C-N-3	0.179		SPACa-C-N-3	3.87
SSPAC-C-N-4	0.177		SPACa-C-N-4	4.04
SSPAC-C-N-5	0.177		SPACa-C-N-5	3.79
SPACa-D-N-1	3.03	Ball mill	PAC-D-N	15.5
SPACa-D-N-2	3.57			
SPACb-D-N-1	0.927	Bead mill	SPACa-D-N-1	3.03
SPACb-D-N-2	0.915		SPACa-D-N-1	3.57
SSPAC-D-N-1	0.169		SPACa-D-N-1	3.03
SSPAC-D-N-2	0.164		SPACa-D-N-1	3.57
SPACa-E-N	3.90	Ball mill	PAC-E-N	19.5
SPACb-E-N	1.19	Bead mill	SPACa-E-N	3.90
SSPAC-E-N	0.177		SPACa-E-N	3.90

(2) Oxidation-inhibitory milling

As-received PACs were placed in a chamber under vacuum condition for 1 hour or longer time to become dry powdered forms, and then were returned to normal atmospheric pressure by filling the chamber with nitrogen (N_2) gas. Then the PACs were rinsed with pure water 3 times in the chamber containing only N2 gas (the PAC obtained was designated as, e.g., PAC-A-R).

The rinsed PAC slurries were adjusted for about 15 % (w/w) concentration. Then each slurry was transferred to a ball mill which was previously filled with N_2 gas, and the milling was conducted. The other milling conditions were same as those of the normal milling. Due to the difficulty of collecting the carbon slurry under N_2 atmosphere after the milling, the collection was conducted under the normal air condition as quickly as possible. The collected carbon slurry was adjusted for 1 % (w/w) concentration with pure water and then purged with N_2 gas for more than 1 hour to reduce the dissolving oxygen concentration < 1 mg/L. The products are designated with "OI" in the third term, e.g., SPACa-A-OI.

The beads milling was conducted under slow milling speed (2590 rpm) while carbon slurry was purged with N_2 gas during the milling (Fig. 3-1). Except that both 0.1-mm beads and 0.3-mm beads were used respectively for milling, other milling conditions were the same as those of the normal milling. After the milling, the carbon slurry was kept under vacuum condition for longer than 1 hour and then filled with N_2 gas to return to normal atmospheric pressure condition. The products are designated with "OI" in the third term, e.g., SPACb-A-OI.

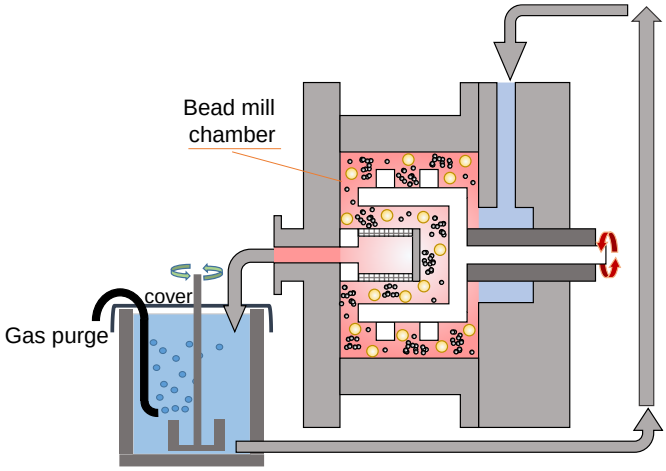

Fig. 3-1. Schematic diagram of gas purge with bead mill.

Table 3-3 Designation of PAC, SPAC, and SSPAC produced by special attempt

Designation	Median diameter D_{50} (μm)	Milling system	Detail Production method			Source carbon
			Rotational speed (rpm)	Bead/ball diameter (mm)	Slurry volume (mL)	
PAC-B-R	21.7	no				PAC-B-N
SPACa-B-OI	no measured	Ball mill – N_2 filled	45	5 & 10	100	PAC-B-R
SPACb-B-OI	0.794	Bead mill – N_2 purge	2590	0.3	400 - 500	SPACa-B-R
SSPAC-B-OI	0.23			0.1		SPACa-B-R
PAC-C-R	22.7	no				PAC-C-N
SPACa-C-OI-1	no measured	Ball mill – N_2 filled	45	5 & 10	100	PAC-C-R
SPACa-C-OI-2	5.15					
SPACa-C-OI-3	3.82					
SPACa-C-OI-4	3.88					
SPACa-C-OI-5	8.11					
SPACa-C-OI-6	2.78					
SPACb-C-OI-1	1.13	Bead mill – N_2 purge	2590	0.3	400 - 500	SPACa-C-OI-1
SPACb-C-OI-2	0.831					SPACa-C-OI-2
SSPAC-C-OI-3	0.213			0.1		SPACa-C-OI-3
SSPAC-C-OI-4	0.200			0.3		SPACa-C-OI-4
SSPAC-C-OI-5	0.229					SPACa-C-OI-5
SSPAC-C-OI-6	0.174			0.1		SPACa-C-OI-6
PAC-D-R	15.3	no				PAC-D-N
SPACa-D-OI-1	3.87	Ball mill – N_2 filled	45	5 & 10	100	PAC-D-R
SPACa-D-OI-2	2.65					
SPACa-D-OI-3	3.21					
SSPAC-D-OI-2	0.197	Bead mill – N_2 purge	2590	0.1	400 - 500	SPACa-D-OI-2
SSPAC-D-OI-3	0.197					SPACa-D-OI-3

The beads milling to produce SSPAC was conducted while carbon slurry was purged with N_2 gas during the milling. Rotational speed of the milling were 2,590 or 3,884 rpm. Beads were of 0.1 or 0.3 mm diameter. The volume of carbon slurry milled was 400 or 800 mL. The milling time was varied in order to get the particles with D_{50} of around 200 nm, but it was from 2 to 6 hours. The products are designated with “OI” in the third term, e.g., SSPAC-A-OI.

All the ACs were stored in a slurry at 4 °C after vacuum conditioning to remove any air from the activated carbon pores.

3.3.3 Characterizations of carbons

Particle size distributions of all ACs were determined by using a laser-light scattering instrument (Microtrac MT3300EXII, Nikkiso Co., Tokyo, Japan). The samples were taken from the stock slurries and then pretreated by the addition of a dispersant (Triton X-100, Kanto Chemical Co., Tokyo, Japan; final concentration, 0.08% w/v) and ultrasonic (150 W, 19.5 kHz, 4 min for 50 mL carbon slurry) dispersion before measurement with the Microtrac.

Field emission scanning electron microscope (FE-SEM; JSM-7400F, JEOL Ltd., Tokyo, JAPAN) was used to observe the particles of SSPAC at accelerating voltage 5.0 kV and working distance 3.0 mm. There was no coating pretreatment because the thickness of coating layer might restrain the accurate observation. The observation was not conducted for SPACa, SPACb, and PAC because these were already observed and the particles sizes were confirmed (Ando et al., 2010).

Elemental analyses were performed on ACs with regard to oxygen, carbon, nitrogen, hydrogen, sulfur and ash by an elemental analyzer (Vario EL Cube, Elementar Japan K.K., Yokohama, Japan) with thermal conductivity and infra-red detectors. The ACs in the slurry form were dried by a vacuum cooling method, which would avoid any oxidation of the AC samples during the drying. Before elemental analysis, the dried samples were stored at a store box under vacuum condition. After N_2 gas was introduced to the store box to reach normal atmospheric pressure, the samples were taken out and transferred to the elemental analyzer promptly. The oxygen content was measured with the O mode of operation while the other elements were with the CHNS mode. Triplicate measurements were conducted for each AC to get the average with error bars.

3.3.4 Adsorbates and working solution

MIB was the main target compound in this study. The concentrations of MIB were detected by either of two systems. In one sysytem, MIB (*m/z* 95 peak) was detected by a purge and trap concentrator (P&T) (Aqua PT 5000 J, GL Sciences, Inc., Tokyo, Japan) coupled to a gas chromatograph-mass spectrometer (GC/MS) (GCMS-QP2010 Plus, Shimadzu Co., Kyoto, Japan) using deuterium-labeled geosmin (geosmin-d3, *m/z* 115 peak) as an internal standard. In the other system, MIB (*m/z* 108 peak) was detected by a headspace solid-phase microextraction (SPME) (PAL RSI 85, Agilent Technologies, Inc., CA, USA) coupled to a GCMS (7820A/5977 E MSD, Agilent Technologies, Inc., CA, USA) using deuterium-labeled 2,4,6-trichloroanisole (TCA-d3, *m/z* 195 peak) as an internal standard.

In addition to MIB, 8 adsorbates were used supplementary: these were geosmin, salicylic acid, phenol, benzothiazole, methidathion-oxon (DMTP-oxon), 4-nitrophenol (PNP), poly (styrenesulfonic acid) sodium salt with average molecular weight (MW) 210 (hereafter PSS-210), PSS-1100 with average MW 1100 and the Suwannee River natural organic matter (SNOM). These compounds were selected for environmental relevancy and/or to cover a variety of hydrophobicity and molecule size dimensions. The concentrations of geosmin were detected by the similar method as MIB, where the *m/z* 112 peak was interpreted as corresponding to geosmin. DMPT-oxon was quantified as by using a hybrid quadrupole-

orbitrap mass spectrometer (Q Exactive, Thermo Fisher Scientific Inc., Waltham, MA, USA) coupled with liquid chromatography (UltiMate3000 LC systems, Thermo Fischer Scientific Inc.) using mepronil as an internal standard. The concentrations of other adsorbates were measured by spectrophotometry (UV-1800, Shimadzu Co., Kyoto, Japan): phenol at 269.5 nm; benzothiazole at 252 nm; salicylic acid at 296 nm; PNP at 317 nm; PSS-210 and PSS-6400 at 261 nm.

Except PSS-210 and PSS-6400 which were purchased from Sigma-Aldrich Co. LLC. (St. Louis, Missouri, USA), the all mentioned chemical reagents were all purchased from Wako Pure Chemical Industries, Ltd., (Osaka, Japan). The working solution in this study is organic-free water containing ion composition same as previous researches (Table 3-4) (Matsui et al., 2015; Pan et al., 2016).

Table 3-4 Ion composition of working solution

Ion	Na^+	K^+	Mg^{2+}	Ca^{2+}	Cl^-	NO^{3-}	SO_4^{2-}	Alkalinity
Concentration (mg/L)	19	3.1	24	18	31	6.9	14	50

3.3.5 Batch adsorption tests

In the adsorption equilibrium tests, aliquots (100 or 110 mL) of the working solutions containing target adsorbates were transferred to 110-mL vials. Specified amounts of PAC, SPAC or SSPAC were immediately added, and the vials were manually shaken and then agitated on a mechanical shaker for 1 week or 3 days at a constant temperature of 20 °C in the dark. Preliminary experiments confirmed that the adsorption equilibrium was reached within 1 week of contact for MIB-PAC (Matsui et al., 2013; Matsui et al., 2012), within 3 days for MIB-SPAC/SSPAC, and within 1 week for the other 8 compounds. Control tests of soultions that did not contain carbon (i.e., blanks) were also conducted to confirm that changes in the concentration of blank adsorbates during long-term mixing were negligible. After certain periods of shaking, the water samples were filtered through 0.2-μm pore size membrane filters, and then concentrations of adsorbates in the aqueous phase were measured. Solid-phase concentrations of adsorbates were calculated from the mass balance.

3.4 Results and discussion

3.4.1 SSPAC production by normal micro-milling

Based on the method described in of section 3.3.2, SSPACs with D_{50} in the range from 140 nm to 240 nm were successfully produced by micro-milling the SPACs which were produced from PACs. The success of SSPAC production with good reproducibility was verified by both the particle size distribution detected by laser-light scattering (Fig. 3-2) and the direct observation under FE-SEM (Fig. 3-3). The information of the carbons produced by the normal milling were listed in Table 3-2.

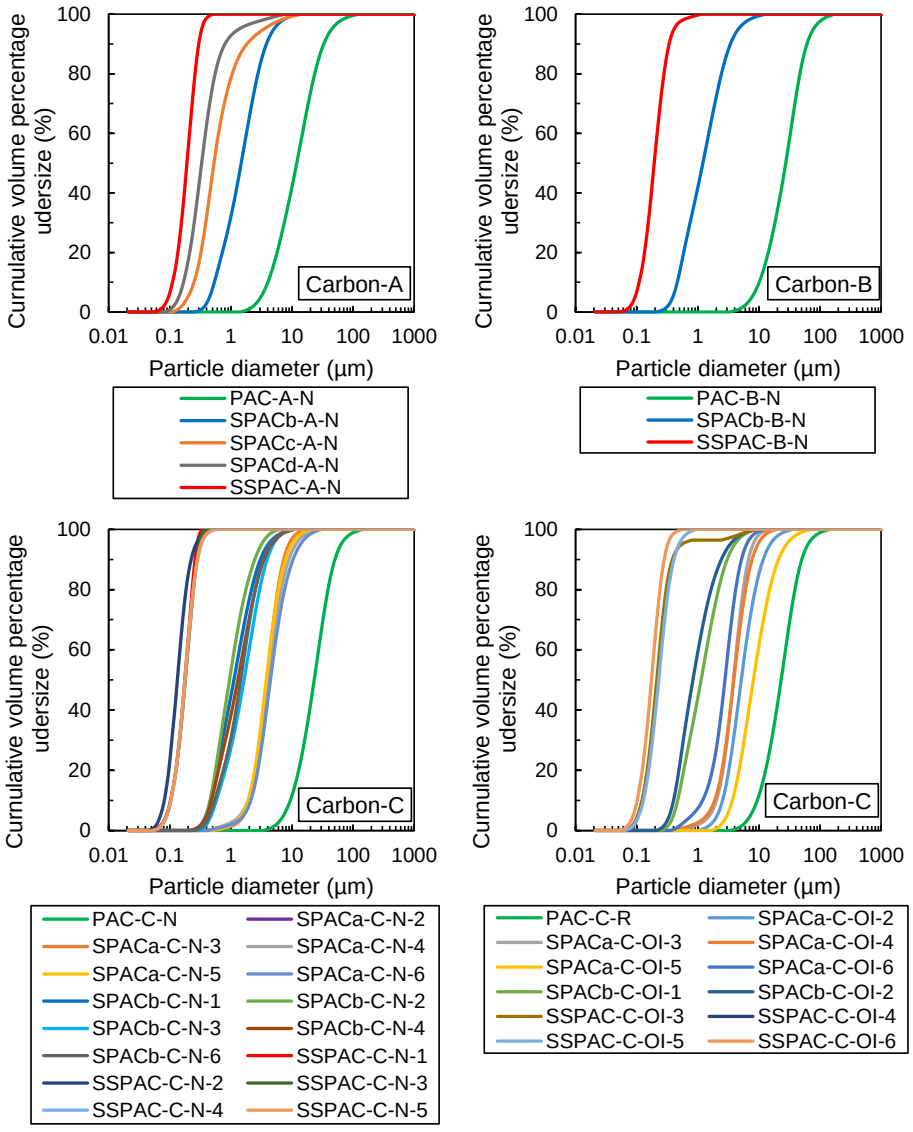

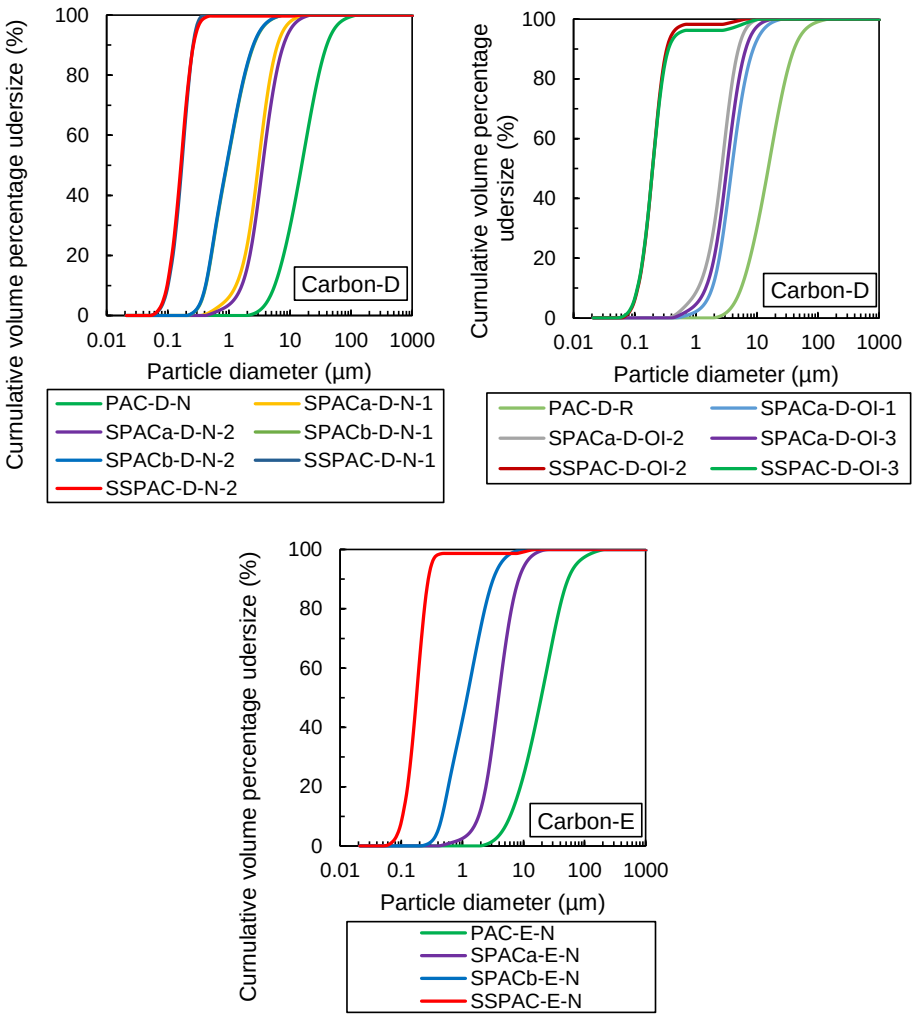

Fig. 3-2. Particle size distributions of PAC, SPAC and SSPAC.

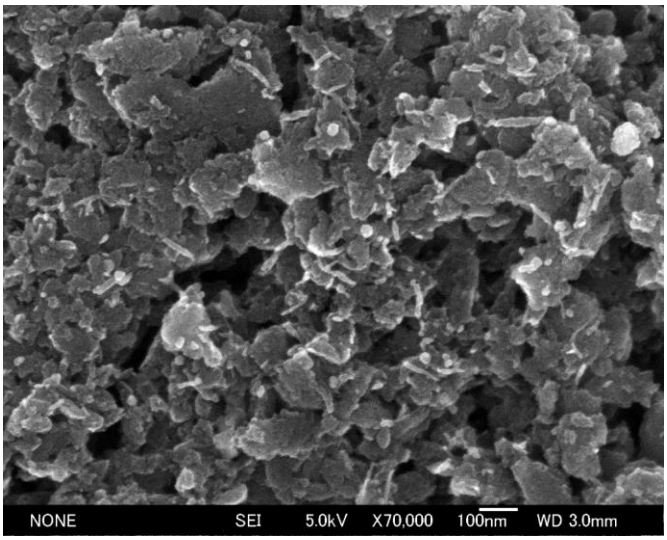

Fig. 3-3. SEM photo of SSPAC-B-N.

3.4.2 Carbon particle size effect on adsorption capacity of MIB.

Carbon-A series with D_{50} varying from 12 μm to 0.20 μm were tested for their MIB adsorption, and the adsorption isotherms under equilibrium were obtained (Fig. 3-4a). Similarly, the adsorption isotherms of the other 4 carbon series (Carbon-B, Carbon-C, Carbon-D and Carbon-E) under equilibrium were obtained (Fig. 3-4b, c, d, and e).

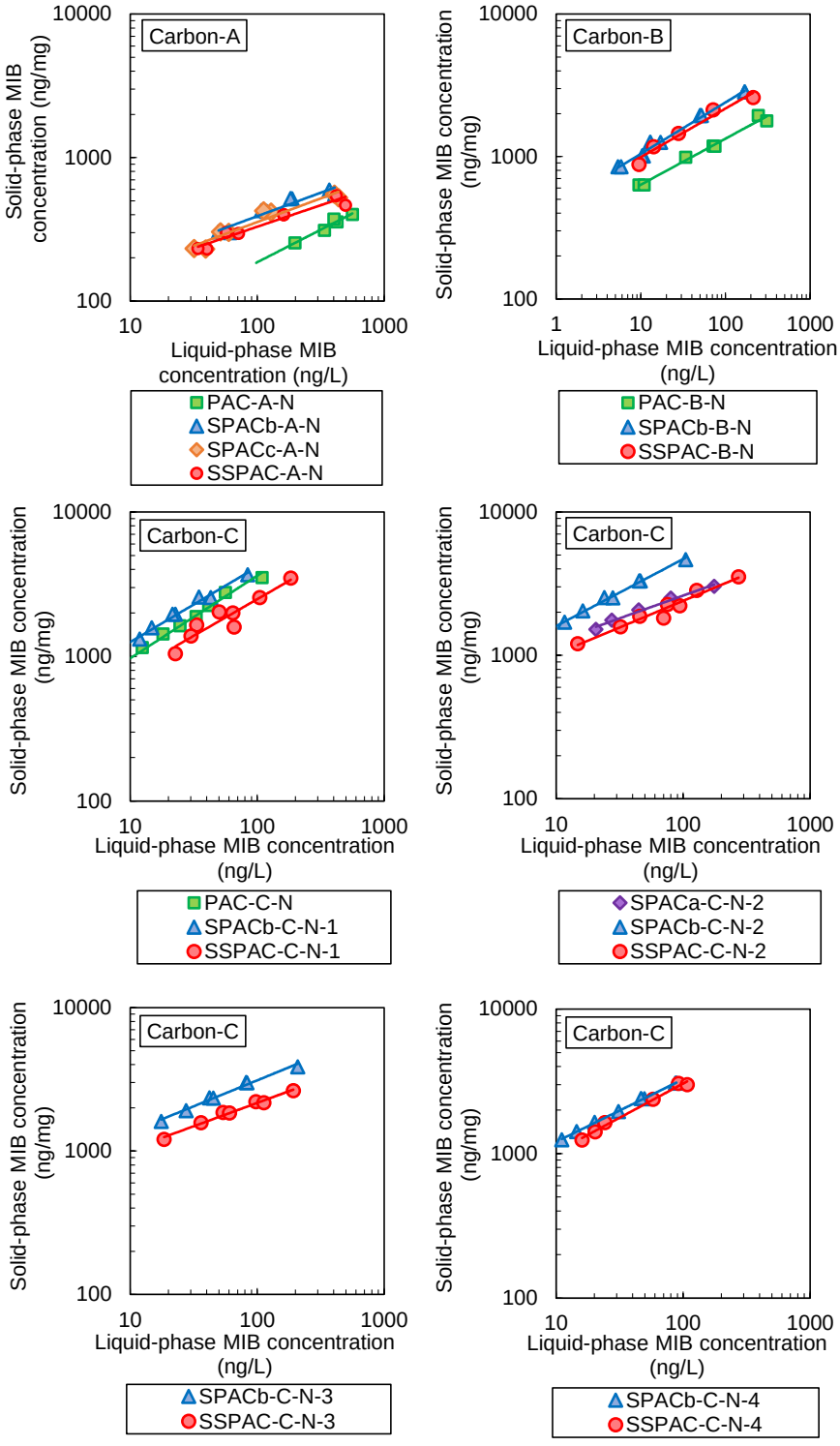

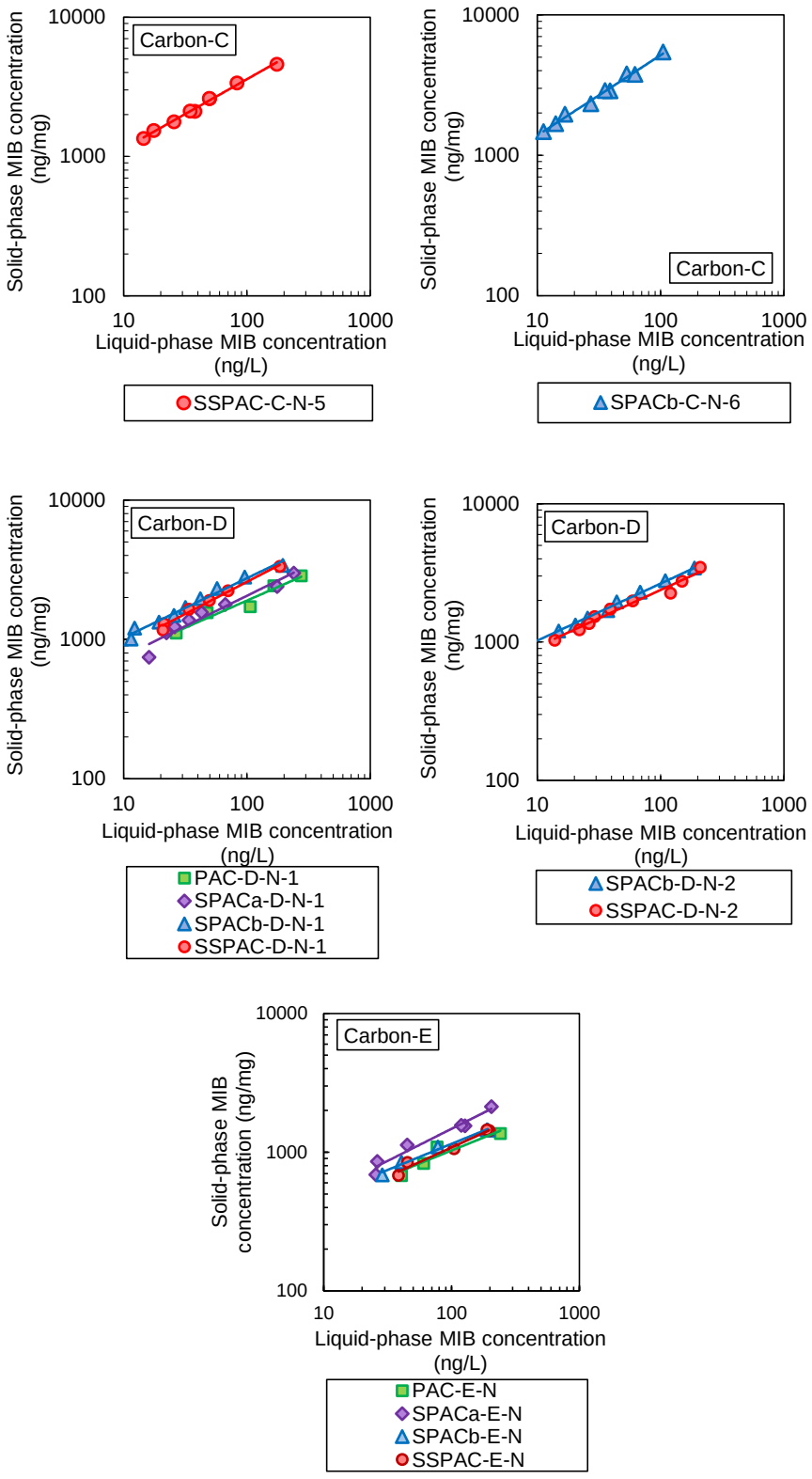

Fig. 3-4. MIB adsorption isotherms of Carbon-A, Carbon-B, Carbon-C, Carbon-D and Carbon-E.

After fitting the isotherm data to Freundlich model, MIB adsorption capacities were quantified in terms of the MIB solid-phase concentration in equilibrium with MIB liquid-phase concentrations of 50

ng/L and 100 ng/L. Then the changes of equilibrium MIB adsorption capacities with carbon particle size were depicted as shown in Fig. 3-5a. From PAC-A-N to SPACb-A-N, D_{50} reduced from 12 µm to 1.47 µm while the adsorption capacities doubled. However, the MIB adsorption capacity was not increased with decreasing carbon particle size when the D_{50} < 1.47 µm. In the case of Carbon-A series, the MIB adsorption capacity of SSPAC-A-N (D_{50} = 0.198 µm) was around 85 % of that of SPACb-A-N (D_{50} = 1.47 µm). The adsorption capacity decrease was observed not only in Carbon-A series but also in the other carbons. For example, the adsorption capacity of SSPAC-B-N was around 90 % of that of SPACb-B-N (Fig. 3-5b), the adsorption capacity of SSPAC-C-N was 51 - 93 % of that of SPACb-C-N [Fig. 3-5(c-1), (c-2)], the adsorption capacity of SSPAC-D-N was 90 % of that of SPACb-D-N (Fig. 3-5d). In the case of Carbon-E, the adsorption capacity started to decrease with particle size in the range of D_{50} < 3.5 µm. The adsorption capacity of SSPAC-E-N was around 74% of that of SPACa-E-N (Fig. 3-5e). Beside the MIB adsorption of our experiments, a similar trend can be seen in a research data of the paper focusing on a pesticide (atrazine) removal by microfiltration pre-coated with SPAC (Amaral et al., 2016). In the data of that study, the trend of the adsorption capacity decrease with carbon size reduction can be seen for on 2 of 3 carbons tested, although the authors of the paper do not comment on this trend.

According to the SAM, the particle size of adsorbent affects the MIB adsorption capacity when the radius of adsorbent is substantially larger than the penetration depth of adsorbate molecules (Matsui et al., 2013; Matsui et al., 2014). In this case, the increase of external surface of adsorbent particles results in the increase of adsorption capacity. Therefore, the increase of adsorption capacity from PAC-A-N (D_{50} = 12 µm) to SPACb-A-N (D_{50} = 1.47 µm) would be due to this mechanism. No increase of the adsorption capacity with decreasing particle size for D_{50} < 1.47 µm (from SPACb to SSPAC) suggests that the particle radii of these carbons were smaller than the penetration depth of MIB and the entire internal pores in carbon particles were utilized by the adsorption of MIB molecule. Once the entire internal pores in carbon particles are utilized for the adsorption, the adsorption capacity becomes independent of carbon particle size. In this case, the pore surface chemistry would play an important role in the adsorption capacity (Li et al., 2002; Matsui et al., 2015; Quinlivan et al., 2005).

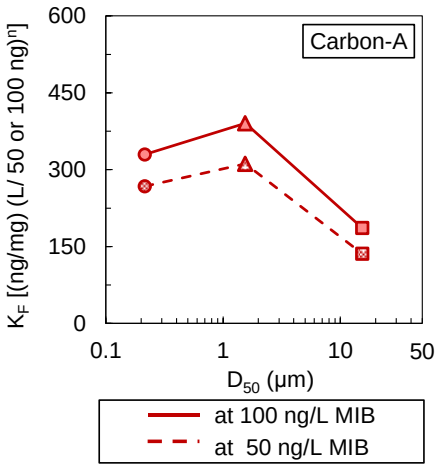

(a)

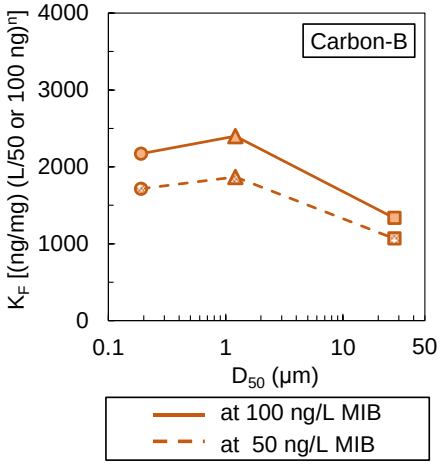

(b)

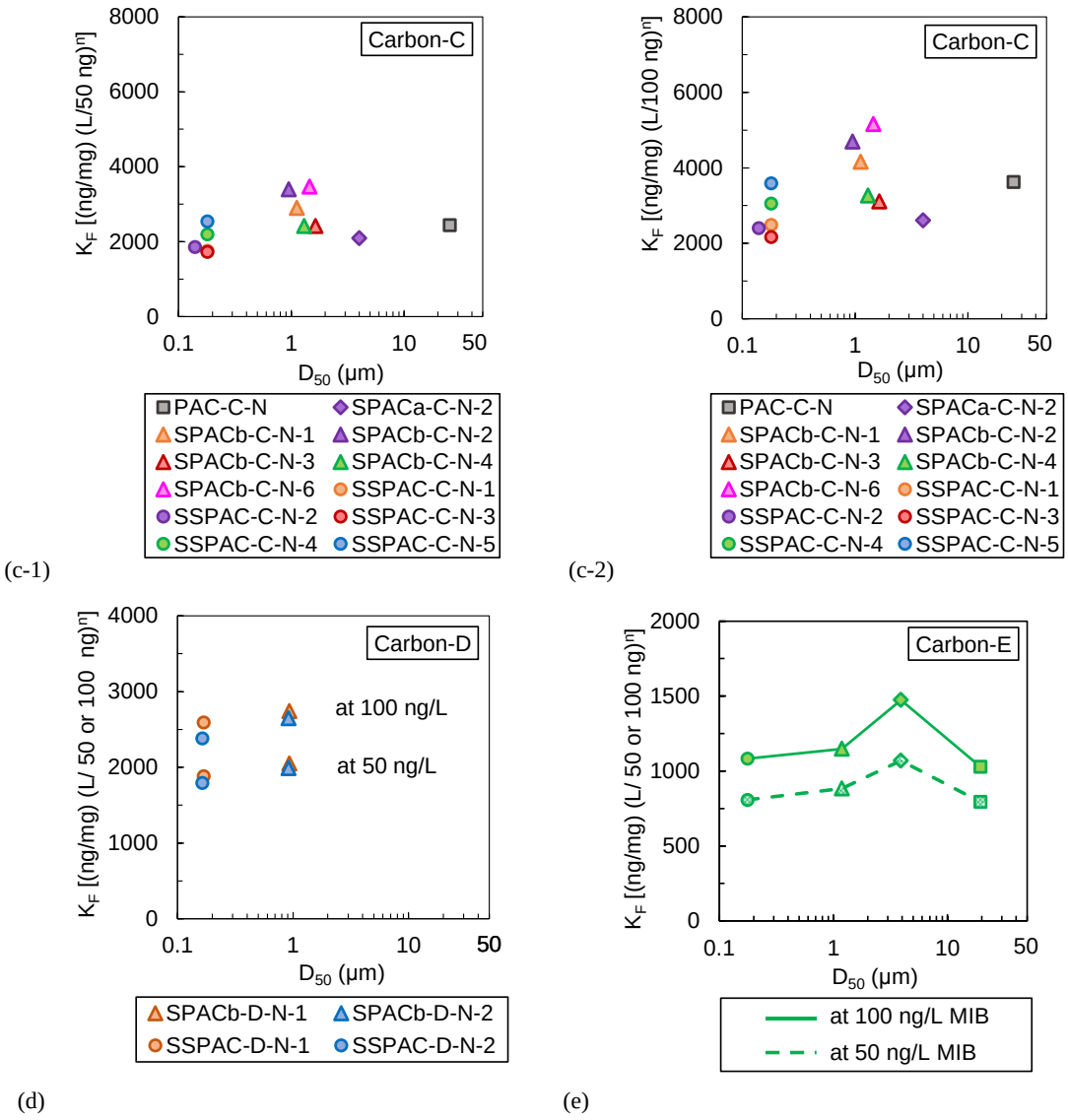

Fig. 3-5. MIB adsorption equilibrium capacity versus carbon particle size [The squares are PAC(s), the demons are SPACa(s), the triangles are SPAC(s), and the circles are SSPAC(s)].

3.4.3 Oxygen contents of carbons

According to the findings of previous researchers (Moreno-Castilla, 2004; Pendleton et al., 1997; Song et al., 2010), the oxygen-containing complexes on the surface of activated carbon, which modifies the hydrophobicity of carbon surface, affects the adsorption capacity of organic compounds, including MIB. The number of oxygen-containing complexes can be reflected by the oxygen content (w/w %) of activated carbon, thereby that is highly correlated with the MIB adsorption capacity (Li et al., 2002; Matsui et al., 2015).

The oxygen contents of Carbon-A series samples are shown in Fig. 3-6a. The oxygen content increased with decreasing particle size, in particular increased largely where the D_{50} < 1 μm. The carbon particles with D_{50} < 1 μm were produced by micro-milling carbons in the bead mill. It is believed that

the external surface of carbon particles is usually more oxidized than the inner region because the diffusion of oxygen in abundant internal narrow pores is very slow (Boehm, 2002). Therefore, the micro-milling opens the inner region of carbon particles and let them contact with oxygen in water, which might accelerates the oxidation speed. Coincidently, the drop of MIB adsorption capacity was seen in the particle size range where the oxygen content increased largely Fig. 3-5a, which suggests that the drop of MIB adsorption capacity would be caused by the oxidation of carbon.

The parent carbons of Carbon-A series, Carbon-B series and Carbon-C series (i.e. PAC-A-N, PAC-B-N, and PAC-C-N) were wood-based carbons, which were produced by the same manufacture but were produced in different batches and were received at different times. The stock periods of the carbons from the receipts to the experiment were different. They were in the order of PAC-A-N series (around 7 years) > PAC-B-N series (around 1 year) > PAC-C-N (less than half year). This order of carbon stock periods just stands in line with the order of oxygen contents: PAC-A-N (9.10 %) > PAC-B-N (7.21 %) > PAC-C-N (2.03 %) (Fig. 3-6a, b, and c). This finding agrees with that the activated carbon will be oxidized while being stocked in air after production (Boehm, 2002). Coincidently, the MIB adsorption capacities of those PACs stands in the opposite order of the oxygen content: the capacity of PAC-A-N was the lowest followed by PAC-B-N and then PAC-C-N (Fig. 3-5a, b, and c). The data supports that the oxidation of carbon causes the decrease of MIB adsorption capacity.

PAC-A-N, PAC-B-N, and PAC-C-N, which had different oxygen contents, presented the increases of oxygen content during the micro-milling by the bead mill (Fig. 3-6a, b, and c). Not only the above three carbons which were produced by the same manufacture, but also Carbon-D-N, which was produced by the other manufacture, also showed the oxygen content increase during the micro-milling (Fig. 3-6d). The external surface area of activated carbon particles are more oxidized than the inter region, and therefore overall carbon particles could be more oxidized when the particle size are reduced the bead milling (Partlan et al., 2016).

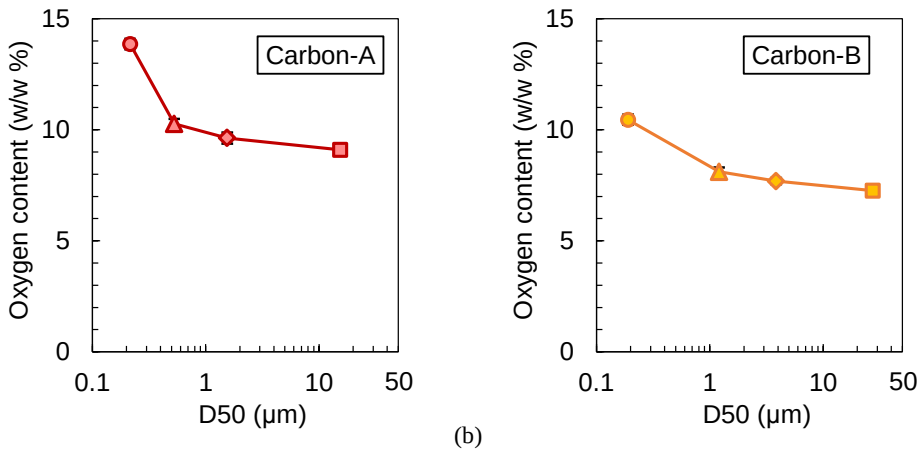

(a) (b)

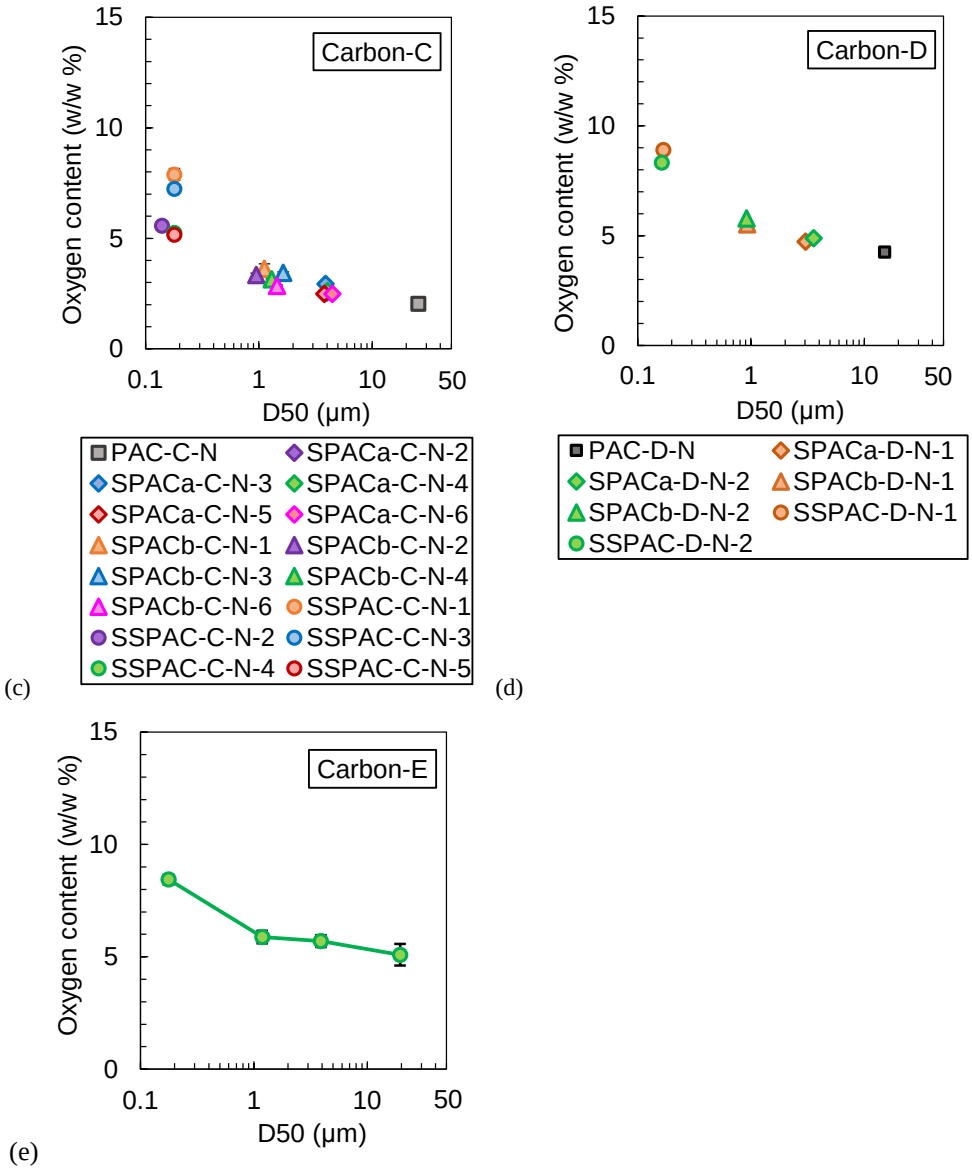

Fig. 3-6. Oxygen content of Carbon-A, Carbon-B, Carbon-C, Carbon-D, and Carbon-E produced under normal milling [The squares are PAC(s), the demons are SPACa(s), the triangles are SPACb(s), and the circles are SSPAC(s)] (Error bars are quite small and almost hidden behind the symbols]**.**

3.4.4 Controlling oxidation during the productions of SPAC and SSPAC

The increase of oxygen content with the progress of milling suggests the introduction of oxygen-containing functional oxidation, which would change the carbon more hydrophilic and then would decrease the adsorption capacities of MIB. This means if the oxidization during milling could be inhibited the decrease of adsorption capacity would be alleviated as well. A quantity of attempts were tried to produce of less-oxidized SSPAC with D_{50} < 250 nm (Table 3-3 and Fig. 3-2). The results are presented in Fig. 3-7.

The oxidation-inhibitory milling was successful in inhibiting oxidation during the milling by which the carbon D_{50} was reduced from 4 µm to 150 - 230 nm. Oxygen content was increased by 2.2 ± 0.5 w/w% when producing SSPAC-C-OI by the oxidation-inhibitory milling as described in the section 2.2.2. On the other hand, the normal milling which produced SSPAC-C-N increased the oxygen content by 3.4 ± 1.2 w/w% (Fig. 3-7a). Similarly, the oxygen content increase of Carbon-D from SPACa to SSPAC produced under oxygen-inhibitory milling was 2.0 ± 0.23 w/w% which is around half of the increase in carbon produced by normal milling (3.8 ± 0.11 w/w%; Fig. 3-7b).

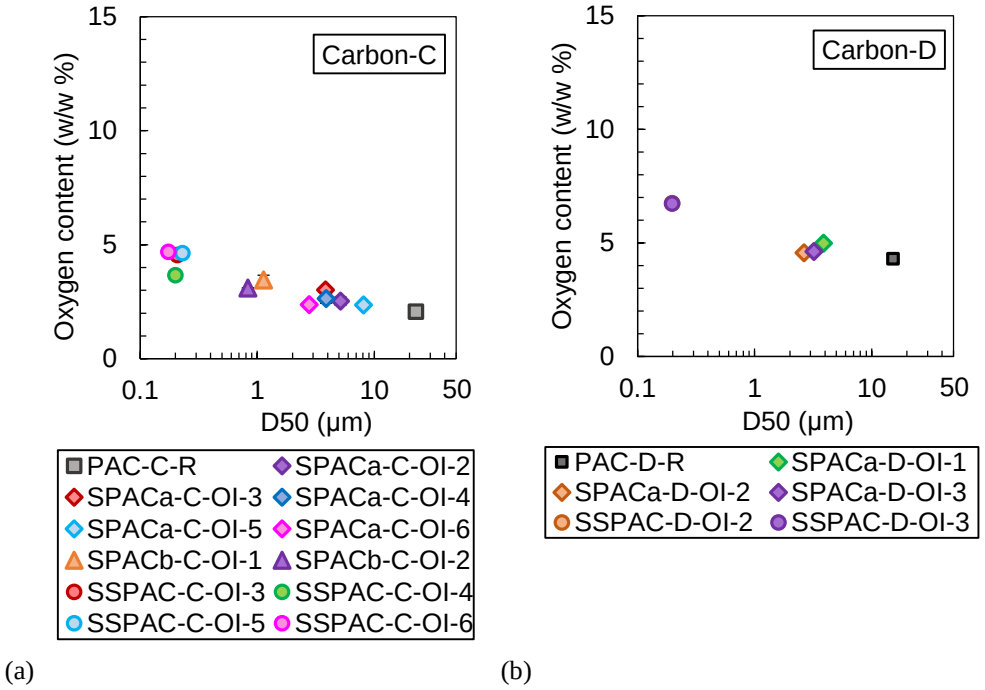

(a) (b)

Fig. 3-7. Oxygen content of Carbon-C and Carbon-D produced under oxidation-inhibitory milling conditions.

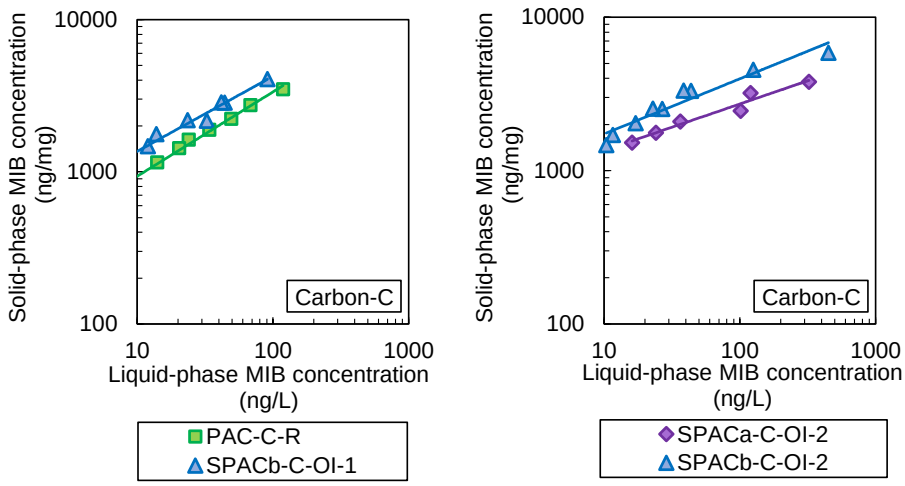

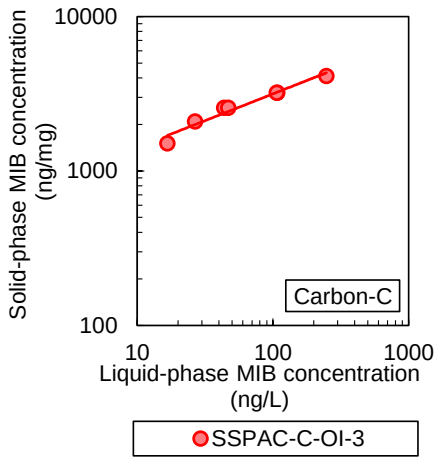
Solid-phase MIB concentration (ng/mg)
10000
1000
100
10
100
1000
Liquid-phase MIB concentration (ng/L)
Carbon-C
SSPAC-C-OI-3

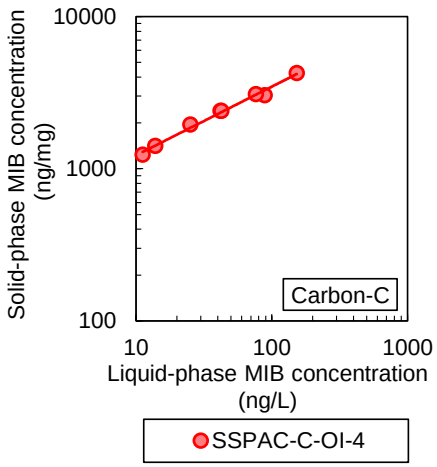
Solid-phase MIB concentration (ng/mg)
10000
1000
100
10
100
1000
Liquid-phase MIB concentration (ng/L)
Carbon-C
SSPAC-C-OI-4

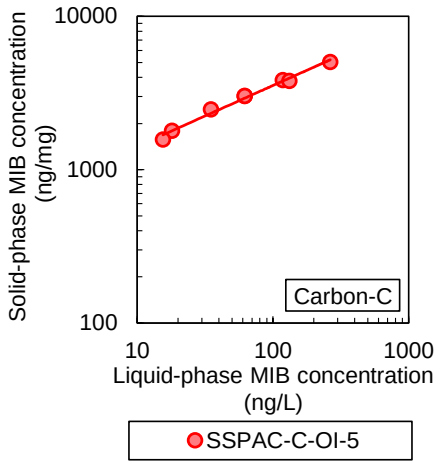
Solid-phase MIB concentration (ng/mg)
10000
1000
100
10
100
1000
Liquid-phase MIB concentration (ng/L)
Carbon-C
SSPAC-C-OI-5

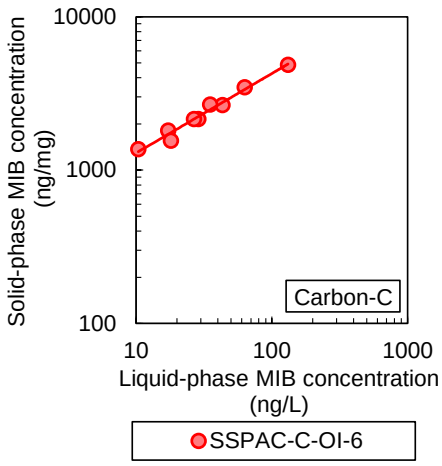
Solid-phase MIB concentration (ng/mg)
10000
1000
100
10
100
1000
Liquid-phase MIB concentration (ng/L)
Carbon-C
SSPAC-C-OI-6

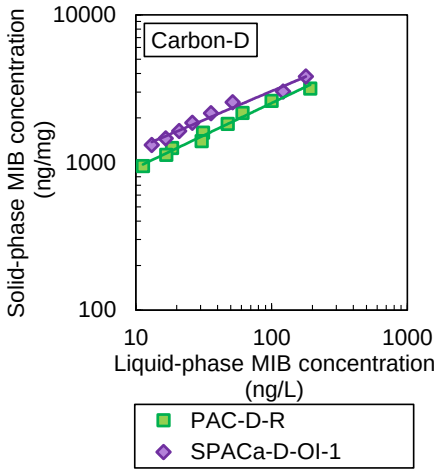
Solid-phase MIB concentration (ng/mg)
10000
1000
100
10
100
1000
Liquid-phase MIB concentration (ng/L)
Carbon-D
PAC-D-R
SPACa-D-OI-1

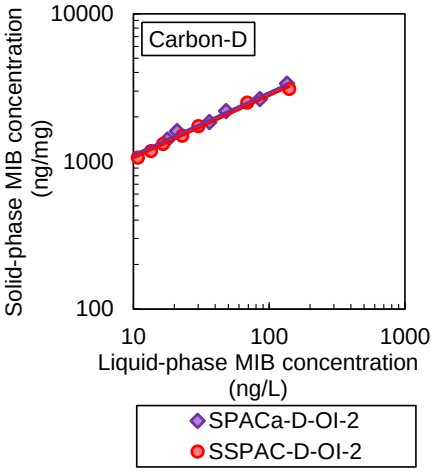
Solid-phase MIB concentration (ng/mg)
10000
1000
100
10
100
1000
Liquid-phase MIB concentration (ng/L)
Carbon-D
SPACa-D-OI-2
SSPAC-D-OI-2

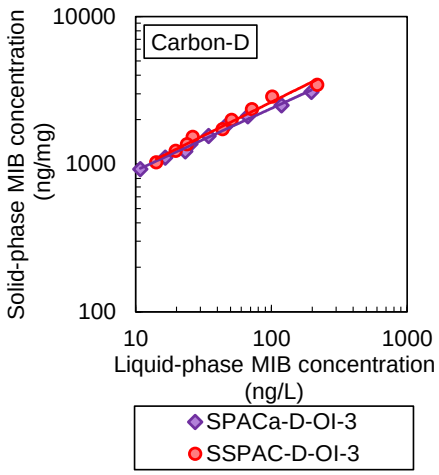

Fig. 3-8. MIB adsorption isotherms of Carbon-C produced under oxidation-inhibited milling conditions.

3.4.5 Correlation between oxygen content and MIB adsorption capacity.

The section 3.3.3 suggests that the decrease of MIB adsorption capacity for the SSPACs that were produced by the normal milling would be caused by the oxidation of the carbons. Regarding the SSPACs with D_{50} of around 200 nm, it was successful to control the oxygen content. Finally SSPACs with low as well as high oxygen contents (SSPAC-C-OI and SSPAC-C-N; SSPAC-D-OI and SSPAC-D-N) were produced from the same PAC. MIB adsorption capacities of these carbons were obtained. SSPAC-C-OI and SSPAC-D-OI of low oxygen content exhibited higher adsorption capacity than SSPAC-C-N and SSPAC-D-N of high oxygen content respectively (MIB adsorption isotherms are in Figs. 3-4 and 3-8. As shown in Fig. 3-9, moreover, the high and negative correlation was observed between oxygen content of carbon particles and their MIB adsorption capacities. These results clearly indicate that the lower MIB adsorption on the SSPAC that were produced by the normal milling than on SPACb was due to the increase of oxygen content, which could make the carbon more hydrophilic.

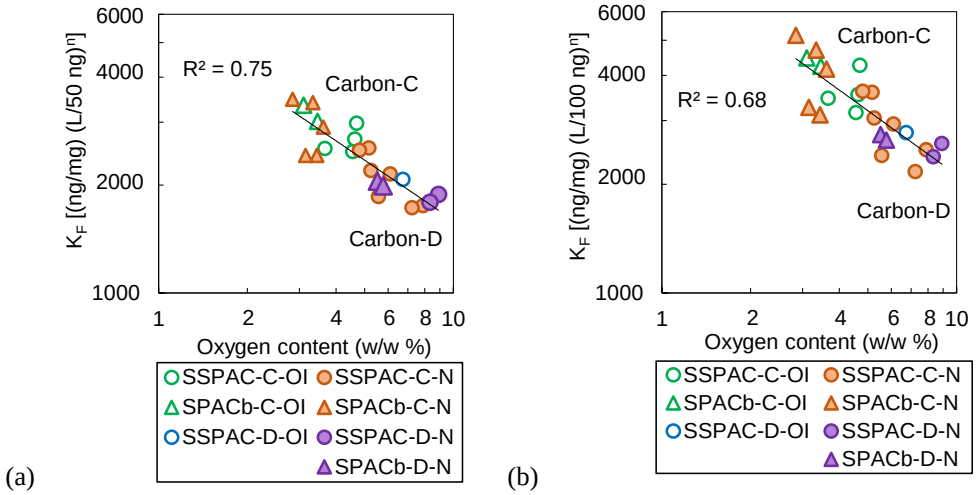

Fig. 3-9. Correlation between oxygen content and MIB adsorption capacity.

The data of the high correlation (Fig. 3-9) includes the data of carbon particles with D_{50} < around 1 μm (all the SPACb and SSPAC). This clearly means that the adsorption capacities were not related to the carbon size, suggesting that the whole carbon particle including internal pores can be accessed by MIB molecule in the adsorption progress, as suggested by the SAM (see the section 3.3.2). It indicates that the adsorption capacities were related to the carbon characteristics, more specifically, hydrophilicity. The oxygen content is a good indicator to evaluate the MIB adsorption capacity of carbons with D_{50} < 1 μm (SPACb and SSPAC).

The oxygen content of the SSPAC produced by the oxidation-inhibitory milling was lower than that produced by the normal milling, but it was still higher than that of the SPAC, from which the SSPAC was produced. The oxidation was not restricted completely during even with the oxidation-inhibitory milling. Finally, the highest adsorption capacity was observed on the SPACb with D_{50} around 1 μm. The energy required for reducing the particle of D_{50} less than 1 μm would not offer any advantage in terms of adsorption capacity. Finally, SPAC of D_{50} around few μm (1.5 μm in the case of Carbon-A and Carbon-B; 4.0 μm in the case of Carbon-C and Carbon-D) would be more reasonable choice for MIB removal in the perspective of the high MIB adsorption capacity and the production with not-excessive energy consumption.

3.4.6 Carbon particle size effects on adsorption capacities of various adsorbates.

The phenomenon of the adsorption capacity increase from PAC to SPACb and the decrease from SPACb to SSPAC was observed on MIB, which is a hydrophobic low-MW (LMW) compound (log-Kow 3.31; 168.3 Da). To see whether this trend of adsorption capacity change with carbon particle size occurs for other adsorbates or not, a plenty of adsorption equilibria tests were conducted on other compounds with environmental relevancy and with wide variety of hydrophobicity and molecular weight (Fig. 3-10). These compounds were geosmin (log-Kow 3.57; 182 Da), DMTP-oxon (log-Kow 0.77; 286 Da), benzothiazole (log-Kow 2.09; 135 Da), phenol (log-Kow 1.46; 94.1 Da), PNP (log-Kow 1.91; 139 Da), salicylic acid (log-Kow 2.06; 138 Da), PSS-210 (average 210 Da), PSS-1100 (average 1100 Da) and SNOM [the log-Kow values of the indicated adsorbate are summarized from database of EPI Suite™ (U.S. Environmental Protection Agency v4.0)]. The adsorption capacities of these compounds were quantified as the solid-phase concentration in equilibrium with each appropriate liquid-phase concentration, and then they were plotted against carbon D_{50} (Fig. 3-11).

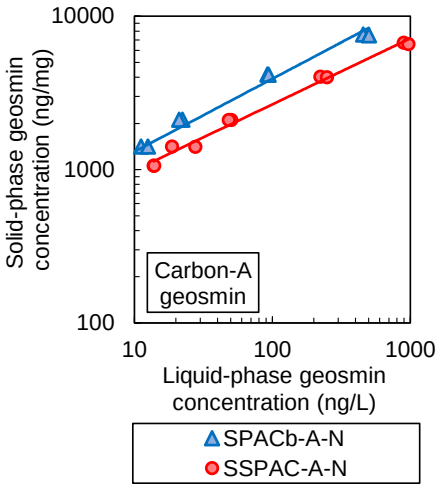
Solid-phase geosmin concentration (ng/mg)
10000
1000
100
Carbon-A geosmin
10
100
1000
Liquid-phase geosmin concentration (ng/L)
SPACb-A-N
SSPAC-A-N

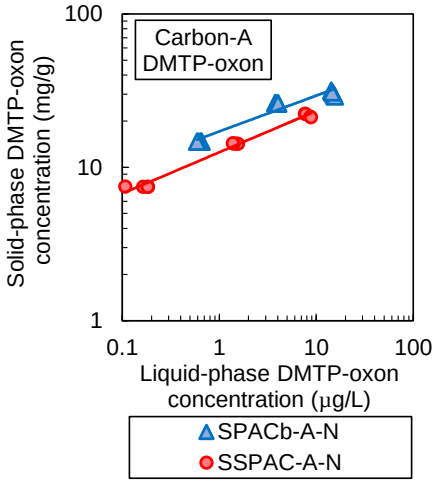
Solid-phase DMTP-oxon concentration (mg/g)
100
10
1
Carbon-A DMTP-oxon
0.1
1
10
100
Liquid-phase DMTP-oxon concentration (μg/L)
SPACb-A-N
SSPAC-A-N

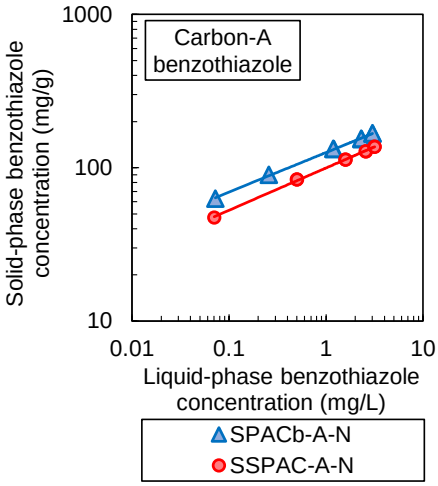
Solid-phase benzothiazole concentration (mg/g)
1000
100
10
Carbon-A benzothiazole
0.01
0.1
1
10
Liquid-phase benzothiazole concentration (mg/L)
SPACb-A-N
SSPAC-A-N

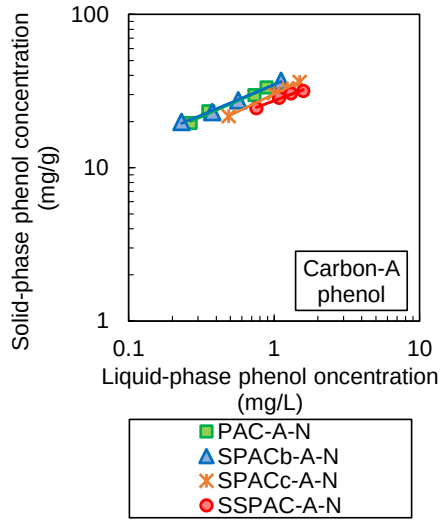
Solid-phase phenol concentration (mg/g)
100
10
1
Carbon-A phenol
0.1
1
10
Liquid-phase phenol oncentration (mg/L)
PAC-A-N
SPACb-A-N
SPACc-A-N
SSPAC-A-N

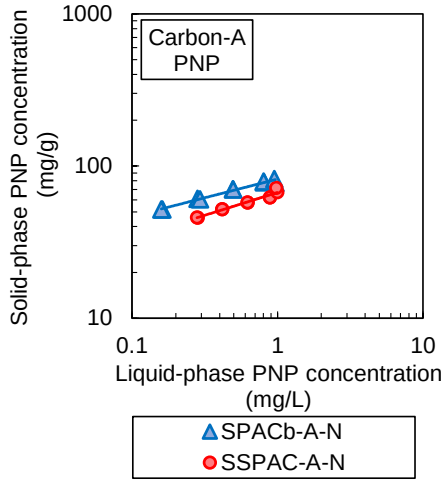
Solid-phase PNP concentration (mg/g)
1000
100
10
Carbon-A PNP
0.1
1
10
Liquid-phase PNP concentration (mg/L)
SPACb-A-N
SSPAC-A-N

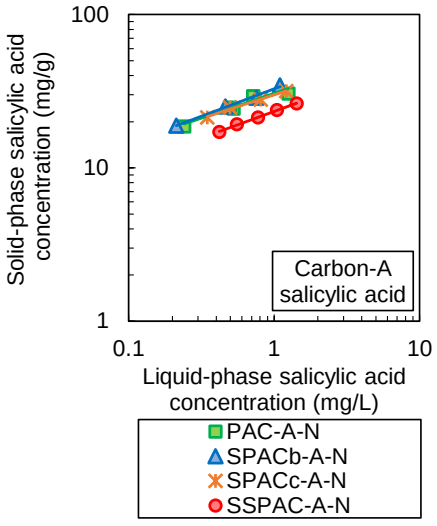
Solid-phase salicylic acid concentration (mg/g)
100
10
1
Carbon-A salicylic acid
0.1
1
10
Liquid-phase salicylic acid concentration (mg/L)
PAC-A-N
SPACb-A-N
SPACc-A-N
SSPAC-A-N

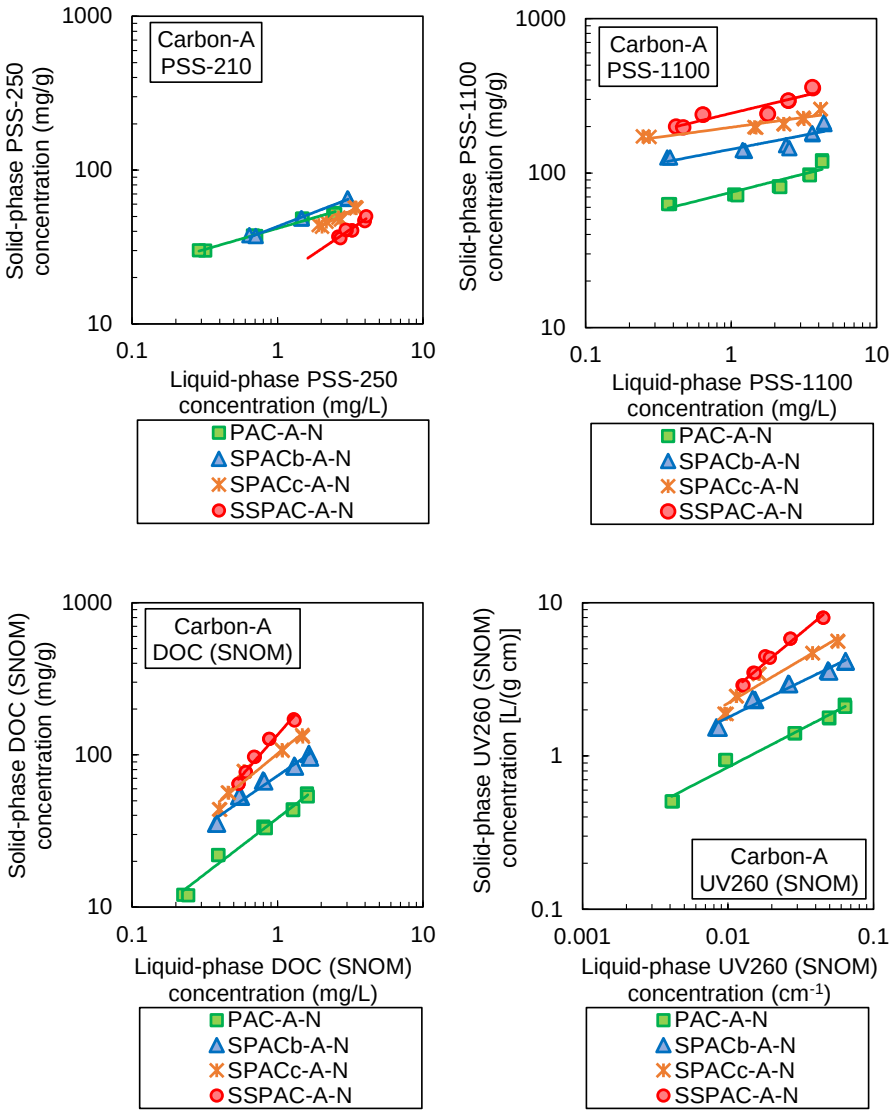

Fig. 3-10. Adsorption equilibria of 7 adsorbates of Carbon-A.

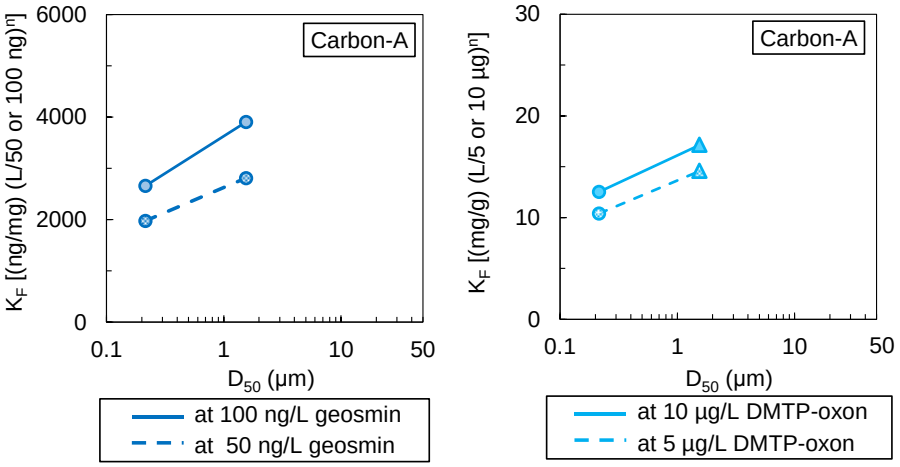

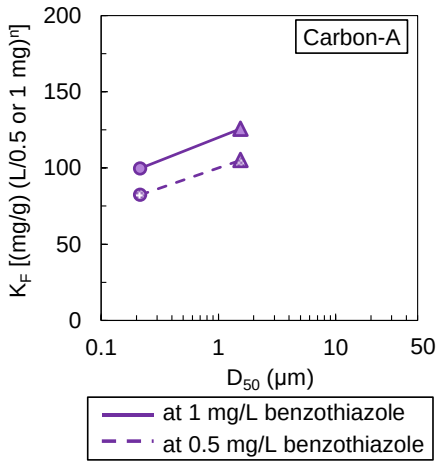
Carbon-A
K_F [(mg/g) (L/0.5 or 1 mg)^n]
200
150
100
50
0
0.1
1
10
50
D_{50} (µm)
at 1 mg/L benzothiazole
at 0.5 mg/L benzothiazole

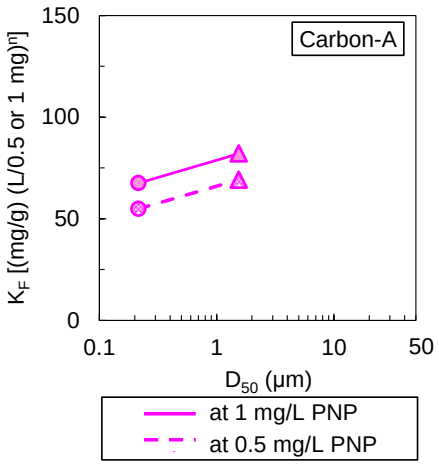
Carbon-A
K_F [(mg/g) (L/0.5 or 1 mg)^n]
150
100
50
0
0.1
1
10
50
D_{50} (µm)
at 1 mg/L PNP
at 0.5 mg/L PNP

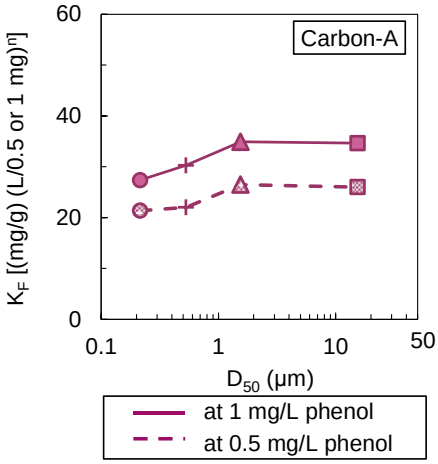
Carbon-A
K_F [(mg/g) (L/0.5 or 1 mg)^n]
60
40
20
0
0.1
1
10
50
D_{50} (µm)
at 1 mg/L phenol
at 0.5 mg/L phenol

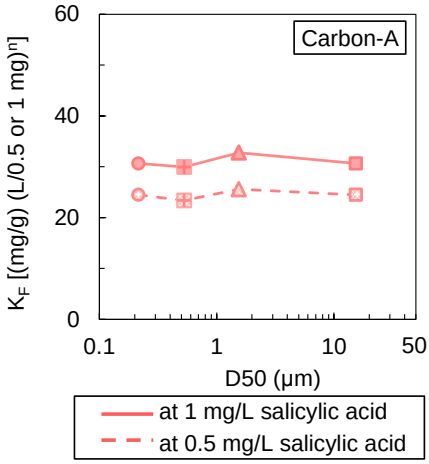
Carbon-A
K_F [(mg/g) (L/0.5 or 1 mg)^n]
60
40
20
0
0.1
1
10
50
D50 (µm)
at 1 mg/L salicylic acid
at 0.5 mg/L salicylic acid

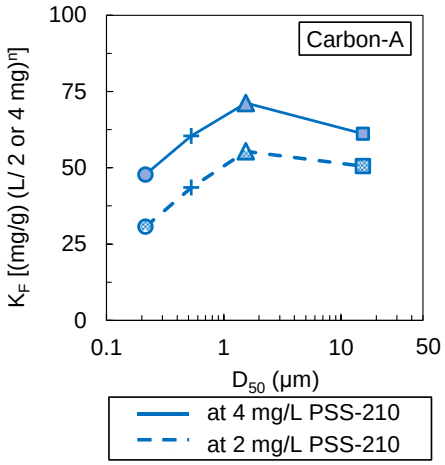
Carbon-A
K_F [(mg/g) (L/ 2 or 4 mg)^n]
100
75
50
25
0
0.1
1
10
50
D_{50} (µm)
at 4 mg/L PSS-210
at 2 mg/L PSS-210

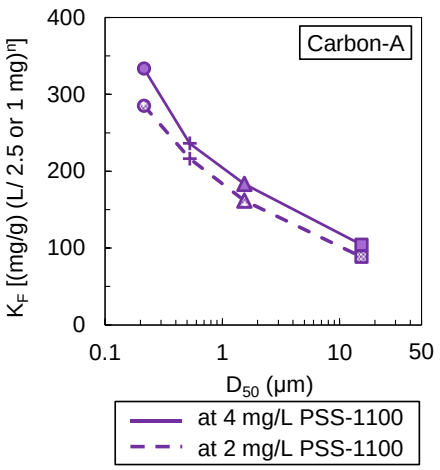
Carbon-A
K_F [(mg/g) (L/ 2.5 or 1 mg)^n]
400
300
200
100
0
0.1
1
10
50
D_{50} (µm)
at 4 mg/L PSS-1100
at 2 mg/L PSS-1100

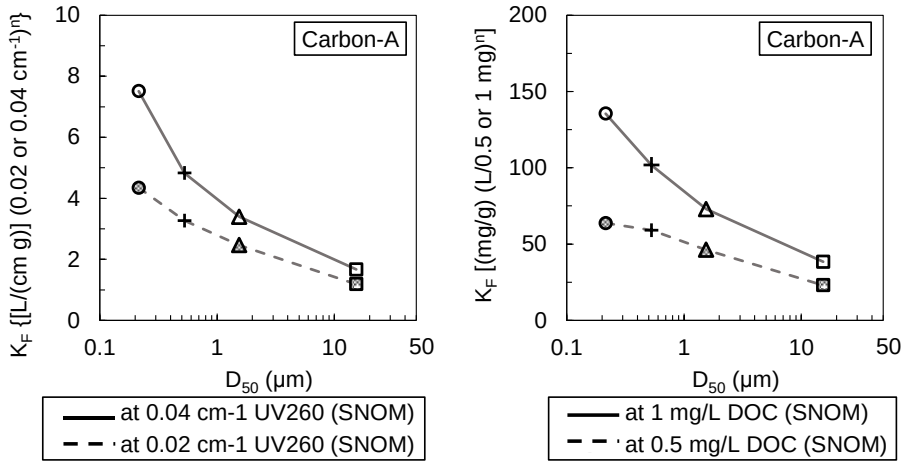

Fig. 3-11. Adsorption equilibrium capacities versus carbon particle size of Carbon-A.

The adsorption capacity decrease from SPACb-A-N to SSPAC-A-N did not occur on the PSS-1100 and SNOM, both of which are high MW (HMW) compounds (MW >1000 Da). The capacity increased from SPACb-A-N to SSPAC-A-N as well as from PAC-A-N to SPACb-A-N. This result stands in line with the previous findings that the adsorption capacity of compounds with HMW increased with carbon particle size reduction (Ando et al., 2010; Ando et al., 2011). For HMW compounds, penetration depth would be very short and shorter than the radius of adsorbents including the PAC and SPAC, and then the inner region of those adsorbents were not accessible for those adsorbates, and thereby the adsorption capacity increased with decreasing adsorbent particle size.

For the other 7 compounds, which were of LMW (MW < 300 Da), the decrease of the adsorption capacities with decreasing the carbon D_{50} from ~1 to 0.2 μm were also observed as in the case with MIB. The adsorption capacity of SSPAC-A-N (D_{50} = 0.20 μm) was lower than that of SPACb-A-N (D_{50} = 1.47 μm) (Fig. 3-5a and 3-11).

The extents of the adsorption capacity decrease from SPACb-A-N to SSPAC-A-N varied depending on compounds. However, any adsorbate property was not found to explain the extents of the adsorption capacity decrease. For example, the extents of the adsorption capacity decrease was not correlated to the log-Kow values of adsorbates (R^2 < 0.02, Fig. 3-12a). The adsorption capacity of geosmin (log-Kow = 3.57), which is similar to or even more hydrophobic than MIB (log-Kow = 3.31), was 30 % lower on SSPAC-A-N than on SPACb-A-N. The adsorption capacity of DMTP-oxon (log-Kow = 0.77), which is a hydrophilic compound, was also 30 % lower on SSPAC-A-N than on SPACb-A-N. Carbon-B series (i.e. SPACb-B-N and SSPAC-B-N) also showed no correlation between the extents of the adsorption capacity decrease and the log-Kow values of the compounds (Fig. 3-12b). Lower adsorption capacity of SSPAC than of SPACb was due to the higher hydrophobicity of SSPAC as indicated by higher oxygen content, as discussed in the section 3.5. Therefore, the different degree of the adsorption capacity deceases from SPACb to SSPAC between the 8 compounds (the 7 compounds plus MIB) indicate that

the adsorption capacities of these compounds have different sensitivity to carbon hydrophobicity (oxygen content).

(a)

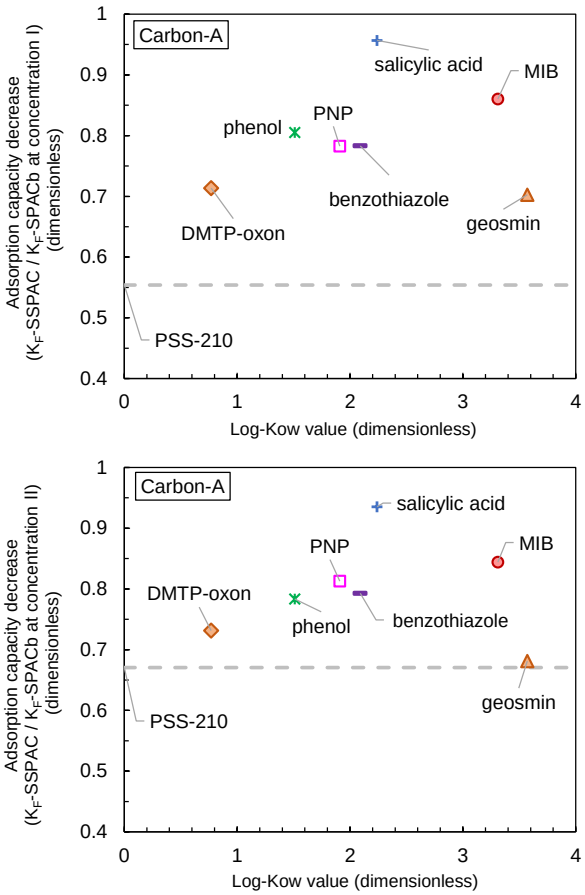

(b)

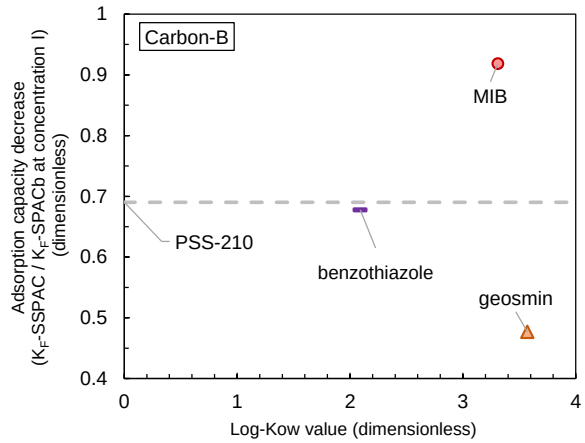

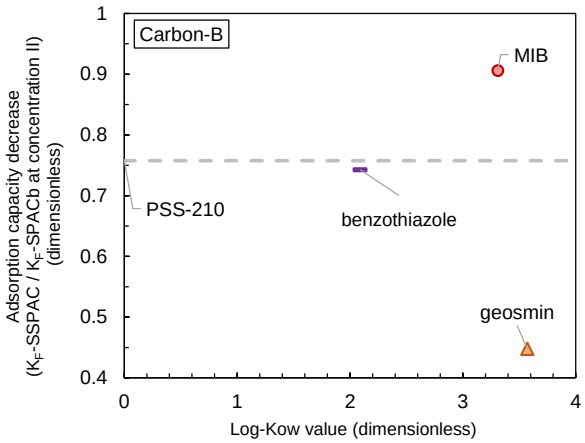

Fig. 3-12. Ratio of adsorption capacity of SPACb and SSPAC versus log-Kow of adsorbates. (Concentration I & II: MIB and geosmin – 50 & 100 ng/L; DMTP-oxon: 5 & 10 µg/L; benzothiazole, phenol, PNP, salicylic acid: 0.5 & 1 mg/L; PSS-210: 2 & 4 mg/L)

Different sensitivity to carbon hydrophobicity is also reported in other studies, although these do not deal with SPAC and SSPAC. A study comparing adsorption capacites of trichloroethene (TCE; log-Kow: 2.42; 131 Da) and methyl tertiary-butyl ether (MTBE; log-Kow: 0.94; 88 Da) indicates that the decrease of adsorption capacity due to the modification of carbon to become hydrophilic is more prominent for MTBE (the adsorbate with lower log-Kow) (Li et al., 2002). However, other study using several fatty acids, including propanoic acid (log-Kow 0.33; 74.1 Da), valeric acid (log-Kow 1.39; 102 Da), enanthic acid (log-Kow 2.42; 130 Da), and pelargonic acid (log-Kow 3.42; 158 Da) reports that the decrease of adsorption capacity due to the modification of carbon to become hydrophilic are not necessarily greater with adsorbate with high log-Kow than with adsorbate with low log-Kow (Kaneko et al., 1989).

The increased formation of water clusters on carbon surface after carbon become more hydrophilic would prevent hydrophobic adsorbates, such as MIB, access to the hydrophobic adsorption sites on carbon surface (Pendleton et al., 1997). It also reduces interaction energy between hydrophilic adsorbates, such as DMTP-oxon, and the carbon surface where the hydrogen bonds were preferentially form to water molecules (Kaneko et al., 1989; Li et al., 2002). Although the adsorption capacities of both hydrophobic and hydrophilic adsorbates decreases with decreasing carbon hydrophobicity, their mechanisms would be different leading to different sensitivity of the adsorption capacity to carbon hydrophobicity.

3.5 Chapter conclusions

(1). The D_{50} of carbon particles after the micro-milling could reach to 140 nm.

(2). The MIB adsorption capacity decreased with decreasing carbon particle size in the range of D_{50} < few μm. This decrease is due to the oxidization of the carbon during the milling.

(3). The oxidation of carbon during milling can be inhibited. In this case, the decrease of MIB adsorption capacity is alleviated.

(4). For the sake of high MIB adsorption capacity and avoiding thankless energy consumption for milling, SPAC with D_{50} around 1 μm is the reasonable choice among other particle size.

(5). The adsorption capacity decrease with decreasing carbon particle size in the range of D_{50} < few μm was also observed for other 7 low-molecular-weight compounds. The extents of the decreases were different in the compounds, but were not simply depend on the hydrophilicity of the compounds.

(6). For HMW adsorbates (SNOM and PSS-1100), the adsorption capacities increased with decreasing adsorbent particle size from PAC to SSPAC.

3.6 Reference

Amaral, P., Partlan, E., Li, M., Lapolli, F., Mefford, O.T., Karanfil, T. and Ladner, D.A., 2016. Superfine powdered activated carbon (S-PAC) coatings on microfiltration membranes: Effects of milling time on contaminant removal and flux. Water Research 100, 429-438.

Ando, N., Matsui, Y., Kurotobi, R., Nakano, Y., Matsushita, T. and Ohno, K., 2010. Comparison of natural organic matter adsorption capacities of super-powdered activated carbon and powdered activated carbon. Water research 44(14), 4127-4136.

Ando, N., Matsui, Y., Matsushita, T. and Ohno, K., 2011. Direct observation of solid-phase adsorbate concentration profile in powdered activated carbon particle to elucidate mechanism of high adsorption capacity on super-powdered activated carbon. Water research 45(2), 761-767.

Boehm, H.P., 2002. Surface oxides on carbon and their analysis: a critical assessment. Carbon 40(2), 145-149.

Bonvin, F., Jost, L., Randin, L., Bonvin, E. and Kohn, T., 2016. Super-fine powdered activated carbon (SPAC) for efficient removal of micropollutants from wastewater treatment plant effluent. Water Research 90, 90-99.

Dudley, L.-A., 2012. Removal of Perfluorinated Compounds by Powdered Activated Carbon, Superfine Powder Activated Carbon, and Anion Exchange Resin.

Dunn, S.E. and Knappe, D.R., 2013. DBP Precursor and Micropollutant Removal by Powdered Activated Carbon [Project# 4294].

Ellerie, J.R., Apul, O.G., Karanfil, T. and Ladner, D.A., 2013. Comparing graphene, carbon nanotubes, and superfine powdered activated carbon as adsorptive coating materials for microfiltration membranes. Journal of Hazardous Materials 261, 91-98.

Flach, F., Konnerth, C., Peppersack, C., Schmidt, J., Damm, C., Breitung-Faes, S., Peukert, W. and Kwade, A., 2016, in press. Impact of formulation and operating parameters on particle size and grinding media wear in wet media milling of organic compounds – A case study for pyrene. Advanced Powder Technology.

Han, S.-W., Shin, J.-W. and Yoon, D.-H., 2012. Synthesis of pure nano-sized Li4Ti5O12 powder via solid-state reaction using very fine grinding media. Ceramics International 38(8), 6963-6968.

Heijman, S.G.J., Hamad, J.Z., Kennedy, M.D., Schippers, J. and Amy, G., 2009. Submicron powdered activated carbon used as a pre-coat in ceramic micro-filtration. Desalination and Water Treatment 9(1-3), 86-91.

Jia, L., Kondoh, K., Imai, H., Onishi, M., Chen, B. and Li, S.-f., 2015. Nano-scale AlN powders and AlN/Al composites by full and partial direct nitridation of aluminum in solid-state. Journal of Alloys and Compounds 629, 184-187.

Kanaya, S., Kawase, Y., Mima, S., Sugiura, K., Murase, K. and Yonekawa, H., 2015. Drinking Water Treatment Using Superfine PAC (SPAC): Design and Successful Operation History in Full-Scale Plant, Salt Lake City, Utah, USA.

Kaneko, Y., Abe, M. and Ogino, K., 1989. Adsorption characteristics of organic compounds dissolved in water on surface-improved activated carbon fibres. Colloids and Surfaces 37, 211-222.

Letterman, R.D., Quon, J. and Gemmell, R.S., 1974. Film transport coefficient in agitated suspensions of activated carbon. Journal (Water Pollution Control Federation), 2536-2546.

Li, L., Quinlivan, P.A. and Knappe, D.R.U., 2002. Effects of activated carbon surface chemistry and pore structure on the adsorption of organic contaminants from aqueous solution. Carbon 40(12), 2085-2100.

Li, M., 2014. Effects of Natural Organic Matter on Contaminant Removal by Superfine Powdered Activated Carbon Coupled with Microfiltration Membranes.

Matsui, Y., Aizawa, T., Kanda, F., Nigorikawa, N., Mima, S. and Kawase, Y., 2007. Adsorptive removal of geosmin by ceramic membrane filtration with super-powdered activated carbon. Journal of Water Supply: Research & Technology-AQUA 56.

Matsui, Y., Ando, N., Sasaki, H., Matsushita, T. and Ohno, K., 2009a. Branched pore kinetic model analysis of geosmin adsorption on super-powdered activated carbon. Water Research 43(12), 3095-3103.

Matsui, Y., Ando, N., Yoshida, T., Kurotobi, R., Matsushita, T. and Ohno, K., 2011. Modeling high adsorption capacity and kinetics of organic macromolecules on super-powdered activated carbon. Water research 45(4), 1720-1728.

Matsui, Y., Hasegawa, H., Ohno, K., Matsushita, T., Mima, S., Kawase, Y. and Aizawa, T., 2009b. Effects of super-powdered activated carbon pretreatment on coagulation and trans-membrane pressure buildup during microfiltration. Water Research 43(20), 5160-5170.

Matsui, Y., Murase, R., Sanogawa, T., Aoki, N., Mima, S., Inoue, T. and Matsushita, T., 2004. Micro-ground powdered activated carbon for effective removal of natural organic matter during water treatment. Water Science & Technology: Water Supply 4(4).

Matsui, Y., Murase, R., Sanogawa, T., Aoki, N., Mima, S., Inoue, T. and Matsushita, T., 2005. <Rapid adsorption pretreatment with submicrometre powdered activated carbon particles before microfiltration.pdf>. Water Science & Technology 51(6-7), 7.

Matsui, Y., Nakano, Y., Hiroshi, H., Ando, N., Matsushita, T. and Ohno, K., 2010. Geosmin and 2-methylisoborneol adsorption on super-powdered activated carbon in the presence of natural organic matter. Water Science & Technology 62(11).

Matsui, Y., Nakao, S., Sakamoto, A., Taniguchi, T., Pan, L., Matsushita, T. and Shirasaki, N., 2015. Adsorption capacities of activated carbons for geosmin and 2-methylisoborneol vary with activated carbon particle size: Effects of adsorbent and adsorbate characteristics. Water Research 85, 95-102.

Matsui, Y., Nakao, S., Taniguchi, T. and Matsushita, T., 2013. Geosmin and 2-methylisoborneol removal using superfine powdered activated carbon: Shell adsorption and branched-pore kinetic model analysis and optimal particle size. Water research 47(8), 2873-2880.

Matsui, Y., Sakamoto, A., Nakao, S., Taniguchi, T., Matsushita, T., Shirasaki, N., Sakamoto, N. and Yurimoto, H., 2014. Isotope Microscopy Visualization of the Adsorption Profile of 2-Methylisoborneol and Geosmin in Powdered Activated Carbon. Environmental Science & Technology 48(18), 10897-10903.

Matsui, Y., Yoshida, T., Nakao, S., Knappe, D.R.U. and Matsushita, T., 2012. Characteristics of competitive adsorption between 2-methylisoborneol and natural organic matter on superfine and conventionally sized powdered activated carbons. Water Research 46(15), 4741-4749.

Mende, S., Stenger, F., Peukert, W. and Schwedes, J., 2003. Mechanical production and stabilization of submicron particles in stirred media mills. Powder Technology 132(1), 64-73.

Mende, S., Stenger, F., Peukert, W. and Schwedes, J., 2004. Production of sub-micron particles by wet comminution in stirred media mills. Journal of Materials Science 39(16), 5223-5226.

Moreno-Castilla, C., 2004. Adsorption of organic molecules from aqueous solutions on carbon materials. Carbon 42(1), 83-94.

Najm, I.N., Snoeyink, V.L., Suidan, M.T., Lee, C.H. and Richard, Y., 1990. Effect of Particle Size and Background Natural Organics on the Adsorption Efficiency of PAC. Journal (American Water Works Association) 82(1), 65-72.

Pan, L., Matsui, Y., Matsushita, T. and Shirasaki, N., 2015. Effect of activated carbon particle size on equilibrium adsorption capacity in the range of 200 nm to 2 mm, Beijing, China.

Pan, L., Matsui, Y., Matsushita, T. and Shirasaki, N., 2016. Superiority of wet-milled over dry-milled superfine powdered activated carbon for adsorptive 2-methylisoborneol removal. Water Research 102, 516-523.

Partlan, E., Davis, K., Ren, Y., Apul, O.G., Mefford, O.T., Karanfil, T. and Ladner, D.A., 2016. Effect of bead milling on chemical and physical characteristics of activated carbons pulverized to superfine sizes. Water Research 89, 161-170.

Patel, C.M., Chakraborty, M. and Murthy, Z.V.P., 2014. Study on the stability and microstructural properties of barium sulfate nanoparticles produced by nanomilling. Advanced Powder Technology 25(1), 226-235.

Patel, C.M., Chakraborty, M. and Murthy, Z.V.P., 2015. Influence of pH on the Stability of Alumina and Silica Nanosuspension Produced by Wet Grinding. Particulate Science and Technology 33(3), 240-245.

Peel, R.G. and Benedek, A., 1980. Attainment of equilibrium in activated carbon isotherm studies. Environmental Science & Technology 14(1), 66-71.

Pendleton, P., Wong, S.H., Schumann, R., Levay, G., Denoyel, R. and Rouquero, J., 1997. Properties of activated carbon controlling 2-Methylisoborneol adsorption. Carbon 35(8), 1141-1149.

Qiu, J.-Y., Hotta, Y., Watari, K., Mitsuishi, K. and Yamazaki, M., 2006. Low-temperature sintering behavior of the nano-sized AlN powder achieved by super-fine grinding mill with Y2O3 and CaO additives. Journal of the European Ceramic Society 26(4–5), 385-390.

Quinlivan, P.A., Li, L. and Knappe, D.R.U., 2005. Effects of activated carbon characteristics on the simultaneous adsorption of aqueous organic micropollutants and natural organic matter. Water Research 39(8), 1663-1673.

Song, X., Liu, H., Cheng, L. and Qu, Y., 2010. Surface modification of coconut-based activated carbon by liquid-phase oxidation and its effects on lead ion adsorption. Desalination 255(1), 78-83.

Stenger, F., Mende, S., Schwedes, J. and Peukert, W., 2005. Nanomilling in stirred media mills. Chemical Engineering Science 60(16), 4557-4565.

Wang, Y., Rao, G.Y. and Hu, J.Y., 2011. Adsorption of EDCs/PPCPs from drinking water by submicron-sized powdered activated carbon. Water Science and Technology: Water Supply 11(6), 711-718.

Chapter 4. Micro-milling of Spent Granular Activated Carbon for Its Possible Reuse as Adsorbent: Remaining Capacity and Characteristics

4.1 Chapter introduction

Adsorption by granular activated carbon (GAC) is widely used in drinking water treatment to remove disinfection byproduct precursors (DBPPs), natural organic matter (NOM), and organic micro-pollutants (OMPs); GAC adsorption also serves as a barrier, inter alia, to occasional spikes of toxic substances in source waters (Corwin et al., 2012; Matsui et al., 2002b; Owen, 1998; Paune et al., 1998). Because of the limited adsorption capacity of GAC, however, removal of these compounds requires that the GAC be replaced from time to time. Otherwise, removal efficiencies deteriorate with time as the GAC filtration operation progresses. Before the breakthrough of a target adsorbate, the GAC needs to be replaced if the removal ability of the adsorbate is to be maintained. Normally, the spent GAC goes through a regeneration process because it is more cost effective to regenerate spent GAC than to purchase virgin GAC (Lambert et al., 2002; Sontheimer et al., 1988). Spent GAC is sometimes replaced with virgin GAC, for example, when the cost of virgin GAC at the market is similar to or somewhat higher than the cost of regeneration (Iwamoto et al., 2014).

In the regeneration process, adsorption sites on the GAC are refreshed by desorption, decomposition, or degradation of the adsorbates loaded on the GAC. Although regeneration restores the adsorption capacity of the GAC to an extent that depends on the regeneration process employed, there are many disadvantages to regeneration. Those disadvantages include 1) for thermal regeneration, high energy demand, loss of GAC itself, accumulation of metals in the GAC, and the high pH of water initially treated by the regenerated GAC (Lambert et al., 2002; San Miguel et al., 2001); 2) for chemical regeneration, the requirement for additional treatment to deal with the regenerants, such as organic solvents, that remain in the regenerated GAC, and the formation of by-products during regeneration (Alvarez et al., 2004; Lim et al., 2005; Martin et al., 1985); 3) for biological regeneration, the long reaction time required for regeneration and the failure of adsorption sites loaded with non-biodegradable adsorbates to recover (Nakano et al., 2000; Scholz et al., 1998). There is hence a need for an alternative option to use spent GAC without regeneration.

As mentioned above, the frequency of GAC replacement is determined by the breakthrough behavior of target compounds. In water treatment plants, where multiple adsorbates are targeted for removal, the frequency of GAC replacement is determined by the earliest breakthrough of the multiple target adsorbates. Previous research has shown that NOM and DBPPs break through GAC adsorbers earlier than OMPs when these compounds coexist as mixtures in water (Kennedy et al., 2015; Summers et al., 2013). Thus, the adsorption capacities may still remain for OMPs even when the GAC has been replaced as a result of the breakthrough of NOMs and/or DBPPs.

The adsorption capacity that remains in spent GAC is likely to be low compared with the capacity of virgin and regenerated GAC. However, the disadvantage of low capacity can be compensated for if the adsorptive kinetics of the carbon is high. When spent GAC is milled into small-size particles, the increase of the exterior specific surface area leads to high adsorption kinetics that enhance the uptake rate of adsorbates. Extremely high adsorption kinetics has been reported for superfine powdered activated carbon (SPAC) with a particle diameter ≅1 μm; SPAC is produced by the micro-milling of virgin powdered activated carbon (Bonvin et al., 2016; Matsui et al., 2004; Matsui et al., 2013a).

Particle size reduction, moreover, can be expected to enhance adsorption capacities as well as adsorption kinetics (Bonvin et al., 2016; Hu et al., 2015; Knappe et al., 1999; Matsui et al., 2010). Enhancement of adsorption capacity may be mandatory for reuse of spent GAC because even very high kinetics cannot compensate for the disadvantage of inadequate capacity.

The objective of this research was to investigate the production of PAC, SPAC, and submicron-sized SPAC from spent GAC and the application of these as adsorbents to remove OMPs, in particular, 2-methylisoborneol (MIB), which is a conventional target OMP due to its association with an unpleasant earthy/musty taste and odor, which impair the palatability of drinking water (Cook et al., 2001; Newcombe et al., 1997). Changes of equilibrium adsorption capacities and adsorptive removal rates with carbon particle size and carbon age are discussed in conjunction with the metrics of standard indicators of activated carbon characteristics.

4.2 Objectives and approaches

The 1st objective of this chapter is to investigate the MIB adsorption performance of PAC, SPAC, and SSPAC produced from used GAC and compare them with that of virgin PAC to clarify the possibility of reuse used GACs by milling them to small adsorbents. For the 2nd objective, it has meaning for practical application if one or more indices of AC evaluation can indicate the remaining MIB adsorption capacity in used AC. Four common indices AC evaluation used in practical use will be tested on the carbons used in this research. Thirdly, the mechanism of different adsorption capacity showed by different sized and different aged AC is explained according to the physiochemical properties of both adsorbates and adsorbents.

4.3 Experimental

4.3.1 Activated carbons (adsorbents)

Table 4-1. The information of collected used GAC

Designation	Water purification plant	Years used	Raw material	Producer	Production area
KM0-GAC	Kanamachi (Bureau of Waterworks Tokyo Metropolitan Government)	0 (virgin)	Bituminouscoal	Norit Japan Co.,Ltd.	USA
KM1-GAC		1 (2012–2013)			
KM2-GAC		2 (2012–2014)			
KM3-GAC		3 (2012–2015)			
KM4-GAC		4 (2007–2011)		Shanxi Xinhua Chemical Co., Ltd	China
KM6-GAC		6 (2006–2012)			
KM9-GAC		9 (2003–2012)	Coal	Calgon Carbon Japan KK.	Japan
AS1-GAC	Asaka (Bureau of Waterworks Tokyo Metropolitan Government)	1 (2014–2015)	Bituminouscoal	Unknown	Unknown
AS2-GAC		2 (2013–2015)			
AS7-GAC		7 (2006–2013)	Unknown	Joint venture of Kuraray Chemical Co. ., Ltd and Osaka Gas Chemicals Co., Ltd	Colombia
KS0-GAC	Kasumigaura (Ibaraki Prefectural Government)	0 (regenerated)	Coconut shell	Serachem Co., Ltd	Japan
KS0.1-GAC		0.1 (2016.06–2016.07)			
KS0.3-GAC		0.3 (2016.04–2016.07)			
IS4-GAC	Ishikari (Ishikari-Seibu Water Supply Association)	4 (2012-2016)	Bituminouscoal	Dainen Co., Ltd	Japan

GACs were collected from GAC beds of drinking water treatment plants operated by the Bureau of Waterworks of the Tokyo Metropolitan Government, the Public Enterprise Bureau of Ibaraki Prefectural Government, and the Ishikari-Seibu Water Supply Authority (Table 4-1). After being thoroughly mixed, each GAC was separated into several portions and kept under a moist condition at 4 °C in a refrigerator. Some portions were sterilized by autoclaving or gamma ray irradiation, which are described in detail in section 4.3.3. Unless specified, the sterilized samples discussed in this paper refer to the samples autoclaved at 63 °C for 30 min.

The GACs were pulverized into fine particles of three particle-size categories according to their median diameter (D50): 1) powdered activated carbon (PAC, D50: 12–42 μm), superfine PAC (SPAC, D50: 0.9–3.5 μm), and submicron-sized SPAC (SSPAC, D50: 0.22–0.29 μm). The GACs had D50s of

1.5–2.3 mm. The details of the pulverization process and the particle size distributions of all carbon samples are described in section 4.3.2. The activated carbon samples were given unique three-term designations as follows. The first term indicates the name of the water treatment plant where the GAC was collected and the number of years the GAC was used. The second term indicates the method of pretreatment of the GAC. An “n” indicates “no pretreatment”, “a” indicates “autoclave pretreatment”, and “g” indicates “gamma irradiation pretreatment”. The final term indicates the particle size category of the carbon: GAC, PAC, SPAC, and SSPAC. KM2-a-SPAC, for example, means SPAC produced by milling from autoclaved GAC, which was sampled at the Kanamachi Water Treatment Plant after being used for 2 years. The carbons produced from the GACs given no pretreatment were used for adsorption experiments with carbon-water contact times < one day. Those produced from the GACs pretreated by autoclaving were used for adsorption experiments with carbon-water contact times > one day to avoid any biodegradation effect. Autoclaving did not substantially influence the equilibrium adsorption capacity (see section 4.4.1). The PAC, SPAC, and SSPAC samples were stored in ultrapure water in the form of slurries at concentrations of 9–22 g/L at 4 °C after vacuum conditioning for 20 min to remove any air from the activated carbon pores.

The pore size distributions of the activated carbons were obtained by using the nitrogen gas adsorption-desorption method (Autosorb-iQ, Quantachrome Instruments, Kanagawa, Japan). The isotherm data for nitrogen gas at 77.4 K was analyzed by (1) the Barrett-Joyner-Halenda (BJH) method for the mesopore region (pore width >2 nm) and (2) the quench solid density functional theory (QSDFT) for the micropore region (pore width = 0.6–2 nm) (ASiQwin, ver.3.01, Quantachrome Instruments). Iodine, phenol, methylene blue (MB), and sodium liner-dodecylbenzene sulfonates (hereafter ABS) numbers were measured according to the standard methods of the Japan Water Works Association (K 113:2005-2) (JWWA, 2005). The details of the measurement methods are described in section 4.3.6.

4.3.2 Production of PAC, SPAC, and SSPAC from GAC

PAC samples were produced from GACs by grinding with a coffee mill under moist conditions followed by grinding with a mortar and pestle under wet conditions after addition of pure water. A 180-µm-sized mesh was used to sieve the ground carbon, and the carbon particles that did not pass the mesh were collected and ground again until they passed the mesh. SPAC with D50 >1.5 µm were produced by milling a PAC slurry in a ball mill (Nikkato Ltd., Osaka, Japan) with a mixture of balls (5-mm and 10-mm balls). To produce SPAC (0.5 µm < D50 <1.5 µm) and SSPAC, the SPAC with D50 >1.5 µm was micro-milled in a bead mill (LMZ015, Ashizawa Finetech Ltd., Chiba, Japan; bead diameter, 0.1 mm).

The particle size (as projected-area diameter) distribution of the GAC was determined by image analysis of pictures taken through a microscope (Viewtrac, MicrotracBEL Corp., Osaka, Japan). Particle size distributions of the SPACs and PACs were determined by using a laser-light-scattering instrument (Microtrac MT3300EXII, Nikkiso Co., Tokyo, Japan) after addition of a dispersant (Triton X-100, Kanto Chemical Co., Tokyo, Japan; final concentration, 0.8 g/L) and subsequent ultrasonic dispersion. All the

size distributions of carbons used are in Fig. 4-1. All activated carbon samples with the related experimental contents were listed in Table 4-2, 4-3, 4-4.

(a)

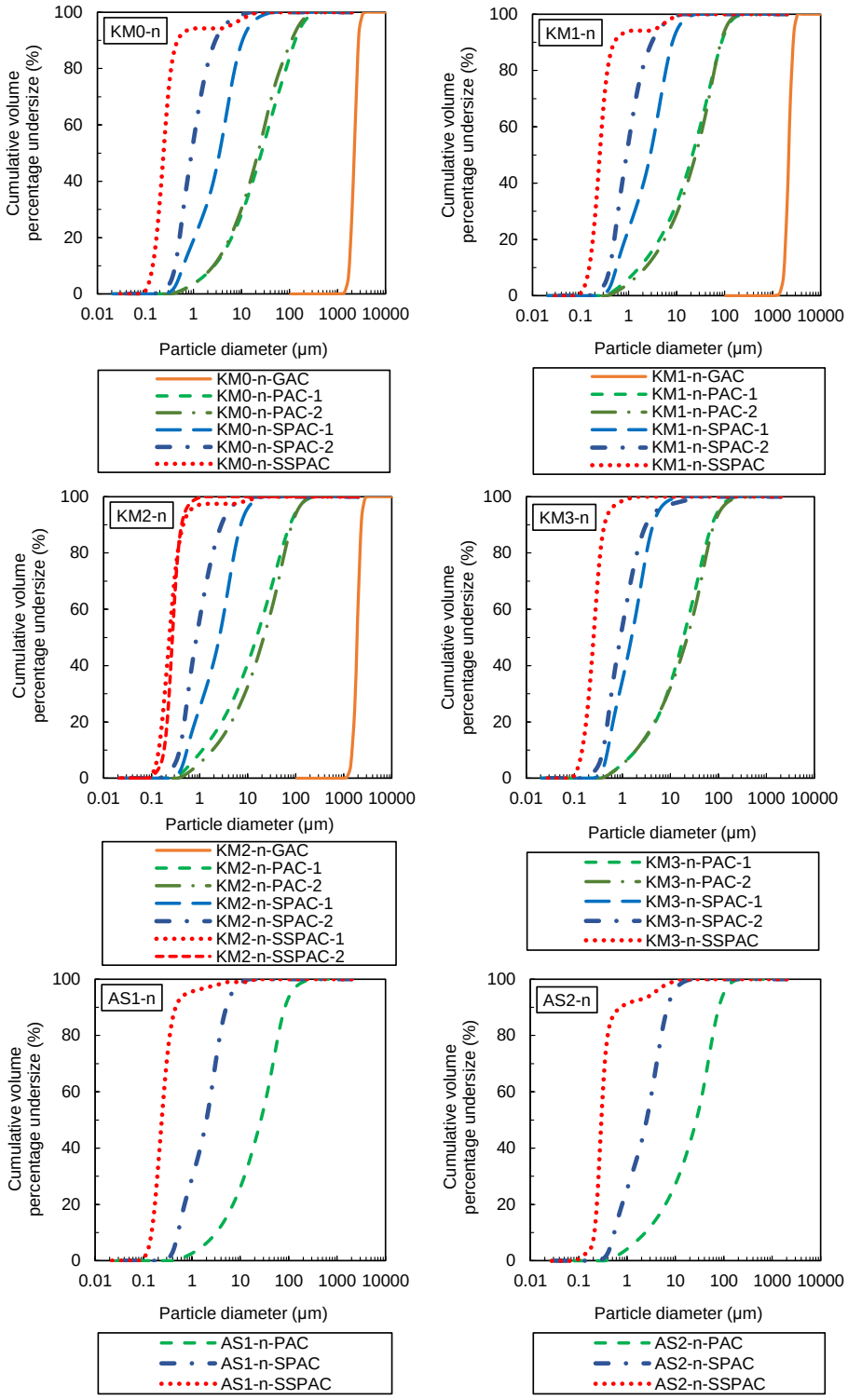

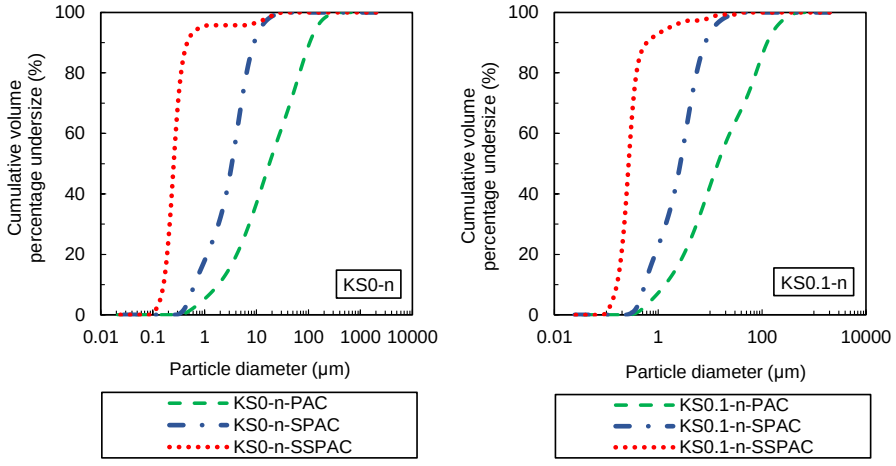
Cumulative volume percentage undersize (%)
Particle diameter (μm)
KS0-n
KS0-n-PAC
KS0-n-SPAC
KS0-n-SSPAC
KS0.1-n
KS0.1-n-PAC
KS0.1-n-SPAC
KS0.1-n-SSPAC

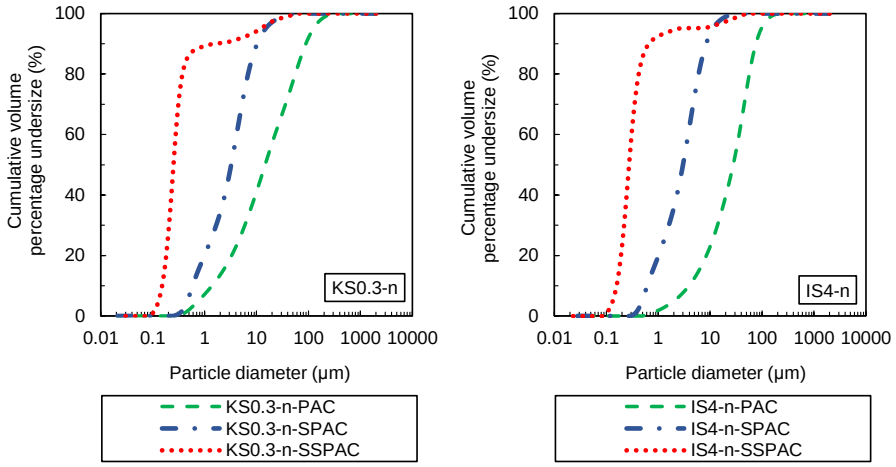
Cumulative volume percentage undersize (%)
Particle diameter (μm)
KS0.3-n
KS0.3-n-PAC
KS0.3-n-SPAC
KS0.3-n-SSPAC
IS4-n
IS4-n-PAC
IS4-n-SPAC
IS4-n-SSPAC

(b)

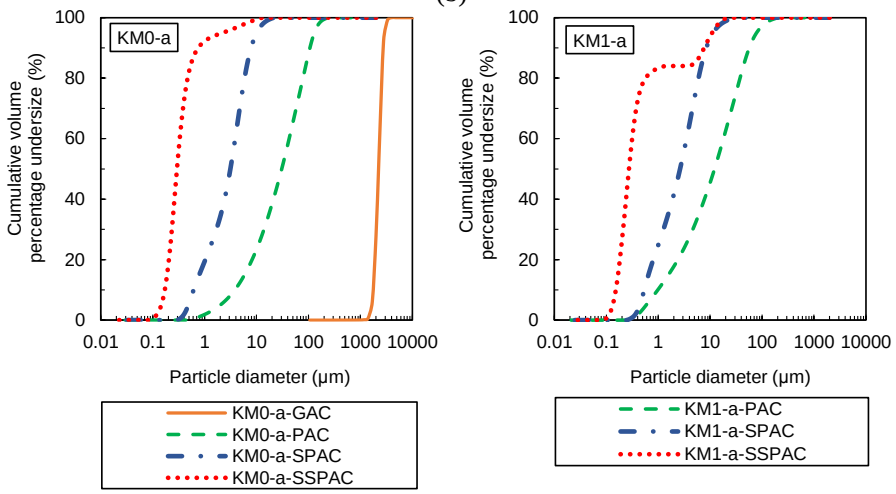
Cumulative volume percentage undersize (%)
Particle diameter (μm)
KM0-a
KM0-a-GAC
KM0-a-PAC
KM0-a-SPAC
KM0-a-SSPAC
KM1-a
KM1-a-PAC
KM1-a-SPAC
KM1-a-SSPAC

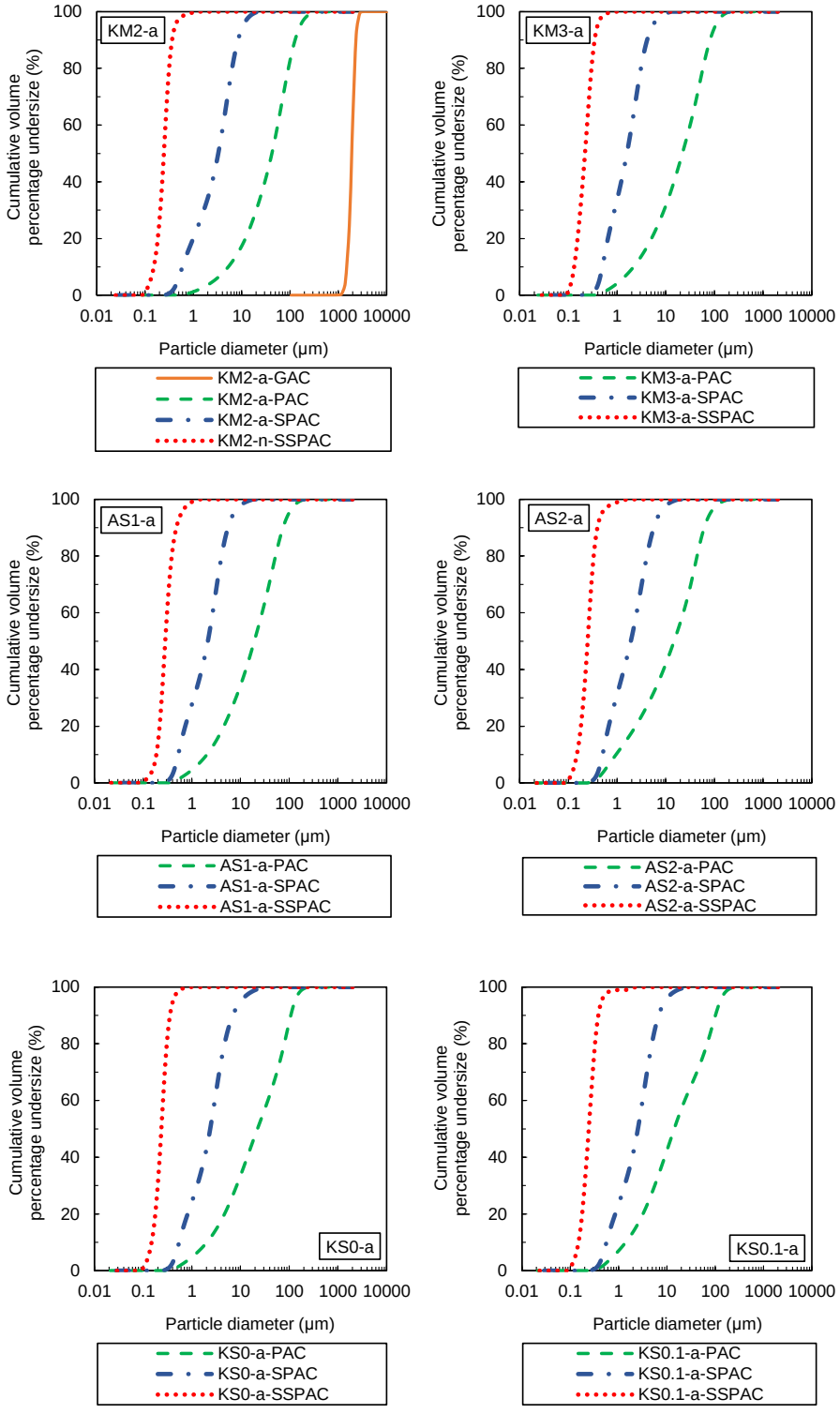
KM2-a
Cumulative volume percentage undersize (%)
Particle diameter (μm)
KM2-a-GAC
KM2-a-PAC
KM2-a-SPAC
KM2-n-SSPAC
KM3-a
KM3-a-PAC
KM3-a-SPAC
KM3-a-SSPAC
AS1-a
AS1-a-PAC
AS1-a-SPAC
AS1-a-SSPAC
AS2-a
AS2-a-PAC
AS2-a-SPAC
AS2-a-SSPAC
KS0-a
KS0-a-PAC
KS0-a-SPAC
KS0-a-SSPAC
KS0.1-a
KS0.1-a-PAC
KS0.1-a-SPAC
KS0.1-a-SSPAC

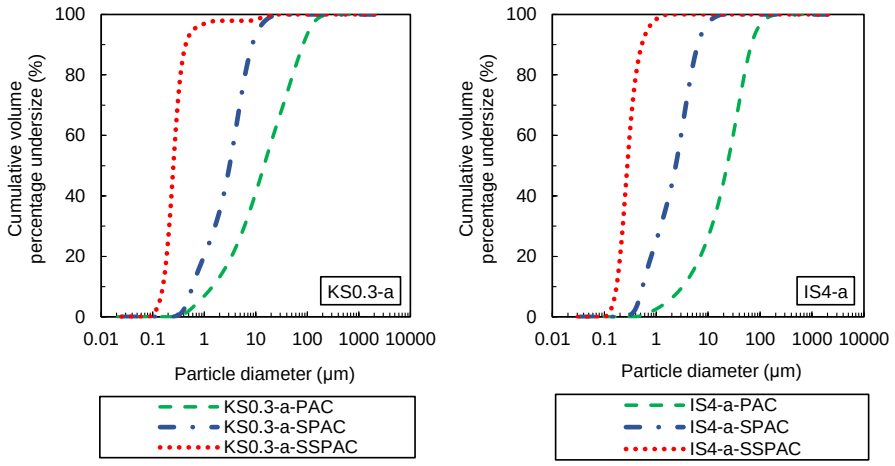

Fig. 4-1. The particle size distribution of GAC/PAC/SPAC/SSPAC used in main script.

Table 4-2. No-autoclave pretreated carbons used for MIB kinetics and adsorption index experiments.

Designation	Parent GAC	Applied experiments	D_{50} (μm)
KM0-n-GAC	KM0-n-GAC	MIB adsorption kinetics	2240
KM0-n-PAC-1		MIB adsorption kinetics; Methylene blue (MB) number	25.9
KM0-n-PAC-2		Iodine number; Phenol number; sodium liner-dodecylbenzene sulfonate (ABS) number	22.1
KM0-n-SPAC-2		MIB adsorption kinetics	0.917
KM0-n-SPAC-1		Iodine number; Phenol number; MB number; ABS number	3.49
KM0-n-SSPAC		MIB adsorption kinetics; Iodine number; Phenol number; MB number; ABS number	0.238
KM1-n-GAC	KM1-n-GAC	MIB adsorption kinetics	2170
KM1-n-PAC-1		MIB adsorption kinetics; MB number	21.5
KM1-n-PAC-2		Iodine number; Phenol number; ABS number	25.1
KM1-n-SPAC-2		MIB adsorption kinetics	0.911
KM1-n-SPAC-1		Iodine number; Phenol number; MB number; ABS number	2.84
KM1-n-SSPAC		MIB adsorption kinetics; Iodine number; Phenol number; MB number; ABS number	0.251
KM2-n-GAC	KM2-n-GAC	MIB adsorption kinetics	1910
KM2-n-PAC-1			15.3
KM2-n-PAC-2		Iodine number; Phenol number; MB number; ABS number	21.5
KM2-n-SPAC-2		MIB adsorption kinetics	0.860
KM2-n-SPAC-1		Iodine number; Phenol number; MB number; ABS number	2.57

KM2-n-SSPAC-1		MIB adsorption kinetics; MB number	0.234
KM2-n-SSPAC-2		Iodine number; Phenol number, ABS number	0.271
KM3-n-PAC-1	KM3-n-GAC	MIB adsorption kinetics	18.8
KM3-n-PAC-2		Iodine number; Phenol number	22.5
KM3-n-SPAC-2		MIB adsorption kinetics;	0.912
KM3-n-SPAC-1		Iodine number; Phenol number	1.56
KM3-n-SSPAC		MIB adsorption kinetics; Iodine number; Phenol number	0.252
AS1-n-PAC	AS1-n-GAC	Iodine number	26.6
AS1-n-SPAC			1.99
AS1-n-SSPAC			0.237
AS2-n-PAC	AS2-n-GAC		27.1
AS2-n-SPAC			2.53
AS2-n-SSPAC			0.294
KS0-n-PAC	KS0-n-GAC		17.6
KS0-n-SPAC			3.34
KS0-n-SSPAC			0.253
KS0.1-n-PAC	KS0.1-n-GAC		14.0
KS0.1-n-SPAC			2.65
KS0.1-n-SSPAC			0.268
KS0.3-n-PAC	KS0.3-n-GAC		14.6
KS0.3-n-SPAC			3.24
KS0.3-n-SSPAC			0.251
IS4-n-PAC	IS4-n-GAC		27.8
IS4-n-SPAC			2.99
IS4-n-SSPAC			0.274

Table 4-3. Autoclave-pretreated carbons used for adsorption equilibrium experiments.

Designation	Parent GAC	Applied experiments	D_{50} (μm)
KM0-a-GAC	KM0-a-GAC	Adsorption equilibrium of MIB in natural water	2240
KM0-a-PAC		Adsorption equilibrium of MIB in natural water; Adsorption equilibrium of MIB, geosmin, acetaminophen, phenol, poly(styrenesulfonic acid) sodium salt MW210 (PSS-210), PSS-6400, MB, ABS in organic-free ionic water; N_2 adsorption (Pore size distribution)	31.1
KM0-a-SPAC			3.13
KM0-a-SSPAC			0.293
KM1-a-PAC	KM1-a-GAC	Adsorption equilibrium of MIB in natural water; N_2 adsorption (Pore size distribution)	12.1
KM1-a-SPAC			2.63
KM1-a-SSPAC			0.273
KM2-a-GAC	KM2-a-GAC	Adsorption equilibrium of MIB in natural water	1910
KM2-a-PAC		Adsorption equilibrium of MIB in natural water;	42.3

KM2-a-SPAC		Adsorption equilibrium of MIB, geosmin, acetaminophen, phenol, PSS-210, PSS-6400, MB, ABS in organic-free ionic water; N_2 adsorption (Pore size distribution)	3.28
KM2-a-SSPAC			0.246
KM3-a-PAC	KM3-a-GAC	Adsorption equilibrium of MIB in natural water; N_2 adsorption (Pore size distribution)	21.9
KM3-a-SPAC			1.59
KM3-a-SSPAC			0.218
AS1-a-PAC	AS1-a-GAC	Adsorption equilibrium of MIB in natural water	19.2
AS1-a-SPAC			2.13
AS1-a-SSPAC			0.284
AS2-a-PAC	AS2-a-GAC		14.8
AS2-a-SPAC			1.91
AS2-a-SSPAC			0.248
KS0-a-PAC	KS0-a-GAC		22.3
KS0-a-SPAC			2.38
KS0-a-SSPAC			0.236
KS0.1-a-PAC	KS0.1-a-GAC		14.2
KS0.1-a-SPAC			2.51
KS0.1-a-SSPAC			0.241
KS0.3-a-PAC	KS0.3-a-GAC		14.5
KS0.3-a-SPAC			3.10
KS0.3-a-SSPAC			0.252
IS4-a-PAC	IS4-a-GAC		23.1
IS4-a-SPAC			2.37
IS4-a-SSPAC			0.277

4.3.3 AC samples used in preliminary tests

Preliminary experiments were conducted to briefly observe the removal of MIB by PAC and SPAC produced from GACs that had been used for ≥4 years at water purification plants in Tokyo. The selection of ≥4 years was based on the fact that GACs were replaced every 4–9 years at the water purification plants. SPACs and PACs were produced from GACs by a combination of pulverization with a food processor and a wet-milling bead mill (size distributions in Fig. 4-2). Table 4-4 provides relevant information about the carbons.

Table 4-4. Carbons usage information in Preliminary Tests

Designation	Parent GAC	Pretreatment of MIB adsorption equilibrium tests	D_{50} (μm)
KM4-n-GAC	KM4-GAC	None	2170
KM4-n-PAC			16.1
KM4-n-SPAC			0.651
KM6-n-GAC	KM6-GAC	None	2100
KM6-n-PAC			22.2
KM6-a-PAC (121 °C)		Autoclave at 121 °C for 15 min	
KM6-a-PAC (63 °C)		Autoclave at 63 °C for 30 min	
KM6-n-SPAC		None	0.725
KM9-n-GAC	KM9-GAC	None	1700
KM9-n-PAC			11.5
KM9-n-SPAC			0.558
AS7-n-GAC	AS7-GAC	None	1290
AS7-n-PAC			10.5
AS7-n-SPAC			0.733
KM2-n-PAC-3	KM2-GAC	None	17.4
KM2-a-PAC		Autoclave at 63 °C for 30 min	42.3
KM2-g-PAC		Gamma ray irradiation under 10.5 ± 0.2 kGy dosage	17.8

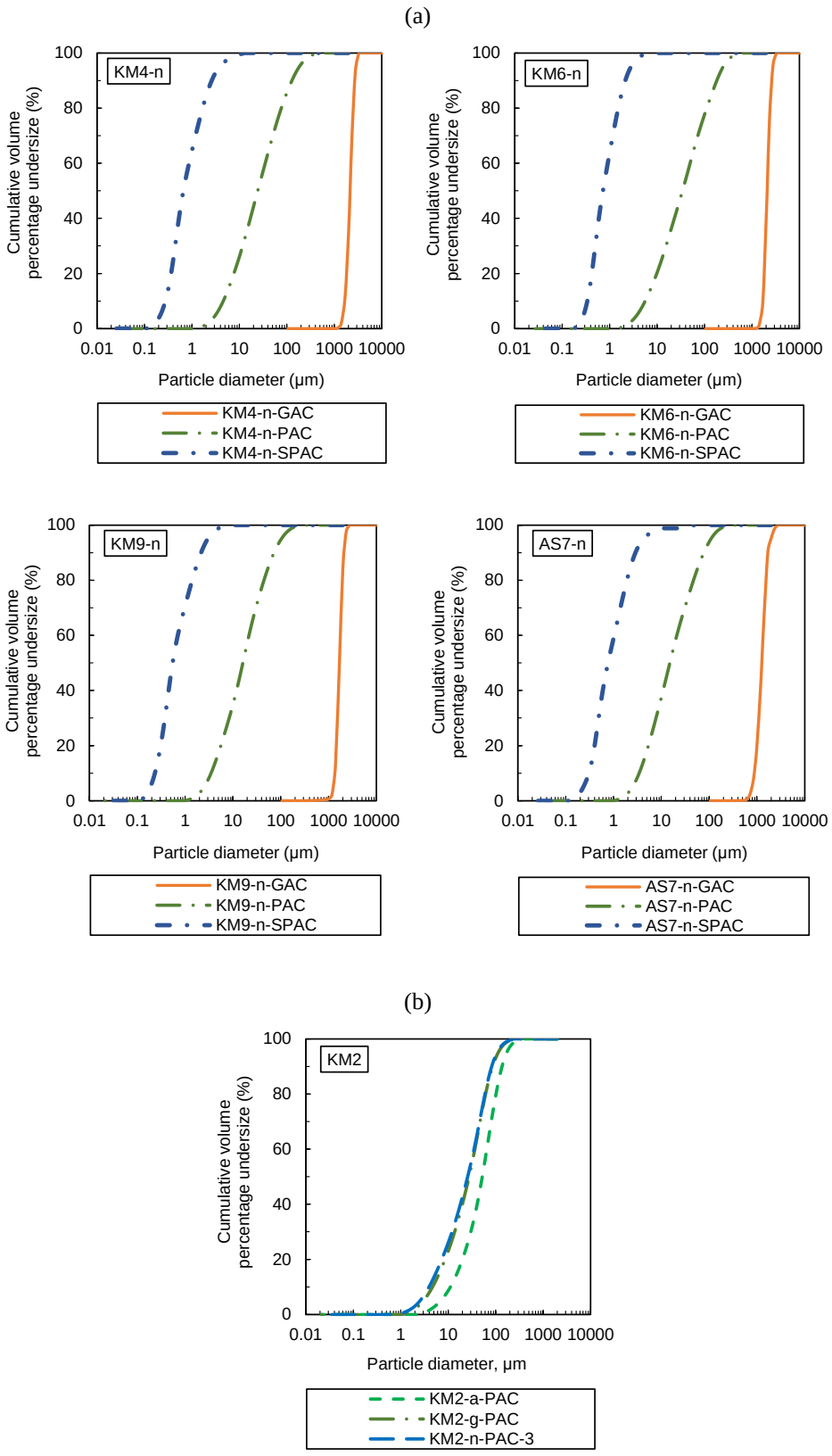

Fig. 4-2. The particle size distribution of carbons used in Preliminary Tests

4.3.4 Adsorbates

MIB was the main target compound in this study. Regent MIB was dissolved in natural water (the raw water entering the Kanamachi Water Purification Plant, the same plant where the main target GACs were collected) or in organic-free ionic water that was made from ultrapure water by adding ions at concentrations identical to their concentrations in the natural water (details are provided in section S4 of the SI). The concentrations of MIB were measured by using deuterium-labeled geosmin (geosmin-d3) as an internal standard in a purge-and-trap concentrator (P&T) coupled to a gas chromatograph-mass spectrometer (GC/MS); the *m/z* 95 peak was assumed to correspond to MIB and the *m/z* 115 peak to geosmin-d3. Two P&T-GC/MS systems were used: (1) a Model 4660 Eclipse (Kinryo Electric Co., LTD, Osaka, Japan) coupled with an Agilent 7890A/5975MSD (Agilent Technologies, Inc., CA, USA); and (2) an Aqua PT 5000 J (GL Sciences, Inc., Tokyo, Japan) coupled with a GCMS-QP2010 Plus (Shimadzu Co., Kyoto, Japan).

In addition to MIB, some compounds with environmental relevancy and compounds used for adsorbability indices were tested as supplementary adsorbates: geosmin, iodine, phenol, acetaminophen, MB, ABS, poly(styrenesulfonic acid) sodium salt with an average molecular weight (MW) of 210 (PSS-210), and PSS-6400 with average MW 6400. These compounds were selected to cover a variety of hydrophobicities and molecular sizes. Geosmin was detected with a method similar to the method used to detect MIB: the *m/z* 112 peak was assumed to correspond to geosmin. Iodine concentrations were measured by titration with sodium thiosulfate ($Na_2S_2O_3$). The concentrations of other adsorbates were measured by spectrophotometry (UV-1800, Shimadzu Co., Kyoto, Japan): phenol at 269.5 nm; high concentrations of acetaminophen (~2 mg/L) at 244 nm; PSS-210 and PSS-6400 at 261 nm; and MB at 665 nm. Concentrations of ABS were measured by spectrophotometry at 223.5 nm or by TOC analyzer (Sievers 900, Ionics Instrument Business Grp., Boulder Co.). The choice of method was based on the working solutions in the experiments because of the effect of ions on spectrophotometry at wavelengths less than 240 nm. Low concentrations of acetaminophen (~10 μg/L) were quantified by using a hybrid quadrupole-orbitrap mass spectrometer (Q Exactive, Thermo Fisher Scientific Inc., Waltham, MA, USA) coupled with liquid chromatography (UltiMate3000 LC systems, Thermo Fischer Scientific Inc.).

Except PSS-210 and PSS-6400 which were purchased from Sigma-Aldrich Co. LLC. (St. Louis, Missouri, USA), the all mentioned chemical reagents were all purchased from Wako Pure Chemical Industries, Ltd., (Osaka, Japan).

4.3.5 Working solutions and batch adsorption tests

In all adsorption kinetics and equilibrium tests, specified amounts of carbon were added to vials containing either 100 or 110 mL of a solution of the target compound, and the vials were manually shaken and then agitated on a mechanical shaker for a pre-determined period of time at a constant temperature of 20 °C in the dark. The carbon-solution contact time ranged from 10 minutes to 24 hours for the MIB adsorption kinetics tests; it was set to 1–2 weeks for the MIB adsorption equilibrium tests. After the pre-determined carbon-solution contact time, the carbon-solution suspension were each filtered through a

0.2-µm membrane filter (DISMIC-25HP; Toyo Roshi Kaisha, Ltd., Tokyo, Japan, SSPAC-solution suspension was filtered twice) to separate carbon, and the concentrations of the adsorbate in the filtrates were then measured. Solid-phase concentrations of adsorbates were calculated from mass balances.

Four working solutions were prepared and used in this research. Solution A was ultrapure water obtained from a Milli-Q Advantage (Millipore Co., Bedford, MA, USA). Solution B (natural water) was the raw water of the Kanamachi Water Purification Plant, the same plant where we collected the virgin and used carbons that were the main targets of this study. Table 4-5 provides information about the ion concentrations, dissolved organic carbon (DOC), and other related information about this water. Solution C (organic-free ionic water) was made from ultrapure water by adding ions at the same concentrations found in the natural water (working solution B). Working solutions B and C were each filtered through a 0.2-µm pore size membrane filter (Advantec H020A; Toyo Roshi Kaisha, Ltd., Tokyo, Japan), and the pH was adjusted to 7.0 ± 0.1 before the solutions were used in the adsorption experiments. Solution D (phosphate buffer water) was a mixture of potassium dihydrogen phosphate (KH_2PO_4) and potassium monohydrogen phosphate (K_2HPO_4) dissolved in ultrapure water; the pH was maintained at 7.0 ± 0.1.

Working solutions B and C were used for the MIB adsorption experiments after adjusting the concentrations of MIB to about 1 µg/L, because MIB usually occurs naturally at concentrations lower than 1 µg/L. The concentration of geosmin in working solution C was also set to about 1 µg/L for the adsorption experiments. In the adsorption tests with iodine, iodine was dissolved in working solution A together with potassium iodide at 6.35 g-I/L. Starch was used as an indicator. The adsorption experiments with MB were conducted in working solution D because of the pH-dependent characteristics of MB; the MB concentrations were 24 and 0.48 mg/L. Working solutions A and C were used for ABS experiments; the concentration of ABS was 5 mg/L. The other compounds were dissolved in working solution C at appropriate concentrations based on the range of concentrations within which individual compounds could be measured with a UV-VIS spectrophotometer: phenol: 1 mg/L; acetaminophen: 2 mg/L; PSS-210 and PSS-6400: 4 mg/L. An adsorption experiment with acetaminophen at 10 µg/L (low concentration) was also conducted.

In all adsorption kinetics and equilibrium tests, aliquots (100 or 110 mL) of the working solutions containing the target compounds were transferred to 110-mL vials. Specified amounts of carbon were immediately added, and the vials were manually shaken and then agitated on a mechanical shaker to keep shaking for a pre-determined period of time at a constant temperature of 20 °C in the dark. After the pre-determined carbon-solution contact time, the carbon-solution mixtures were each filtered through a 0.2-µm pore size membrane filter (SSPAC-solution mixture was filtered twice), and the concentrations of the adsorbate in the aqueous phase were measured. The carbon-solution contact time ranged from 10 minutes to 24 hours for MIB adsorption kinetics experiments, but it was set to two weeks for the MIB adsorption equilibrium experiments with natural water (working solution B) because of the slow rate of adsorption onto GAC and used carbons in natural water. Adsorption experiments in organic-free ionic water (working solution C) were conducted with PAC, SPAC, and SSPAC to check the adsorption capacity of single target compounds when there was no adsorption competition. The carbon-solution contact time for adsorption equilibrium in organic-free ionic water was shortened to 7 days for all

compounds except phenol (0.5 days), acetaminophen of low concentration (0.5 days), and iodine (15 min) while adsorption equilibria were confirmed.

Table 4-5. The information of natural water working solution

pH	Turbidity	Chroma	Ammonia nitrogen	Conductivity	$KMnO_4$ consumption
7.8	14	7	0.04 mg/L	27 μS/m	8.8 mg/L
Alkalinity	DOC	UV265	MIB	Geosmin	
48 mg/L	1.2 mg/L	0.04 cm^{-1}	5 ng/L	Undetectable	

Ion	Na^+	K^+	Mg^{2+}	Ca^{2+}	Cl^-	NO_3^-	SO_4^{2-}
Concentration (mg/L)	20	3.8	4.9	24	8.0	4.1	31

4.3.6 Absorbability Indices

The amounts of iodine, phenol, MB, and ABS adsorbed onto the carbons at specified liquid-phase concentrations after specified adsorbate-adsorbent contact times were termed the iodine number, phenol number, MB number, and ABS number, respectively. The iodine number was equated to the solid-phase concentration at equilibrium with a liquid-phase concentration of 2.5 g/L after a 15-min contact time in working solution A (see section 4.3.5); the phenol number was equated to the solid-phase concentration measured after a 60-min contact time in working solution C with a liquid-phase concentration of 0.5 mg/L; the MB number was equated to the solid-phase concentration after a 30-min contact time in working solution D at a liquid-phase concentration of 0.24 mg/L; the ABS number was equated to the solid-phase concentration after a 90-min contact time in working solution A at a liquid-phase concentration of 2.5 mg/L. These values were measured according to the standard methods of the Japan Water Works Association (K 113:2005-2) (JWWA, 2005).

(1). Measurement methods for the iodine number and MB number:

A carbon slurry was added to an Erlenmeyer flask that contained 25-mL of 6.35-g/L iodine in an iodine/KI solution or 24 mg/L of MB in a phosphate-buffer solution. After shaking for 15 min for iodine adsorption or 30 min for MB adsorption at 100 rpm at 20 °C, the mixed carbon-solution suspensions were each filtered through a 0.2-μm pore size membrane filter (DISMIC-25HP; Toyo Roshi Kaisha, Ltd., Tokyo, Japan, SSPAC-solution suspension was filtered twice). The concentrations of iodine or MB in the aqueous phase were then measured by titration or spectrophotometry, respectively. The solid-phase concentrations of iodine adsorbed onto the carbon samples at a liquid-phase concentration of 2.5 g/L were calculated based on the obtained adsorption isotherms and defined as iodine numbers. Similarly, the MB number was the carbon solid-phase concentration of MB at a liquid-phase concentration 0.24 mg/L.

(2). Measurement methods for phenol number and ABS number:

Carbon slurries were added to 110-mL vials that contained 1-mg/L phenol in an organic-free ionic solution or 5 mg/L of ABS in pure water. After shaking for 90 min (ABS) or 60 min (phenol) at 100 rpm at 20 °C, the carbon-solution suspensions were each filtered through a 0.2-μm pore size membrane filter (the SSPAC-solution suspension was filtered twice), and then the concentrations of phenol or ABS in the aqueous phase were measured by spectrophotometry. The phenol number and ABS number were equated to the carbon solid-phase concentration of phenol and ABS at liquid-phase concentrations of 0.5 mg/L and 2.5 mg/L, respectively.

4.4 Results and discussion

4.4.1 Preliminary tests for used activated carbons

I. Effect of biological degradation in isotherm experiments

In the batch adsorption equilibrium tests using the spent GACs and the PAC/SPACs produced from the spent GACs, a two-week contact time was used to allow adsorption to reach equilibrium. This contact time was longer than the time (one week or less) used to obtain MIB adsorption isotherms of PAC/SPAC in previous studies (Graham et al., 2000; Matsui et al., 2015; Newcombe et al., 2002a). The reason for choosing a longer contact time was that MIB adsorption by GAC was considered to require a longer contact time to reach adsorption equilibrium than PAC/SPAC due to the larger particle size of GAC and consequently the slow uptake rate. The results were that MIB was not removed by spent GACs and their SPACs, even under the high carbon dosage of 200 mg/L (KM4-n-GAC, KM4-n-SPAC, etc., Fig. S1). However, some of the used carbons with an intermediate size (KM-6-n-PAC, etc.) showed marked MIB removals. These results were obtained for old carbons with ages ≥6 years; more than 90% of the MIB could be removed with a carbon dose of 200 mg/L. Such a high removal was not attained with the 4-year-old carbons.

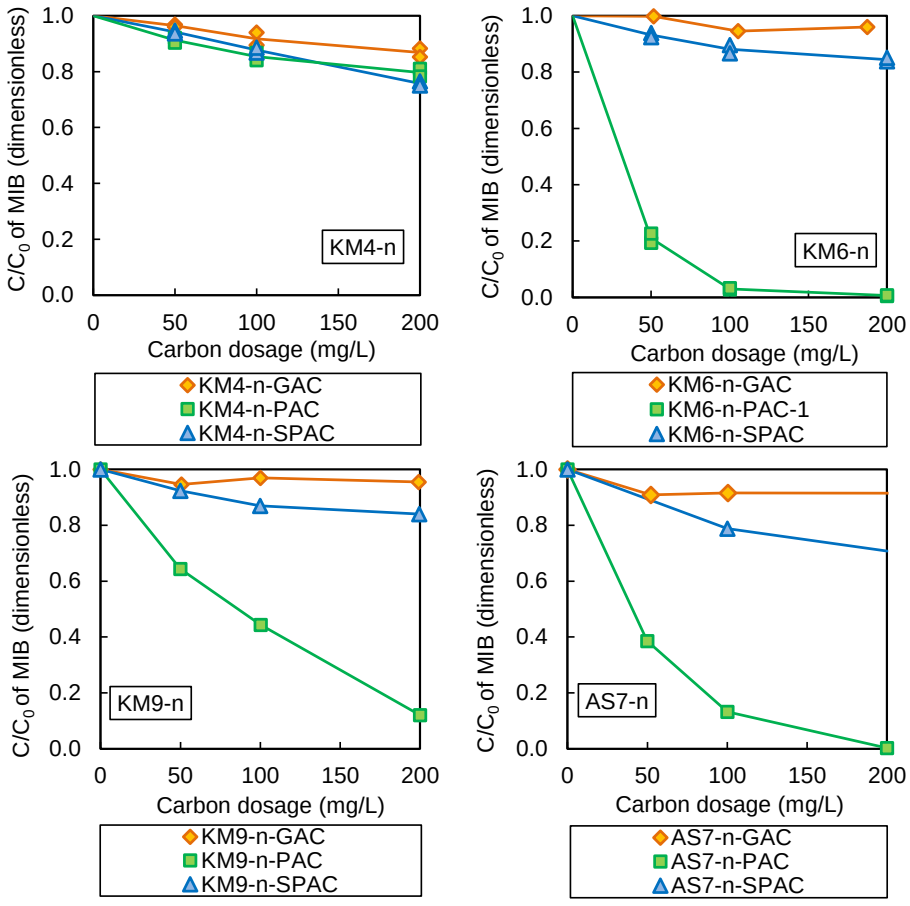

Fig. 4-3. MIB removal rate against carbon dosage at the carbon-water contact time of 2 weeks.

Among possible reasons why only PAC produced from used carbon ≥ 6 years old achieved high MIB removal, we hypothesized that biological degradation might be the reason, and tested this hypothesis. We observed a change of the liquid-phase MIB concentration with the carbon-solution contact time (Fig. 4-4). The concentration of MIB did not decline during the initial two days, but it started to decrease after the 3rd day, and for several days the removal rate accelerated. After the MIB concentration reached <5% of the initial concentration on the 14th day, the MIB stock solution was spiked into a carbon-solution system to raise the MIB concentration back to about 1 μg/L, similar to the MIB concentration at the beginning of the experiment. The MIB concentration decreased immediately after the spike. This behavior is typical of biodegradation. We regard the delay of the onset of the decrease of the MIB concentration during the first two days as a reflection of the acclimation period of the bacteria.

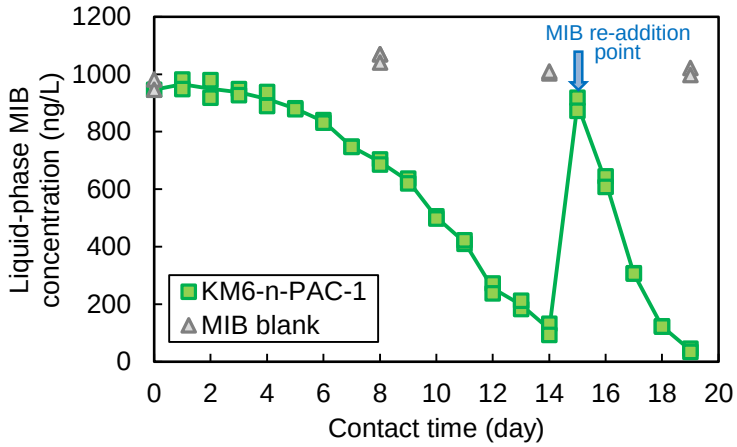

Fig. 4-4. Change of MIB concentration after the addition of KM6-n-PAC with carbon dosage 100 mg/L.

II. Sterilization treatment of used carbons.

To test the biodegradation hypothesis, we sterilized carbons for 30 min and 15 min in an autoclave at 63 °C and 121 °C, respectively. Then we conducted the MIB removal experiments by using the sterilized PACs (KM6-a-PACs), and we carried out a control experiment using un-sterilized PACs (KM6-n-PAC). The MIB concentration did not decrease in the experiment with the sterilized PACs, but it decreased in the experiment with the un-sterilized PACs (Fig. 4-5). The MIB removals attained with the un-sterilized PACs during very long carbon-solution contact, which is typical of isotherm experiments, were a result of biodegradation. The reason for the lack of MIB removal with spent GACs (Fig. 4-3) was likely due to the small surface area exposed to the bulk solution. SPACs showed little or no MIB removal as well (Fig. 4-3), possibly because the bacteria attached to the carbon were physically destroyed in the milling process used to produce the SPAC. SPAC particles are smaller than bacteria. These results also indicated that the MIB adsorption capacity was exhausted after 4 years of service in the water purification plant. We therefore focused on used carbons younger than 4 years in this study.

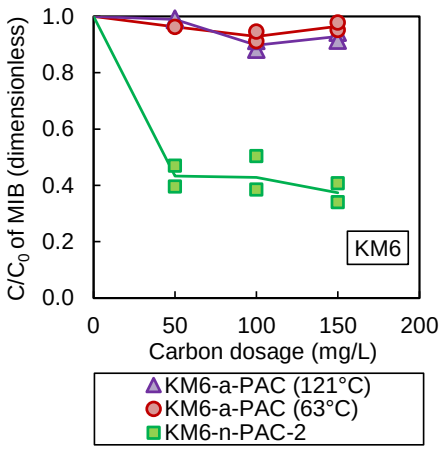

Fig. 4-5. Effect of autoclave treatment on MIB removal under 2-week's carbon-water contact time.

To confirm that there was little effect from autoclaving on the equilibrium MIB adsorption capacity, bottle-point adsorption experiments were conducted with three PACs. KM2-n-PAC was produced by milling two-year-old GAC (KM2-GAC). KM2-a-PAC was produced by autoclaving KM2-n-PAC at 63 °C for 30 min. KM2-g-PAC was produced by sterilizing KM2-n-PAC via gamma ray irradiation at 10.5 ± 0.2 kGy. The MIB removal rates by the three PACs were similar, the indication being that biological degradation of MIB did not occur in the KM2-n-PAC bottles. The lack of biological degradation with the KM2-n-PAC, in contrast to the biological degradation with the KM-6-n-PAC (Fig. 4-3), could be due to the younger age of the KM2-n-PAC. The similarity of the MIB adsorption isotherms of the three PACs (Fig. 4-6) suggests that autoclaving and gamma irradiation pretreatment did not modify the carbon characteristics with respect to adsorption capacity. Finally, we used autoclaved carbons in adsorption equilibrium isotherm tests, which require a long carbon-water contact time, in order to avoid any possible biodegradation effect.

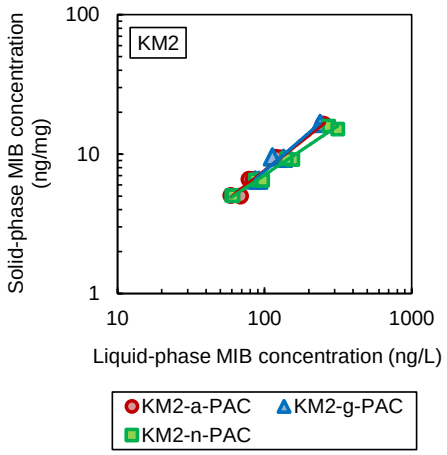

Fig. 4-6. Effect of autoclave and gamma irradiation treatments on the adsorption isotherms of MIB.

III. NOM desorption

The other issue regarding the adsorption experiments with spent carbons was the possibility of NOM desorption from the spent carbons. We monitored the total organic carbon (TOC) and UV absorbance at 260 nm (UV260) of the solution after adding spent carbons (KM9) in natural water supplemented with MIB. In all experiments, the TOC and UV260 did not increase, the indication being that NOM was removed rather than discharged (Fig. 4-7). Even in the experiment with KM2-n-PAC and organic-free ionic water, the increase of UV260 after a high carbon dosage (200 mg/L) was very small (<0.004 cm^{-1}; no graph attached).

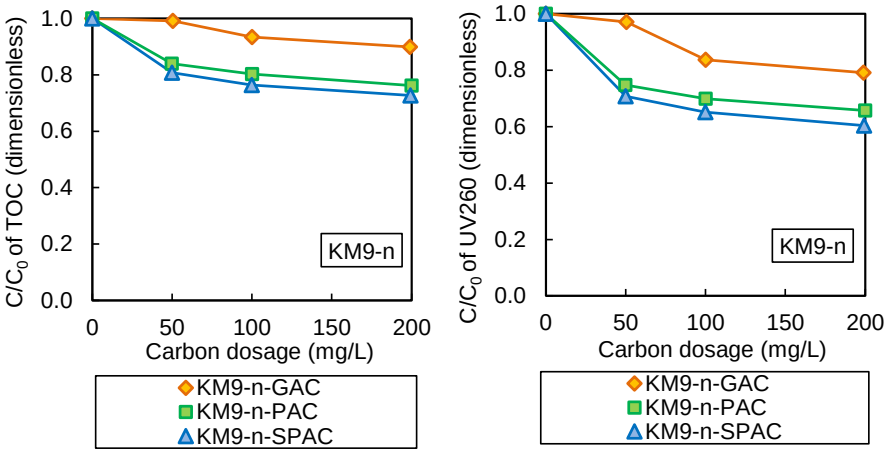

Fig. 4-7. Change of TOC against carbon dosage in adsorption equilibrium (The carbon-water contact time was 2 weeks. Initial TOC and UV260 were 1.15 ± 0.35 mg/L and 0.045 ± 0.25 cm^{-1})**.**

4.4.2 MIB adsorption kinetics.

We tested KM0, KM1, KM2, and KM3 after having determined that four-year old carbons had no adsorptive removal ability (Fig. 4-3). Fig. 4-8 shows the time-course changes of normalized MIB concentrations in the adsorption kinetic tests. Fig. 4-8a shows the results of KM0 (virgin GAC and the PAC and the SPAC produced from it). There were clear increases of MIB removal rates with decreasing particle size when the GAC was milled to PAC and SPAC. The MIB removal rate was higher for SPAC than PAC, as reported elsewhere (Matsui et al., 2007; Matsui et al., 2013a; Pan et al., 2016). Improvements of MIB removal rates with decreasing carbon size were also observed for 1-to-3-year-old spent carbons (Fig. 4-8b,c,d).

To further clarify the MIB removal efficiencies of spent carbons, we performed adsorption experiments with varying dosages and a fixed carbon-water contact time of 30 min, a time that is often used in actual water purification treatment. Fig. 4-9 shows the results. The SPAC and SSPAC produced from one-year-old carbons (KM1-n-SPAC) achieved the same removal rate as virgin PAC (KM0-n-PAC), a removal rate that might be regarded as a feasible goal from a practical standpoint. In the two-year-old carbon series, SPAC did not achieve the same reduction rate as the virgin PAC, but SSPAC did. None

of the three-year-old carbons, including its SSPAC, achieved the same removal rate as the virgin PAC (KM0-n-PAC).

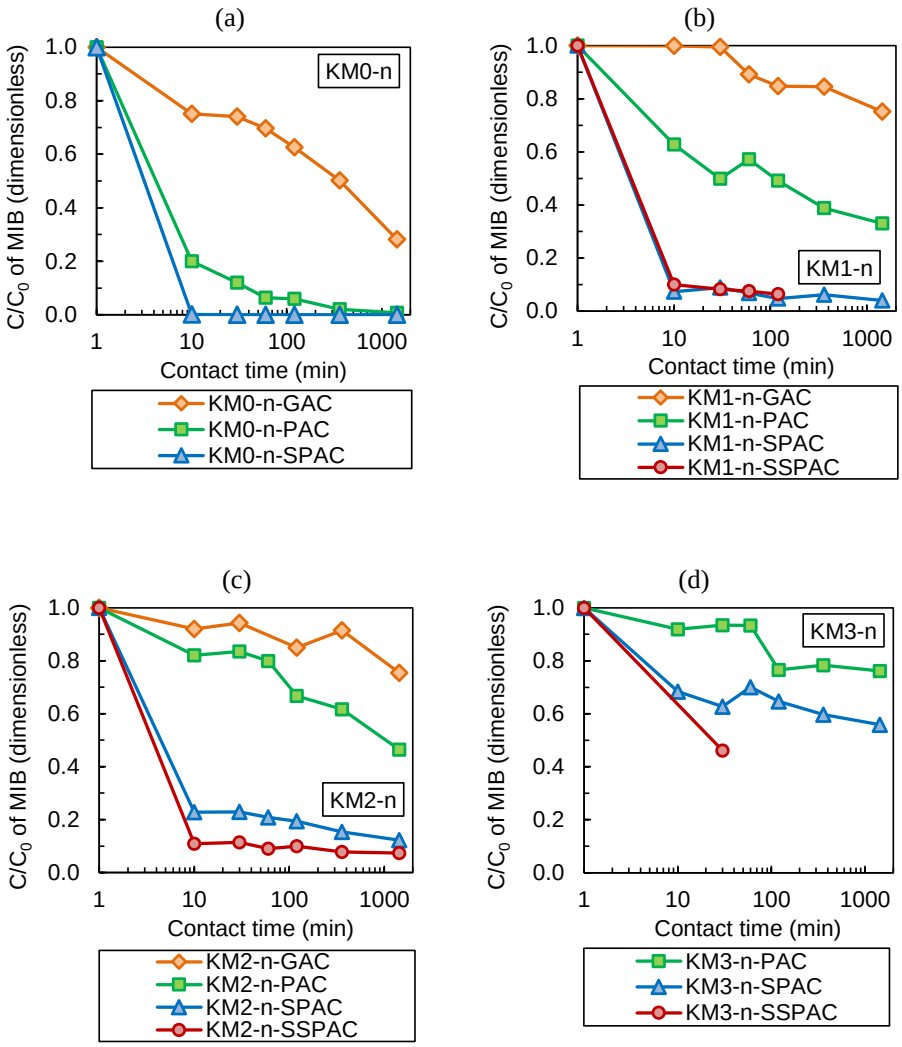

Fig. 4-8. MIB removal rates against carbon-solution contact time (PAC/SPAC/SSPAC dosage was 40 mg/L in natural water; GAC dosage was 210 ± 10 mg/L in natural water)**.**

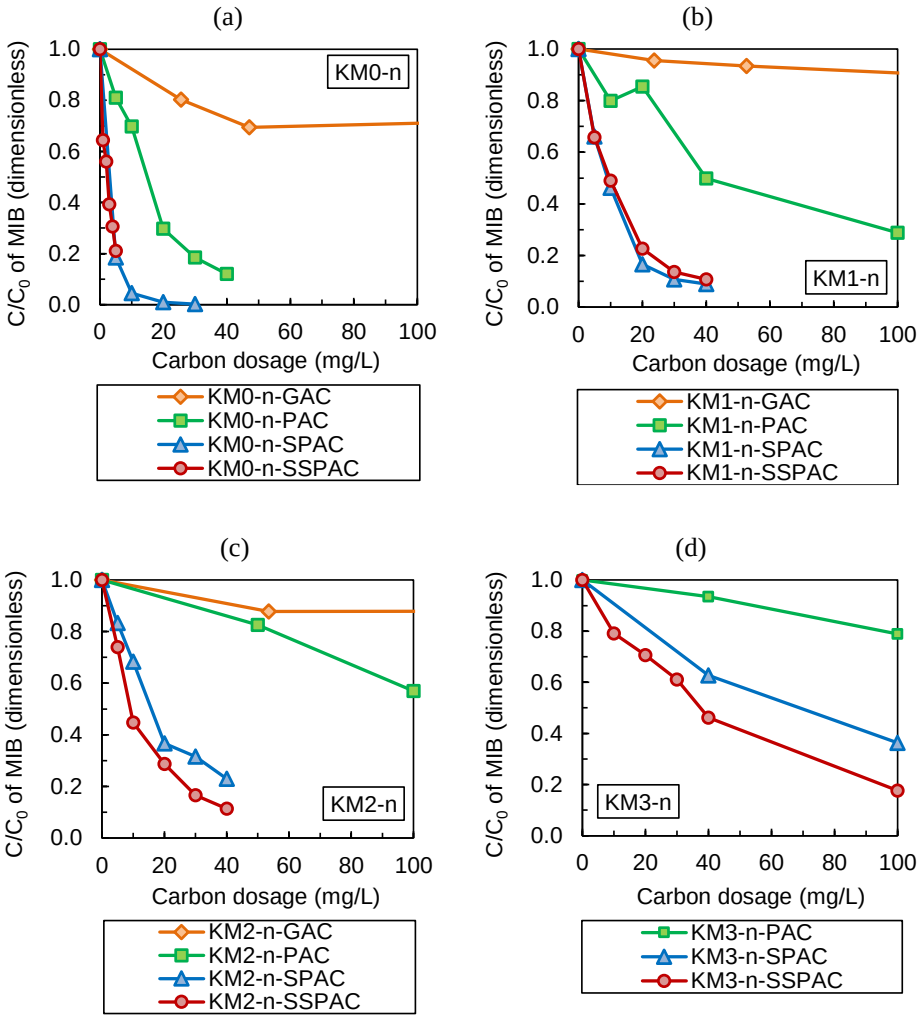

Fig. 4-9. MIB removal rates against carbon dosages at a carbon-water contact time of 30 min (natural water)**.**

In a word, the influence of carbon size on MIB adsorptive removal was observed for the used carbon as well as the virgin carbons, but the influence was more prominent for the older used carbons (Fig. 4-10).

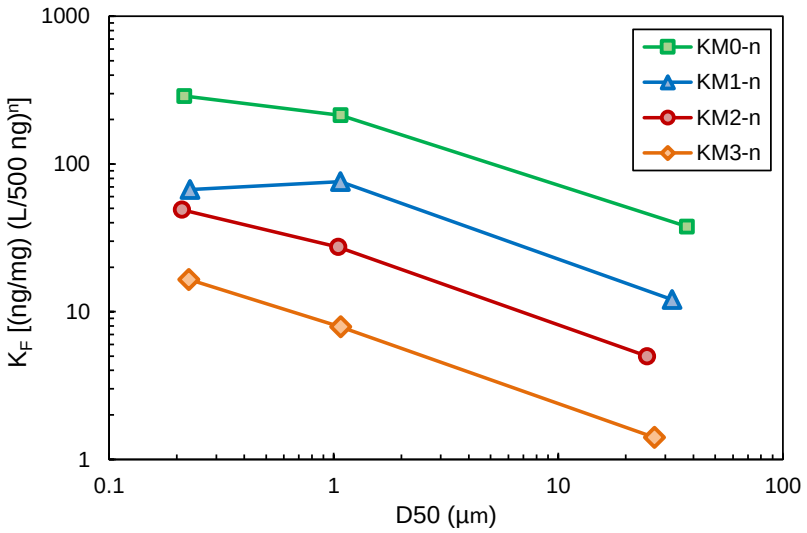

Fig. 4-10. MIB removal ability against carbon particle size (the ability was evaluated as solid-phase concentration with the liquid-phase concentration of 500 μg/L after 30-min contact time)**.**

4.4.3 MIB adsorption capacities.

As described in section 4.4.2, the one-year-old and two-year-old carbons, when milled to micron- and submicron-diameter particles, respectively, were similar to the virgin PAC in terms of MIB removal ability. However, the uptake rate of MIB by carbon with ages ≥3 years was less than that of virgin PAC, even if the particle sizes were decreased to enhance the uptake rate of MIB. Because sufficient adsorbate uptake cannot be expected when the carbon does not have a certain level of equilibrium adsorption capacity, we examined the equilibrium adsorption capacities of the spent carbons. Fig. 4-11 shows the adsorption isotherms of the 32 carbons. The equilibrium MIB adsorption capacities decreased with increasing carbon age and increased as the particle size decreased.

To clarify these trends, the equilibrium adsorption capacities of carbon with different ages were plotted against the carbon particle sizes. Equilibrium adsorption capacities were quantified in terms of the MIB solid-phase concentration in equilibrium with a MIB liquid-phase concentration of 100 ng/L after fitting the isotherm data to the Freundlich model. A reduction of the MIB adsorption capacities with carbon age was clearly apparent (Fig. 4-12). The longer the carbon aged, the lower the MIB adsorption capacity of the carbon. A similar phenomenon has previously been observed for adsorption of a pesticide (atrazine) onto PAC, which was used for a few months in an immersed microfiltration membrane system (Lebeau et al., 1999). Equilibrium adsorption capacities in our study also increased with decreasing carbon particle size. A similar phenomenon has been reported for virgin PAC and its SPAC (Matsui et al., 2010; Matsui et al., 2012) as well as for one-year-old used GAC and its PAC (Hu et al., 2015; Knappe et al., 1999).

Among the spent carbons up to three years old, the oldest carbon (KM3-a series) showed the most dramatic increase of adsorption capacity: the adsorption capacity increased 6.8-fold when the carbon diameter decreased from 22 μm to 200 nm. Adsorption capacity increased 12-fold when the diameter of

two-year-old carbon decreased from 1.9 mm to 250 nm. Finally, the capacity of SSPAC produced from two-year-old GAC was similar to that of virgin PAC. Adsorption capacities decreased with increasing age of carbons, but they increased as the particle size decreased. As described in section 4.4.2, when used GAC was milled to micron- and submicron-size particles, its ability to remove MIB at a given contact time was enhanced, and the adsorption capability of the carbon was similar to that of virgin PAC. This enhancement can be explained by the faster adsorbate uptake rate due to the broadening of the outer surface area (carbon-water contact area) and reduction of the intra-particle diffusion path length. The results presented in this section clearly reveal that the enhancement of MIB removal efficiency was due to both an increase of equilibrium adsorption capacity and an increase of adsorbate uptake rate.

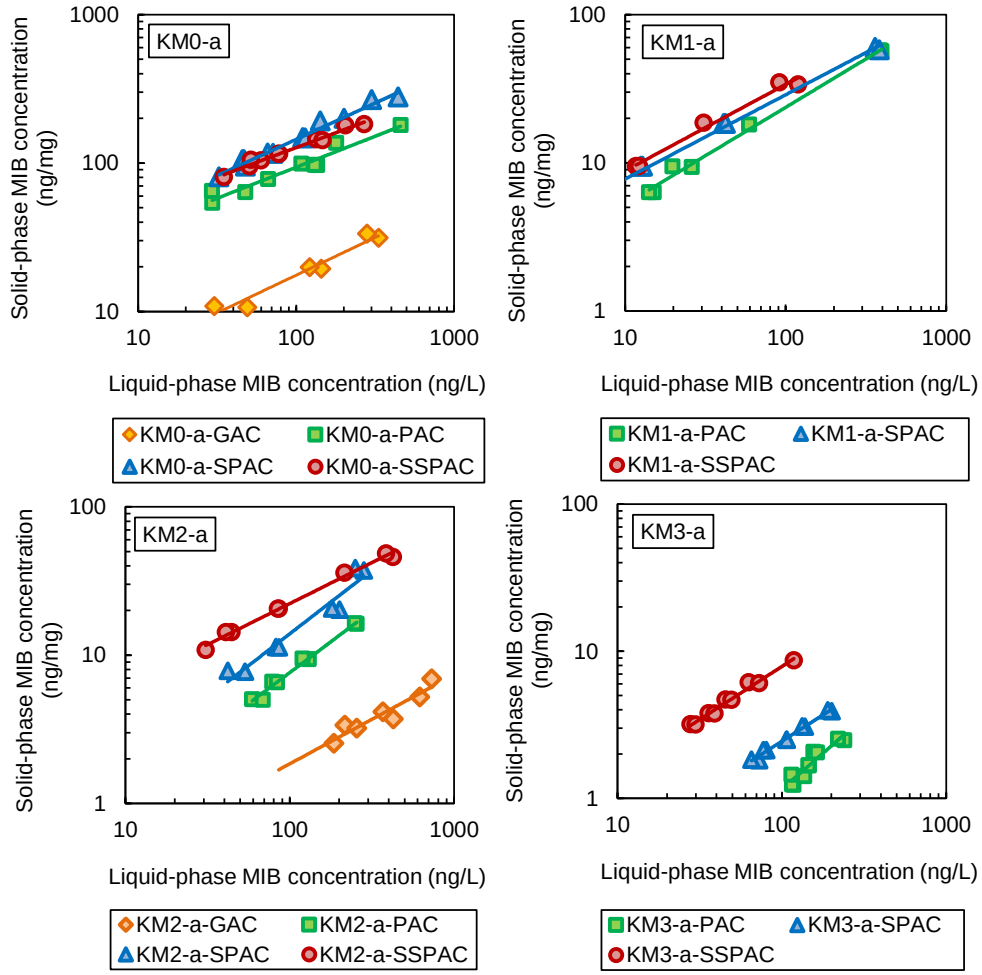

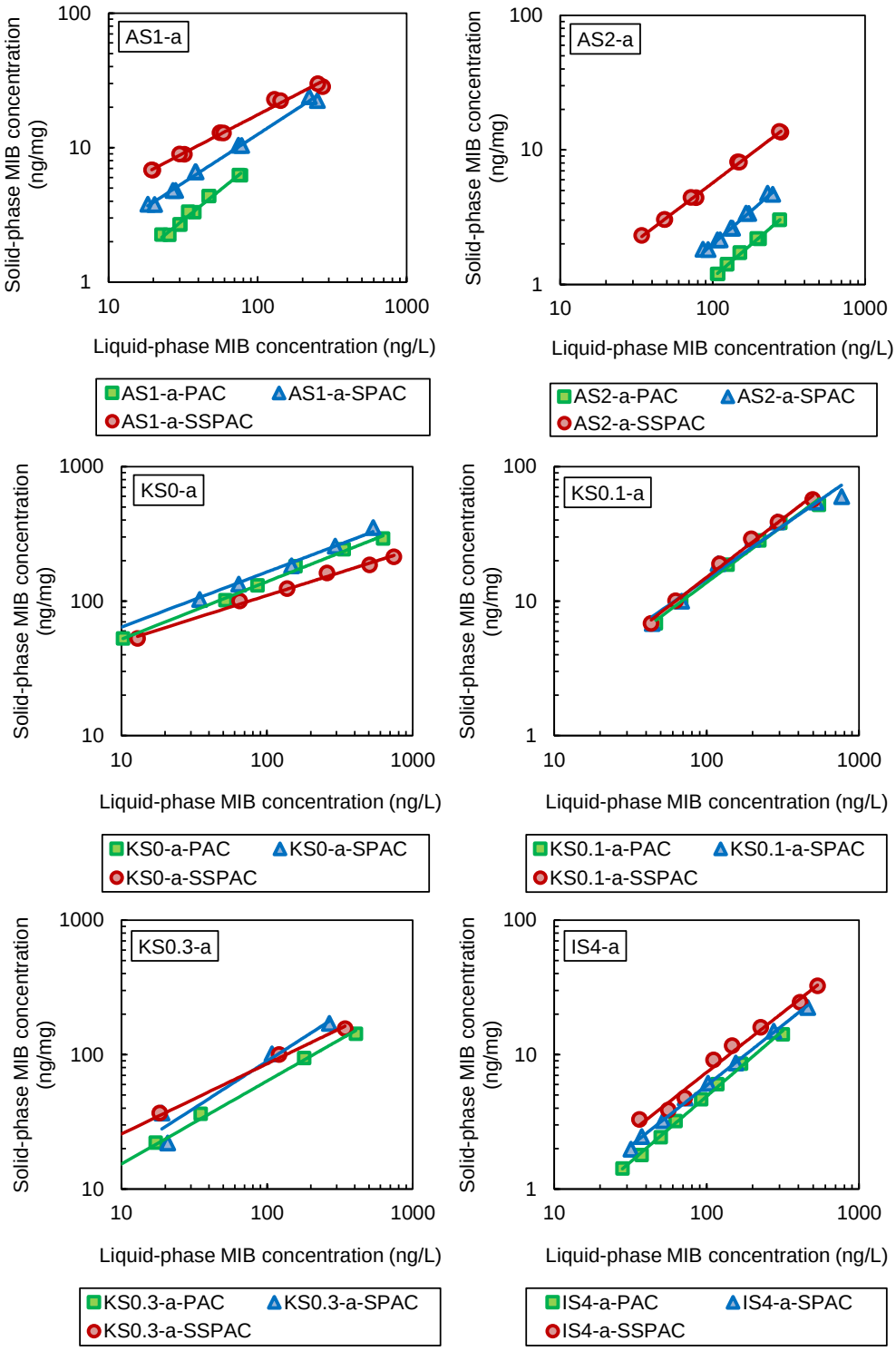

Fig. 4-11. MIB adsorption isotherms.

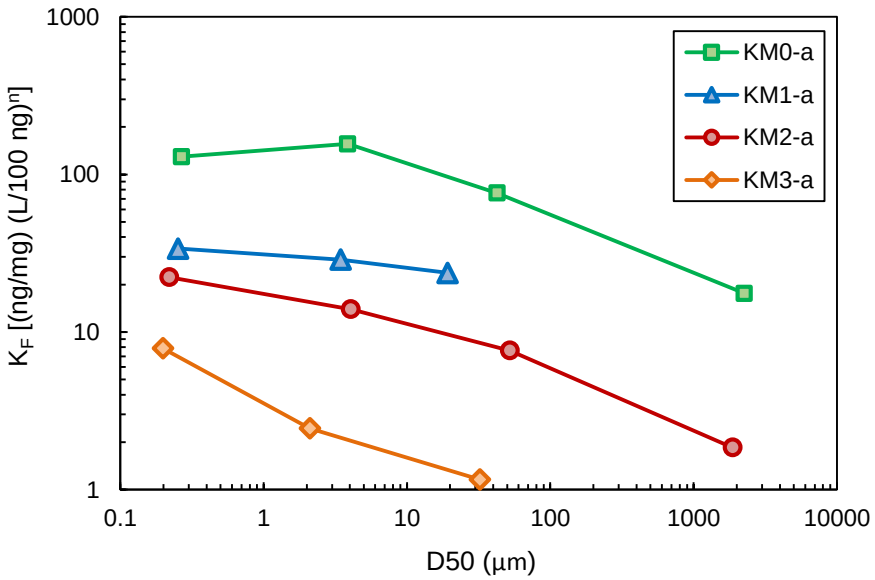

Fig. 4-12. MIB adsorption equilibrium capacity versus carbon particle size (The metric of the capacity was the solid-phase concentration in equilibrium with a liquid-phase concentration of 100 ng/L in natural water)**.**

4.4.4 Pore size distributions

The pore size distribution of activated carbon particles is an important parameter related to their equilibrium adsorption capacity. It has been reported previously that the change in carbon particle size by micro-milling does not result in any substantial change in pore size distribution (Ando et al., 2010; Matsui et al., 2015). The results of our study also confirmed that the pore size distributions were similar for different-size particles (PAC, SPAC, and SSPAC) with the same age, although experimental errors were apparent in the data for one-year-old carbon (Fig. 4-13). We therefore considered the effect of carbon age on pore size distribution after averaging data for carbons of the same age.

Between carbons of different ages, clear differences were apparent in the distribution of small-size micropores (pores with widths 0.6–0.9 nm) (Fig. 4-14a). In contrast, no large difference was apparent in the distribution of pores with widths >0.9 nm, including mesopores (Fig. 4-14). The volume of the small-size micropores decreased with age from 0 to 3 years; it decreased mainly during the first year, whereas the volume of the larger-size pores did not decrease. If loading of NOM on carbon is the main cause of carbon fouling, this result is intriguing, because NOM is believed to adsorb mainly onto mesopores rather than micropores (Li et al., 2002b; Li et al., 2003; Newcombe et al., 2002a). A previous study of four-year-old used GAC (Kameya et al., 1997), however, has revealed a similar phenomenon, namely that micropore volume decreases to a larger extent than mesopore volume, and it decreases rapidly at the beginning of an operation of a GAC bed. A change of the volume of micropores could be caused by accumulation of synthetic organic micro-pollutants as well as low-MW NOM present in the raw waters because the effluents from wastewater treatment plants are discharged into the upstream of the river.

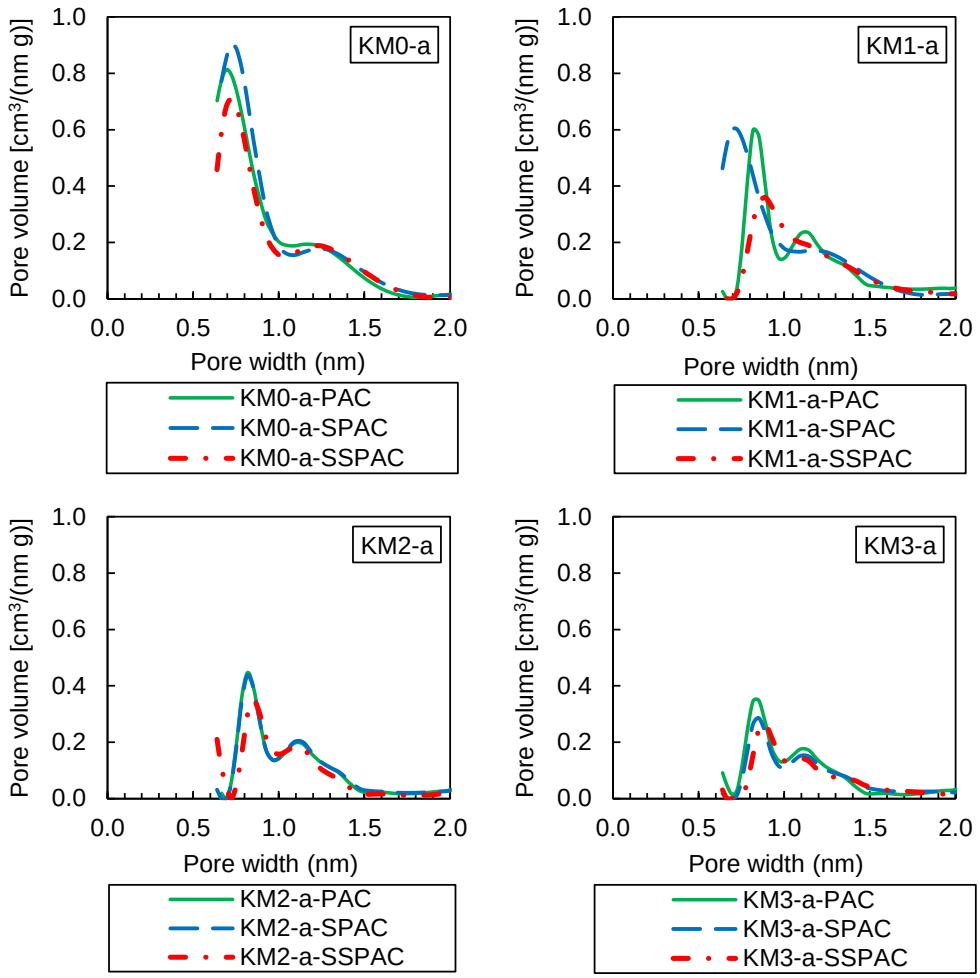

Fig. 4-13. Micropore size distributions of PAC, SPAC, and SSPAC.

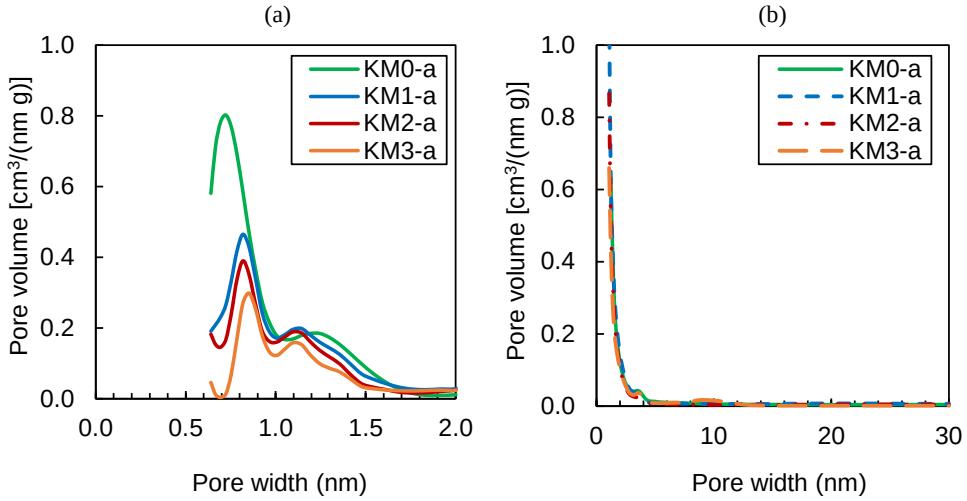

Fig. 4-14. Pore size distributions of KM series carbon.

In our experiment, the rapid drop of micropore volume after one year was concomitant with the decrease of MIB adsorption capacity: the adsorption capacity dropped relatively rapidly during the first year and declined more slowly afterward (Fig. 4-12, note that the ordinate is at log scale). The similarity between the trends of micropore volume and MIB adsorption capacity is in accord with the common understanding that MIB is mainly adsorbed in micropores (Greenwald et al., 2015; Newcombe et al., 1997; Quinlivan et al., 2005; Yu et al., 2007).

4.4.5 Iodine, phenol, methylene and ABS numbers

The amounts of iodine, phenol, MB, and ABS adsorbed under specified conditions are called the iodine, phenol, MB, and ABS numbers, respectively. These numbers were used as metrics of the adsorptive removal ability of activated carbons. Fig. 4-15 shows the changes of these numbers for carbons of different ages against carbon particle size calculated from the data in Fig. 4-16.

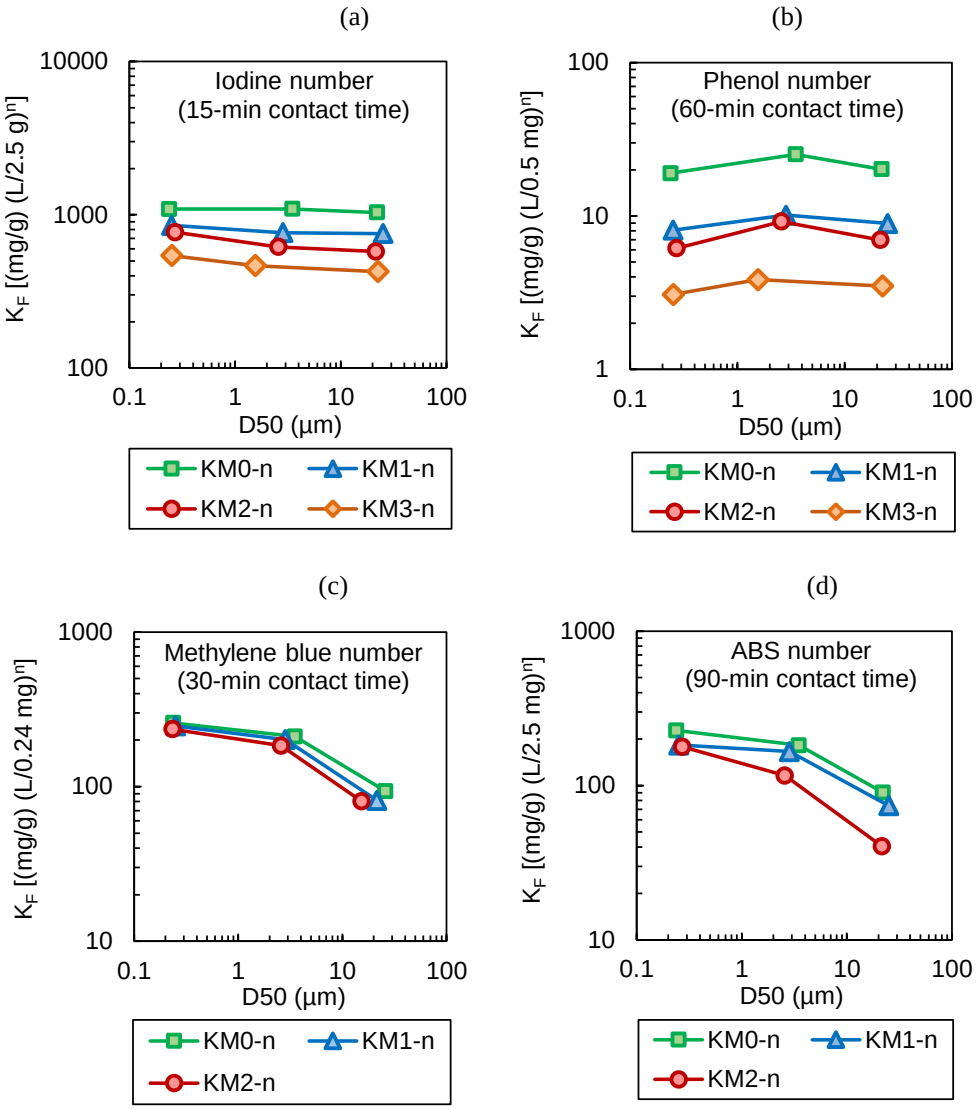

Fig. 4-15. Adsorption indices versus carbon particle size

(a) (Iodine)

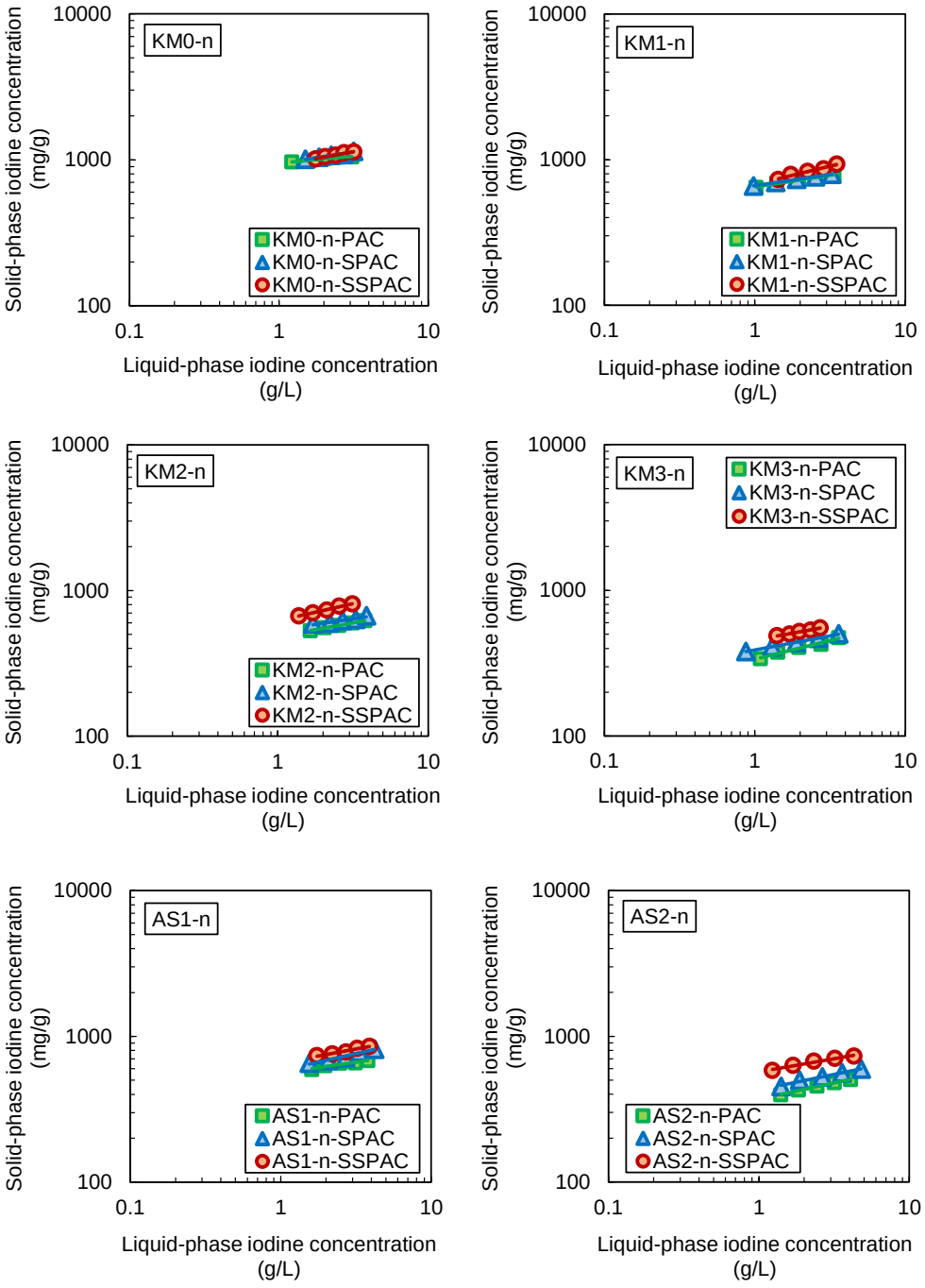
KM0-n
KM0-n-PAC
KM0-n-SPAC
KM0-n-SSPAC
KM1-n
KM1-n-PAC
KM1-n-SPAC
KM1-n-SSPAC
KM2-n
KM2-n-PAC
KM2-n-SPAC
KM2-n-SSPAC
KM3-n
KM3-n-PAC
KM3-n-SPAC
KM3-n-SSPAC
AS1-n
AS1-n-PAC
AS1-n-SPAC
AS1-n-SSPAC
AS2-n
AS2-n-PAC
AS2-n-SPAC
AS2-n-SSPAC
Solid-phase iodine concentration (mg/g)
Liquid-phase iodine concentration (g/L)
10000
1000
100
0.1
1
10

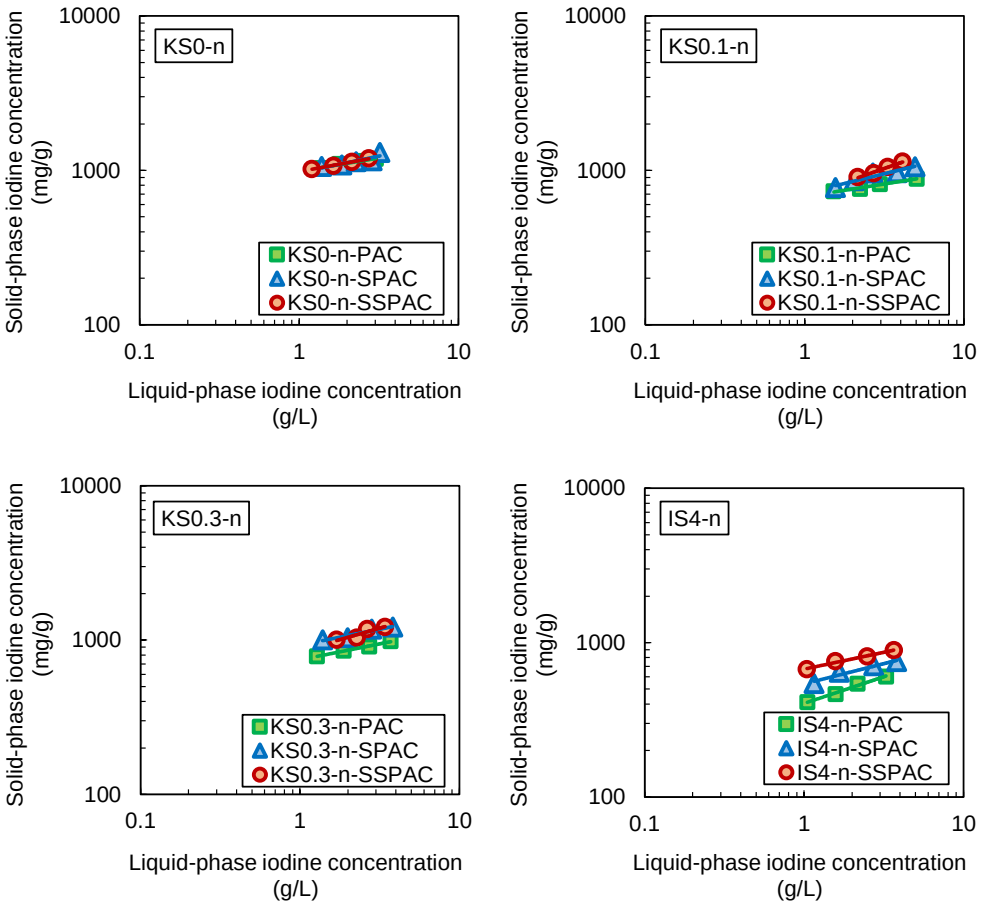
KS0-n
KS0-n-PAC
KS0-n-SPAC
KS0-n-SSPAC
KS0.1-n
KS0.1-n-PAC
KS0.1-n-SPAC
KS0.1-n-SSPAC
KS0.3-n
KS0.3-n-PAC
KS0.3-n-SPAC
KS0.3-n-SSPAC
IS4-n
IS4-n-PAC
IS4-n-SPAC
IS4-n-SSPAC
Solid-phase iodine concentration (mg/g)
Liquid-phase iodine concentration (g/L)
10000
1000
100
0.1
1
10

(b) (Phenol)

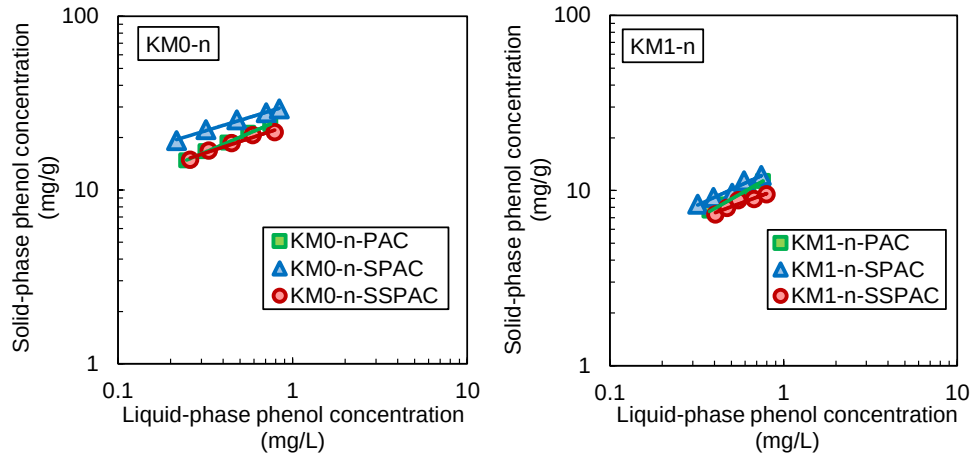
KM0-n
KM0-n-PAC
KM0-n-SPAC
KM0-n-SSPAC
KM1-n
KM1-n-PAC
KM1-n-SPAC
KM1-n-SSPAC
Solid-phase phenol concentration (mg/g)
Liquid-phase phenol concentration (mg/L)
100
10
1
0.1
1
10

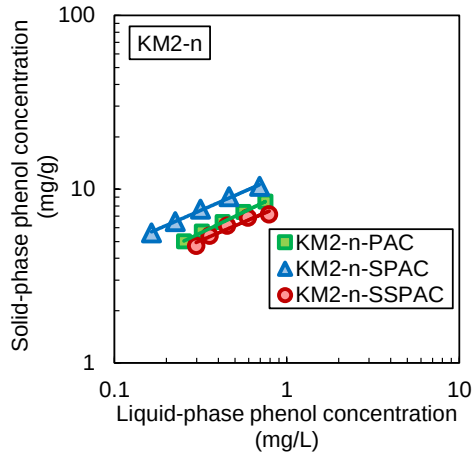
KM2-n
KM2-n-PAC
KM2-n-SPAC
KM2-n-SSPAC
Solid-phase phenol concentration (mg/g)
Liquid-phase phenol concentration (mg/L)
100
10
1
0.1
1
10

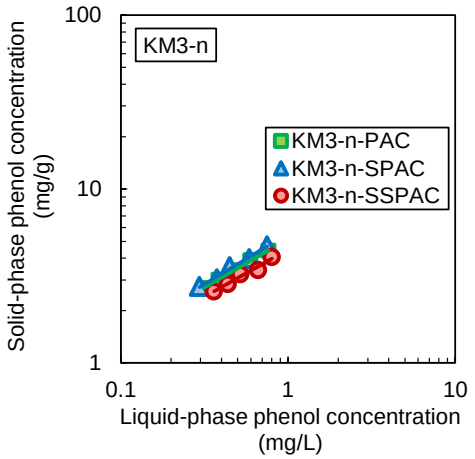
KM3-n
KM3-n-PAC
KM3-n-SPAC
KM3-n-SSPAC
Solid-phase phenol concentration (mg/g)
Liquid-phase phenol concentration (mg/L)
100
10
1
0.1
1
10

(c) (MB)

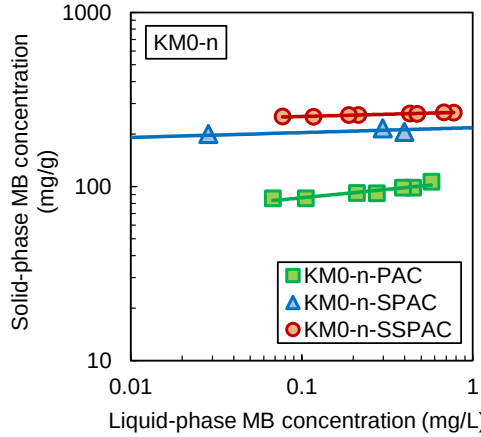
KM0-n
KM0-n-PAC
KM0-n-SPAC
KM0-n-SSPAC
Solid-phase MB concentration (mg/g)
Liquid-phase MB concentration (mg/L)
1000
100
10
0.01
0.1
1

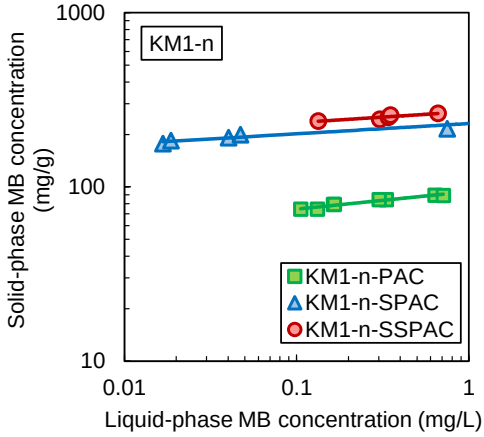
KM1-n
KM1-n-PAC
KM1-n-SPAC
KM1-n-SSPAC
Solid-phase MB concentration (mg/g)
Liquid-phase MB concentration (mg/L)
1000
100
10
0.01
0.1
1

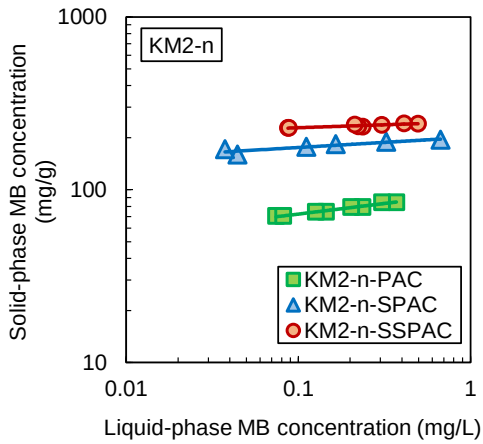
KM2-n
KM2-n-PAC
KM2-n-SPAC
KM2-n-SSPAC
Solid-phase MB concentration (mg/g)
Liquid-phase MB concentration (mg/L)
1000
100
10
0.01
0.1
1

(d) (ABS)

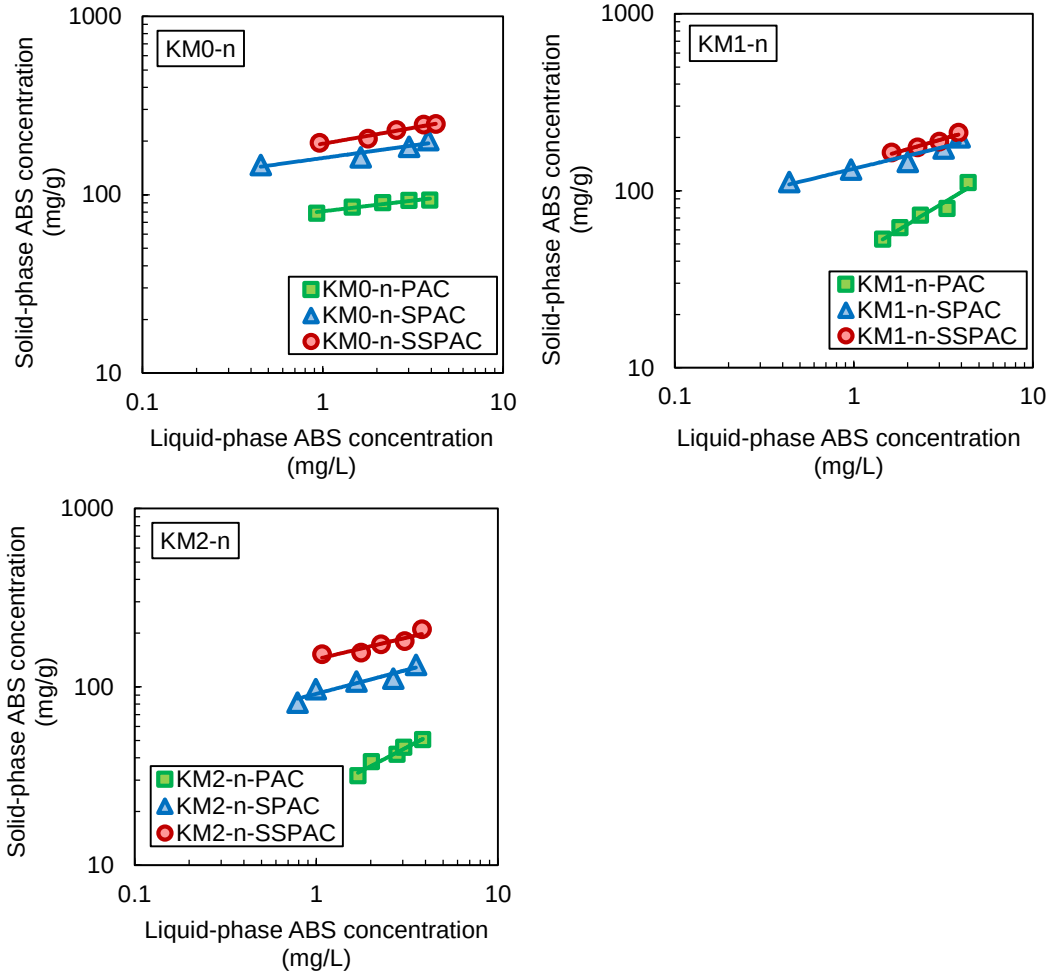

Fig. 4-16. Solid-phase vs. liquid-phase concentrations used to determine iodine number, phenol number, MB number, and ABS number.

For both the iodine number and phenol number (Figs. 4-15a and b, respectively), dependencies on carbon age were clearly apparent: the older spent carbons adsorbed smaller amounts of iodine and phenol. The dependencies on carbon age were small for the MB number (Fig. 4-15c). For the ABS number (Fig. 4-15d), the dependence on carbon age was also small at a carbon particle diameter of about 0.2 μm – 0.3 μm, but it was large at a carbon particle diameter greater than a few microns. With respect to dependence on carbon particle size, iodine numbers increased slightly with decreasing particle size. In the case of the phenol number, no increase and even slight decreases were observed when the size of the carbon particles was reduced. In the case of the MB and ABS numbers (Figs. 5c and d, respectively), a dependency on carbon particle size was clearly apparent. Among the four index numbers of the KM carbon series, the iodine number showed the highest correlation (R^2 = 0.97) with the MIB adsorption capacity (Fig. 4-16). The correlation was high (R^2 = 0.88), even when the data included carbons from different materials and carbons used in different treatment plants that treated different waters (Fig. 4-17). The MIB adsorption capacity increased with increasing iodine number, even when the data came from carbons with the same

age. Such a trend was not apparent for phenol, for which the correlation was second highest among the four indices (R^2 = 0.83). The iodine number was therefore a good index for roughly estimating the remaining MIB adsorption capacity of the spent carbons. The MIB removal ability of SSPAC produced from two-year-old GACs was similar to that of virgin PAC, as described in the section 3.1, and the iodine numbers of the two-year-old carbons were about 600 mg/g (Fig. 4-17). Therefore, if spent carbon still has an iodine number > 600 mg/g, it could be reused as SSPAC (or possibly as SPAC), regardless of the raw material that was the source of the carbon and the history of carbon use.

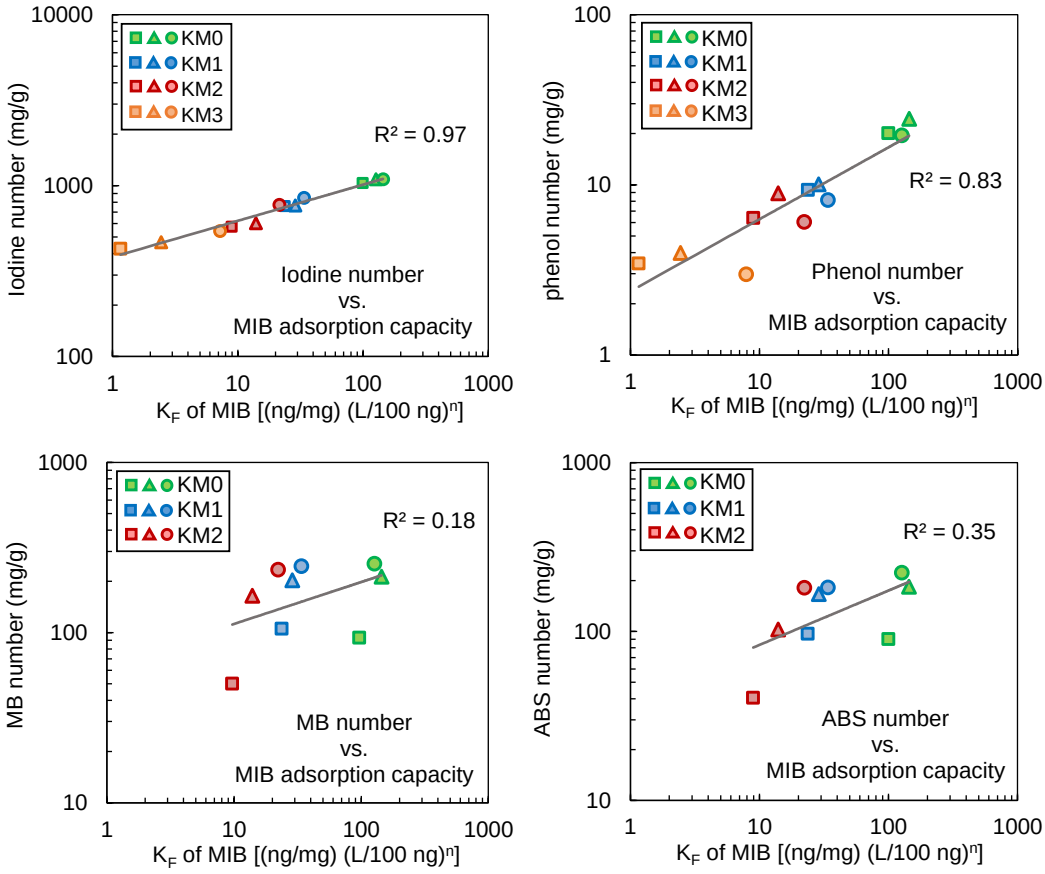

Fig. 4-16. Correlation between MIB adsorption capacity and four indices of the KM-series carbon (The squares are PACs, the triangles are SPACs, and the circles are SSPACs).

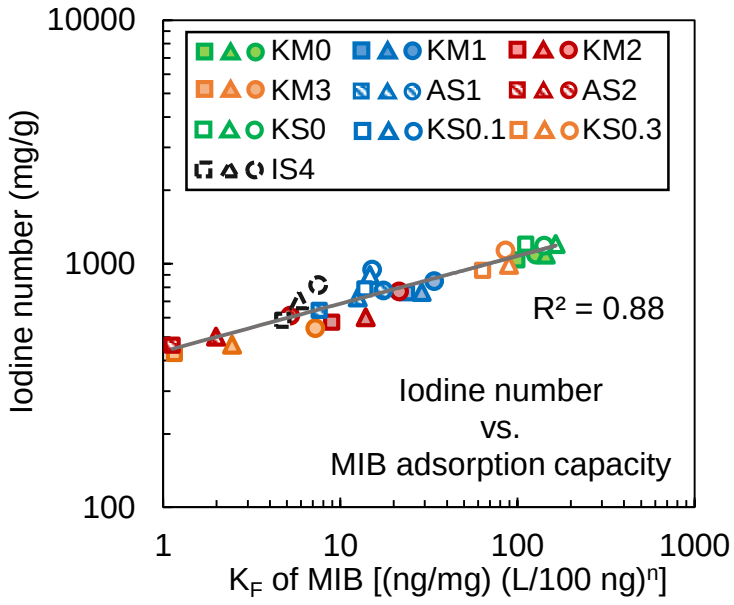

Fig. 4-17. Correlation between MIB adsorption capacity and iodine number of carbons (The squares are PACs, the triangles are SPACs, and the circles are SSPACs).

4.4.6 Influence of adsorbates properties on the adsorption capacity

Among the four indices, the iodine number (Fig. 4-17) was most highly correlated with MIB adsorption capacity (section 4.4.5). This correlation reflects the large degree of the adsorption capacity dependence on carbon age and to a certain degree its dependence on carbon size (Fig. 4-15a). To determine which properties of the adsorbates led to the adsorption capacity dependencies on carbon particle size and carbon age, we measured the adsorption isotherms of a variety of compounds on PAC, SPAC, and SSPAC that were produced from two-year-old used GAC (KM2-GAC) and virgin GAC (KM0-GAC). The adsorption capacity of each carbon sample for each adsorbate was calculated from the corresponding adsorption isotherm at equilibrium (Fig. 4-18). The calculation was carried out using the same procedure explained in section 4.4.3 for the MIB adsorption capacity. To avoid the effect of background adsorptive substances (including NOMs) in natural water, especially for adsorption onto virgin carbons, all the adsorption experiments were conducted in organic-free water, the ionic composition of which was the same as that of the natural water. For MIB and geosmin, the adsorption capacities were calculated at equilibrium with a liquid-phase concentration of 100 ng/L. For phenol, acetaminophen, PSS-210, iodine, MB, ABS, and PSS-6400, half of the initial concentrations was used as an equilibrium liquid-phase concentration to calculate the adsorption capacity (data for lower concentrations were not obtainable because of analytical errors). The degree of the capacity dependence on carbon age was then quantified from the ratio of the adsorption capacities of virgin SPAC and spent SPAC. This ratio is hereafter called the age-dependency index. The degree of the capacity dependence on carbon particle size was quantified in terms of the slopes of log-log plots of capacities vs. carbon particle diameters (Matsui et al., 2012). This slope is hereafter called the size-dependency index.

Among the several properties of the adsorbates that could possibly have influenced the adsorption capacities of the spent carbon, we first focused on molecular size, because changes were observed in the volume of the small-size micropores as the carbon aged (section 4.4.4). As a metric of molecular size, we used the minimal projection diameter (MPD) because it is the property that decides which carbon pores are available for the adsorbate molecule (Kasaoka et al., 1989; Li et al., 2002a; Pelekani et al., 2000; Sontheimer et al., 1988). MPDs were calculated from the three-dimensional structures of molecules predicted by using Marvin Sketch (v.16.5.16.0, ChemAxon Ltd, Hungary).

The age-dependency and size-dependency indices of the nine compounds are plotted against their MPDs in Figs. 4-19 and 4-20, respectively. The age dependencies of ABS and PSS-6400 were low, perhaps because of their large sizes. Because pores with widths >0.9 nm did not change much with age (section 4.4.4), ABS and PSS-6400, which have MPDs of 1.22 nm and 2.52 nm, respectively, would not have been influenced from loading of (probably) NOM during the GAC operation. Among the compounds with MPDs of 0.6–0.9 nm, MIB and geosmin exhibited high age dependency (Fig. 4-19). MIB and geosmin are hydrophobic compounds with high log-Kow values of 3.31 and 3.57, respectively, and they adsorb on hydrophobic basal plane sites (Ahnert et al., 2003; Considine et al., 2001; Moreno-Castilla, 2004). Hydrophilic compounds such as acetaminophen, which adsorb on specific sites as well as basal planes (Rey-Mafull et al., 2014), exhibited small age-dependency, which is in accord with a previous study that suggests a small effect from the loading of background matrix on acetaminophen adsorption (Coimbra et al., 2015).

It has therefore been suggested that the hydrophobic basal plane sites contained in the pores (0.6–0.9 nm) were probably intensively occupied by hydrophobic compounds during the long-term operation of the GAC. These hydrophobic compounds would be low-MW NOM (Kilduff et al., 1998; Newcombe et al., 1997; Newcombe et al., 2002b). Although low-MW NOMs might be overall more hydrophilic than hydrophobic (Aiken et al., 1992; Croué, 2004; Velten et al., 2011), hydrophobic fractions of low-MW NOMs with a benzene moiety, phenolic structures, and conjugated double bonds (Świetlik et al., 2004), which would promote hydrophobic interactions, would occupy the hydrophobic sites in the micropores and thus reduce the capacities of MIB and similar compounds to adsorb (Matsui et al., 2002a; Schmit et al., 2002; Zietzschmann et al., 2016). Hydrophobic synthetic organic micro-pollutants, which would be present in waters treated by the GACs, would also occupy hydrophobic adsorption sites in the micropores and thereby reduce the adsorption capacities of MIB and similar compounds. Overall, this research suggests that age dependency results from micropores and adsorbates with molecular diameters of 0.6–0.9 nm and high hydrophobicity.

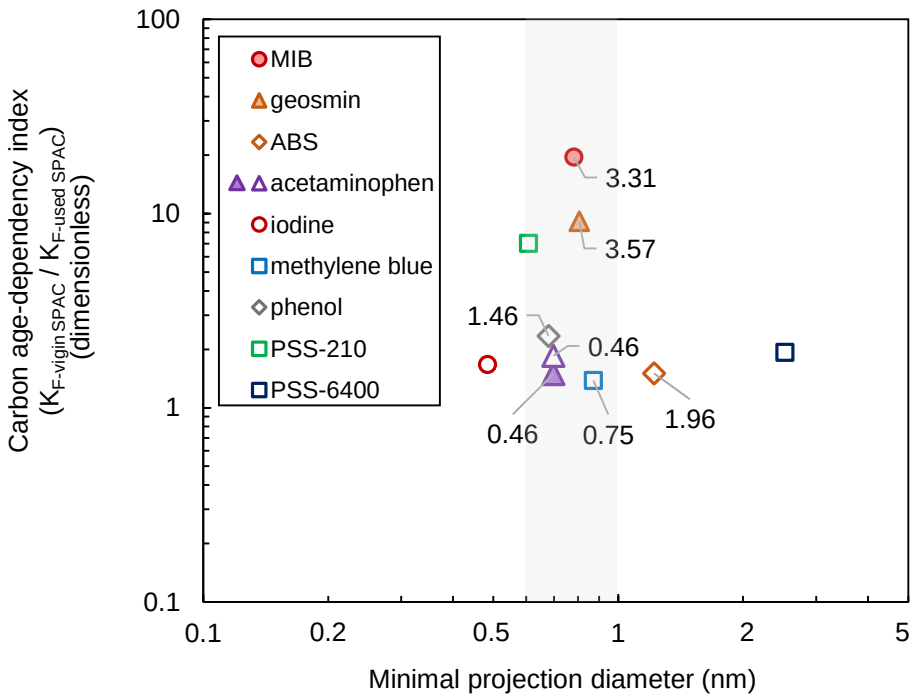

Fig. 4-19 – Carbon age-dependency index of adsorbates, quantified in terms of the ratio of the adsorption capacity between virgin and used SPAC (D50: 3 µm), against the minimal projection diameter of the adsorbates. Each number in the figure is the log-Kow value of the indicated adsorbate summarized by EPI Suite™ (U.S. Environmental Protection Agency v4.0). The log-Kow of iodine, PSS-210, and PSS-6400 were not obtainable. Closed symbols correspond to data with low initial concentrations (<10 µg/L). Open symbols correspond to data with high initial concentrations (>0.5 mg/L).

Of relevance to the carbon-size-dependency is the fact that early researchers discovered that some hydrophobic organic micro-pollutants and high-MW compounds were adsorbed mainly on the exterior of carbon particles due to their limited penetration distances (Matsui et al., 2013a; Matsui et al., 2014). The capacity of MIB, geosmin, and humic substances to adsorb onto GAC and PAC would thus increase when the GAC/PAC particle was milled to a smaller size (Amaral et al., 2016; Ando et al., 2010; Bonvin et al., 2016; Knappe et al., 1999; Matsui et al., 2015; Matsui et al., 2013b). The high dependencies on carbon particle size of the capacities of MIB, geosmin, PSS-6400, and ABS to adsorb onto spent carbons (Fig. 4-20) are in line with this previous finding, which was reported for virgin carbons. Similarly, for large molecular-size compounds and hydrophobic compounds with even small molecular sizes, the equilibrium adsorption capacities on spent as well as virgin carbons would increase when carbon particle size was decreased by milling.

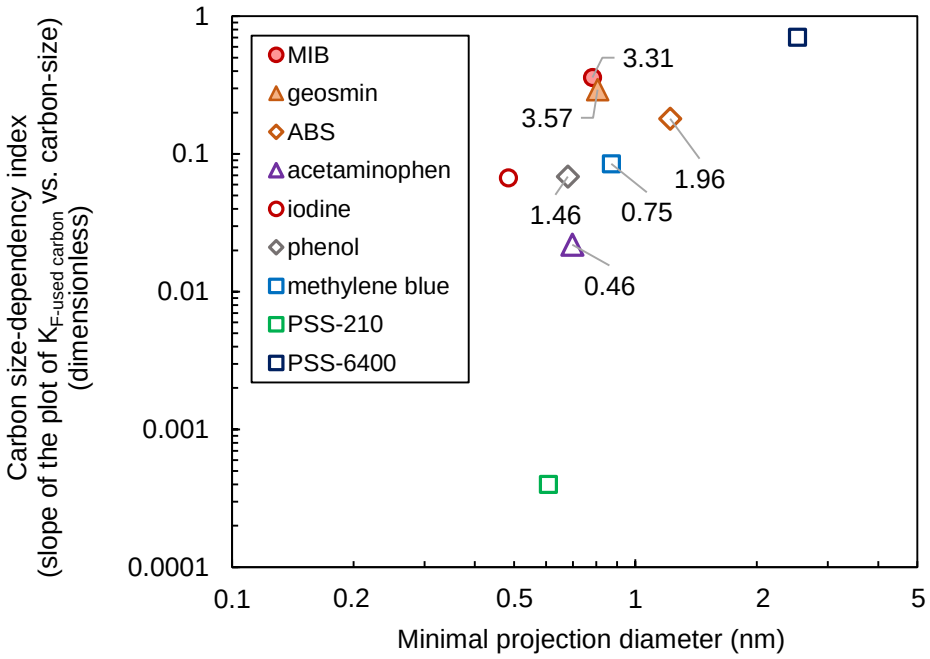

Fig. 4-20. Carbon size-dependency index of adsorbates, quantified by the absolute value of the slopes of plots of adsorption capacities of used carbons vs. carbon size, against the minimal projection diameter of the adsorbates. Each number in the figure is the log-Kow value of each adsorbate summarized by EPI Suite™ (U.S. Environmental Protection Agency v4.0).

(a) (phenol with 1-mg/L initial concentration [0.5-day contact time], working solution C [organic-free ionic water])

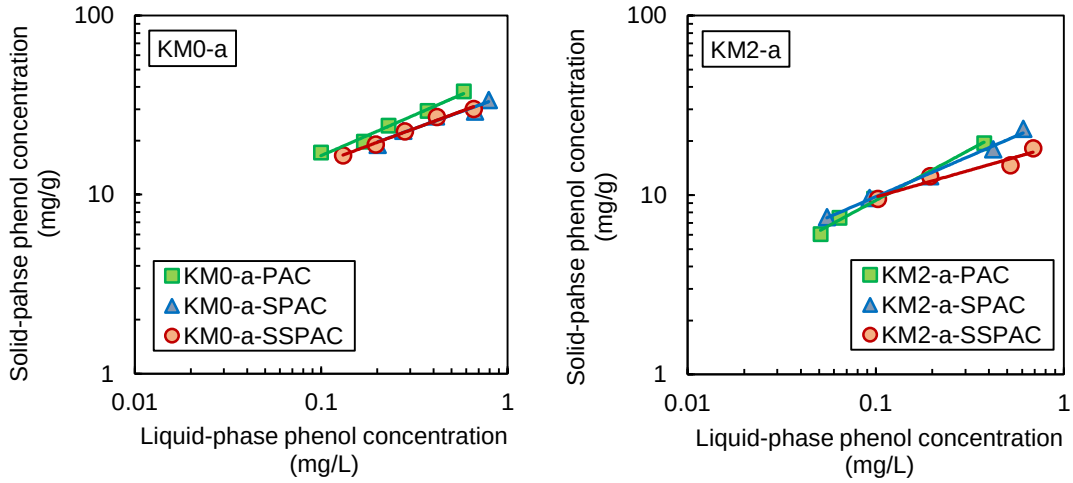

(b) (acetaminophen with 2-mg/L initial concentration [7-day contact time], working solution C [organic-free ionic water])

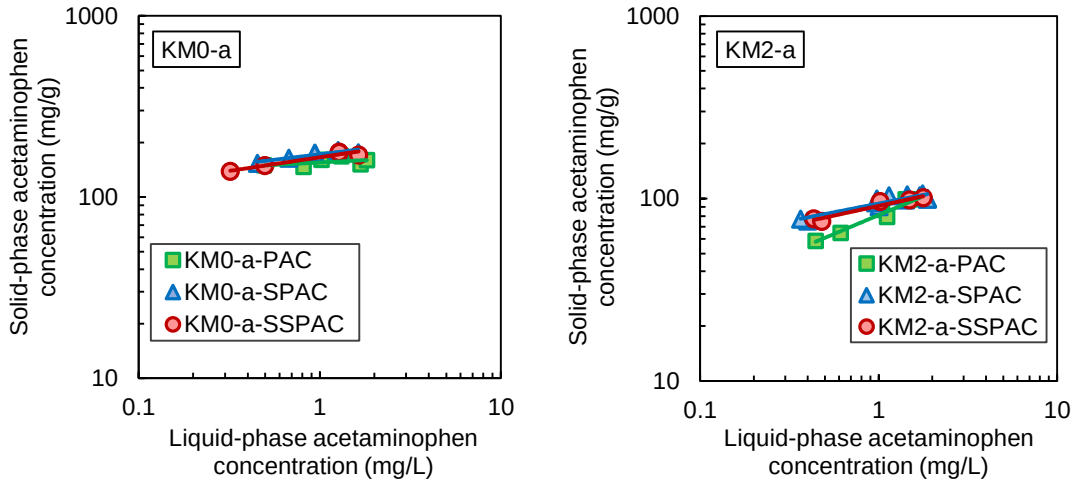

(c) (acetaminophen with 10-µg/L initial concentration [0.5-day contact time], working solution C [organic-free ionic water])

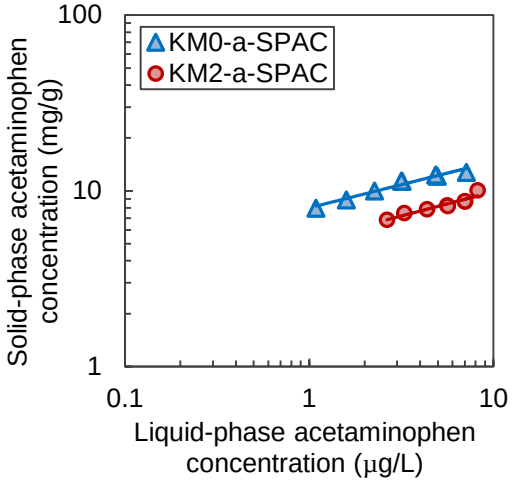

(d) (MIB with 1-µg/L initial concentration [7-day contact time], working solution C [organic-

free ionic water])

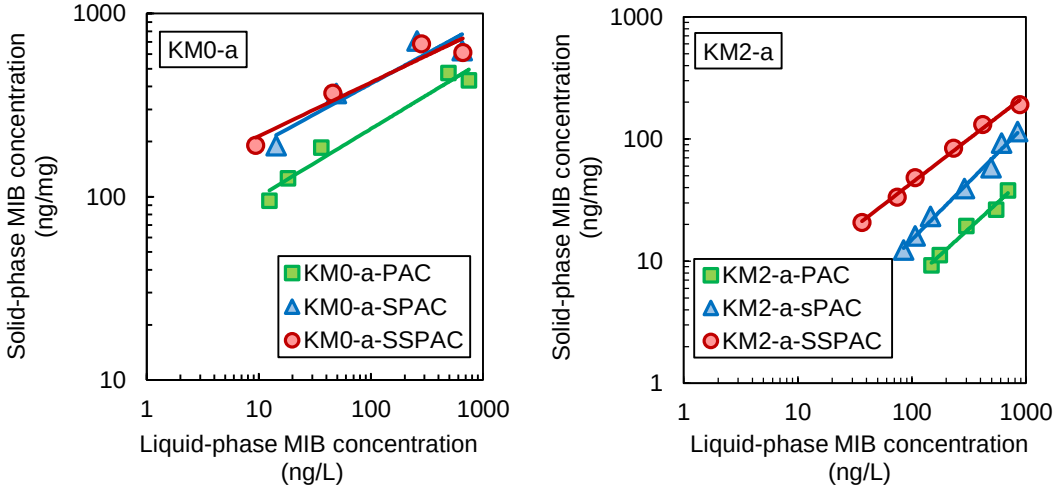

(e) (geosmin with 1-µg/L initial concentration [7-day contact time], working solution C [organic-free ionic water])

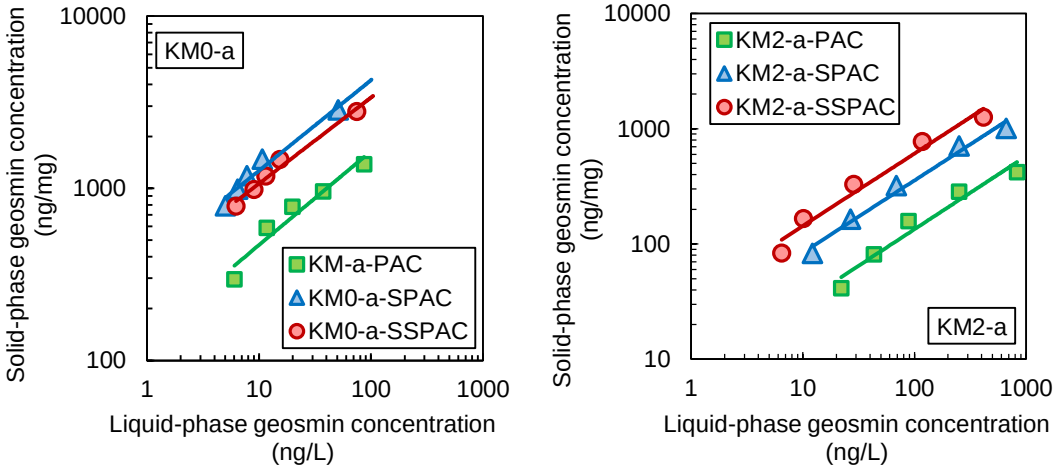

(f) (MB with 0.48-mg/L initial concentration [7-day contact time], working solution D [phosphate buffer water])

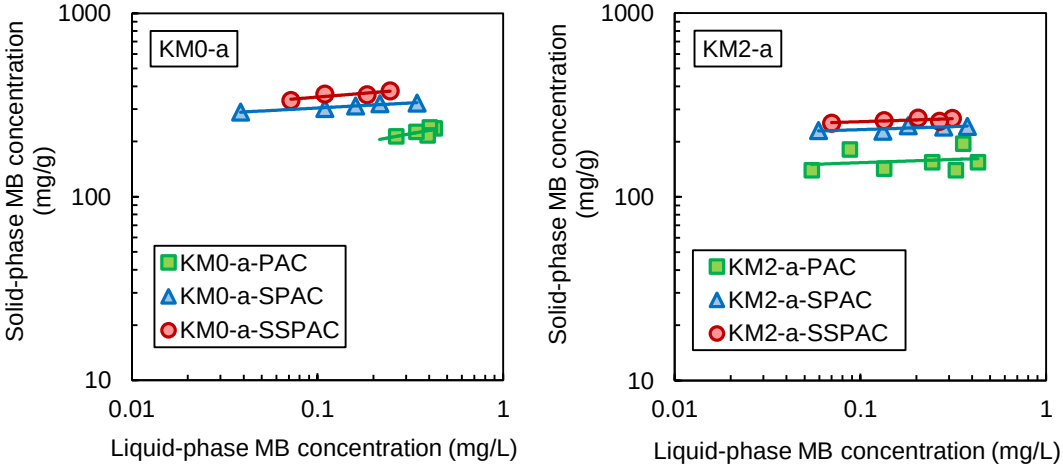

(g) (ABS with 5-mg/L initial concentration [7-day contact time], working solution C [ultrapure water])

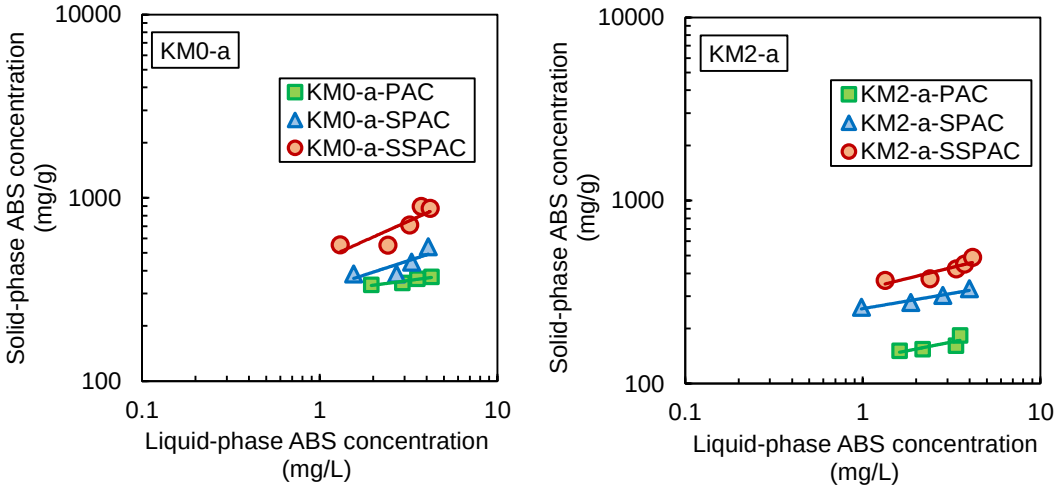

(h) (PSS-210 with 4-mg/L initial concentration [7-day contact time], working solution C [organic-free ionic water])

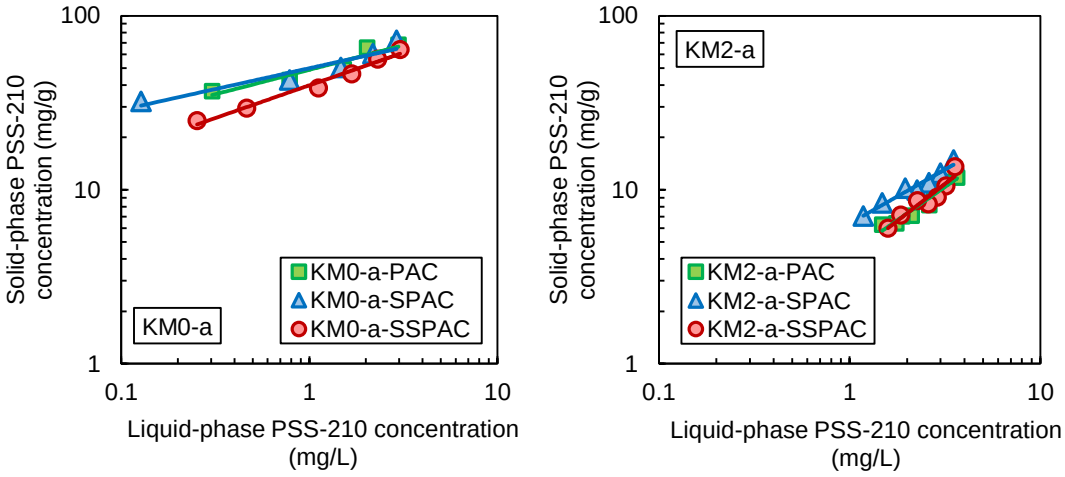

(i) (PSS-6400 with 4-mg/L initial concentration [7-day contact time], working solution C [organic-free ionic water])

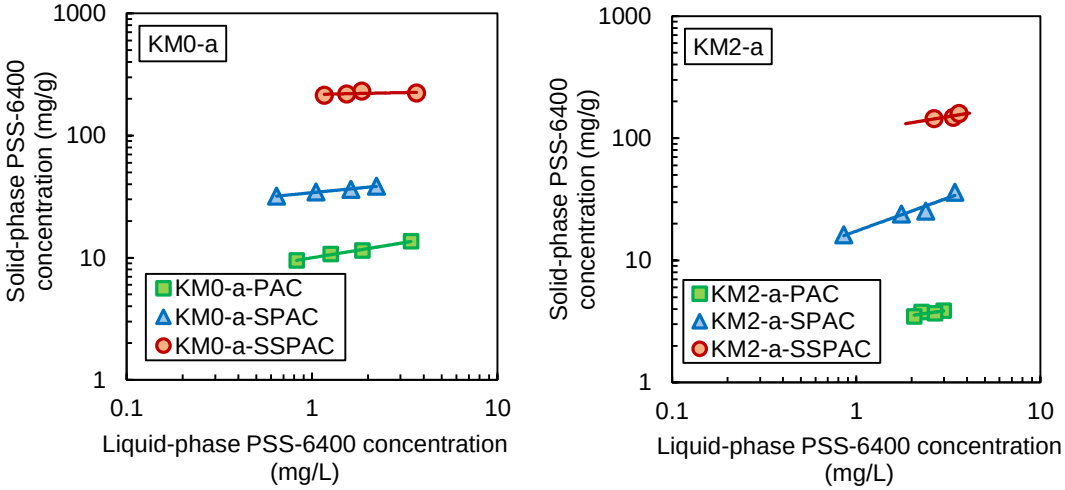

Fig. 4-20. Adsorption isotherms of the eight adsorbates.

4.5 Chapter conclusions

(1). Equilibrium MIB adsorption capacities of GACs used in water treatment plants for 1–3 years increased when the GACs were milled to PAC, SPAC, and SSPAC, which are characterized by progressively smaller particle sizes.

(2). By milling the GACs used in water purification plants for 1–2 years, it is possible to reuse them as SPAC or SSPAC adsorbents to remove MIB. This reusability reflects the increased adsorption capacity and higher adsorptive kinetics of smaller particles.

(3). The MIB adsorption capacity of spent carbons was well correlated with iodine numbers. Therefore, iodine number can be a metric of remaining MIB adsorption capacity.

(4). During the three years of GAC use, the volume of the micropores with widths of 0.6–0.9 nm was greatly reduced compared with that of pores with larger widths.

(5). The adsorption capacity of spent carbon for hydrophobic compounds with MPDs of 0.6–0.9 nm, including MIB, depended on carbon age; the capacity decreased greatly with carbon age.

(6). The adsorption capacity of spent carbon for compounds with large MPDs and/or high hydrophobicities depended on the carbon particle size; the capacity increased with decreasing particle size.

4.6 Reference

Ahnert, F., Arafat, H.A. and Pinto, N.G., 2003. A Study of the Influence of Hydrophobicity of Activated Carbon on the Adsorption Equilibrium of Aromatics in Non-Aqueous Media. Adsorption 9(4), 311-319.

Aiken, G.R., McKnight, D.M., Thorn, K.A. and Thurman, E.M., 1992. Isolation of hydrophilic organic acids from water using nonionic macroporous resins. Organic Geochemistry 18(4), 567-573.

Alvarez, P.M., Beltran, F.J., Gomez-Serrano, V., Jaramillo, J. and Rodriguez, E.M., 2004. Comparison between thermal and ozone regenerations of spent activated carbon exhausted with phenol. Water Res 38(8), 2155-2165.

Amaral, P., Partlan, E., Li, M., Lapolli, F., Mefford, O.T., Karanfil, T. and Ladner, D.A., 2016. Superfine powdered activated carbon (S-PAC) coatings on microfiltration membranes: Effects of milling time on contaminant removal and flux. Water Research 100, 429-438.

Ando, N., Matsui, Y., Kurotobi, R., Nakano, Y., Matsushita, T. and Ohno, K., 2010. Comparison of natural organic matter adsorption capacities of super-powdered activated carbon and powdered activated Carbon. Water Research 44(14), 4127-4136.

Bonvin, F., Jost, L., Randin, L., Bonvin, E. and Kohn, T., 2016. Super-fine powdered activated carbon (SPAC) for efficient removal of micropollutants from wastewater treatment plant effluent. Water Research 90, 90-99.

Coimbra, R.N., Calisto, V., Ferreira, C.I.A., Esteves, V.I. and Otero, M., 2015. Removal of pharmaceuticals from municipal wastewater by adsorption onto pyrolyzed pulp mill sludge. Arabian Journal of Chemistry, In Press.

Considine, R., Denoyel, R., Pendleton, P., Schumann, R. and Wong, S.-H., 2001. The influence of surface chemistry on activated carbon adsorption of 2-methylisoborneol from aqueous solution. Colloids and Surfaces A: Physicochemical and Engineering Aspects 179(2–3), 271-280.

Cook, D., Newcombe, G. and Sztajnbok, P., 2001. The application of powdered activated carbon for mib and geosmin removal: predicting pac doses in four raw waters. Water Research 35(5), 1325-1333.

Corwin, C.J. and Summers, R.S., 2012. Controlling trace organic contaminants with GAC adsorption. American Water Works Association. Journal 104(1), 43.

Croué, J.-P., 2004. Isolation of Humic and Non-Humic NOM Fractions: Structural Characterization. Environmental Monitoring and Assessment 92(1), 193-207.

Graham, M.R., Summers, R.S., Simpson, M.R. and MacLeod, B.W., 2000. Modeling equilibrium adsorption of 2-methylisoborneol and geosmin in natural waters. Water Research 34(8), 2291-2300.

Greenwald, M.J., Redding, A.M. and Cannon, F.S., 2015. A rapid kinetic dye test to predict the adsorption of 2-methylisoborneol onto granular activated carbons and to identify the influence of pore volume distributions. Water Research 68, 784-792.

Hu, J., Shang, R., Heijman, B. and Rietveld, L., 2015. Reuse of spent granular activated carbon for organic micro-pollutant removal from treated wastewater. Journal of Environmental Management 160, 98-104.

Iwamoto, T., Tasaki, T. and Kanami, T., 2014. Renewal and Selection of Granular Activated Carbon in Advanced Drinking Water Purification in Tokyo, Nagoya, Japan.

JWWA, 2005. Powdered activated carbon for water treatment (K 113:2005-2), Japan Water Works Association, Tokyo, Japan.

Kameya, T., Hada, T. and Urano, K., 1997. Changes of adsorption capacity and pore distribution of biological activated carbon on advanced water treatment. Water Science and Technology 35(7), 155-162.

Kasaoka, S., Sakata, Y., Tanaka, E. and Naitoh, R., 1989. Design of molecular-sieve carbon. Studies on the adsorption of various dyes in the liquid phase. International Journal of Chemical Engineering 29(4), 734-742.

Kennedy, A.M., Reinert, A.M., Knappe, D.R.U., Ferrer, I. and Summers, R.S., 2015. Full- and pilot-scale GAC adsorption of organic micropollutants. Water Research 68, 238-248.

Kilduff, J.E. and Karanfil, 1998. TCE adsorption by GAC preloaded with humic substances. Journal - American Water Works Association 90(5), 76.

Knappe, D.R., Snoeyink, V.L., Roche, P., Prados, M.J. and Bourbigot, M.-M., 1999. Atrazine removal by preloaded GAC. American Water Works Association. Journal 91(10), 97.

Lambert, S.D., San Miguel, G. and Graham, N.J.D., 2002. Deleterious effects of inorganic compounds DURING THERMAL REGENERATION of GAC: A Review. Journal (American Water Works Association) 94(12), 109-119.

Lebeau, T., Lelièvre, C., Wolbert, D., Laplanche, A., Prados, M. and Côté, P., 1999. Effect of natural organic matter loading on the atrazine adsorption capacity of an aging powdered activated carbon slurry. Water Research 33(7), 1695-1705.

Li, L., Quinlivan, P.A. and Knappe, D.R.U., 2002a. Effects of activated carbon surface chemistry and pore structure on the adsorption of organic contaminants from aqueous solution. Carbon 40(12), 2085-2100.

Li, Q., Snoeyink, V.L., Campos, C. and Mariñas, B.J., 2002b. Displacement Effect of NOM on Atrazine Adsorption by PACs with Different Pore Size Distributions. Environmental Science & Technology 36(7), 1510-1515.

Li, Q., Snoeyink, V.L., Mariñas, B.J. and Campos, C., 2003. Pore blockage effect of NOM on atrazine adsorption kinetics of PAC: the roles of PAC pore size distribution and NOM molecular weight. Water Research 37(20), 4863-4872.

Lim, J.-L. and Okada, M., 2005. Regeneration of granular activated carbon using ultrasound. Ultrasonics Sonochemistry 12(4), 277-282.

Martin, R.J. and Ng, W.J., 1985. Chemical regeneration of exhausted activated carbon—II. Water Research 19(12), 1527-1535.

Matsui, Y., Aizawa, T., Kanda, F., Nigorikawa, N., Mima, S. and Kawase, Y., 2007. Adsorptive removal of geosmin by ceramic membrane filtration with super-powdered activated carbon. Journal of Water Supply: Research & Technology-AQUA 56.

Matsui, Y., Knappe, D.R.U., Iwaki, K. and Ohira, H., 2002a. Pesticide Adsorption by Granular Activated Carbon Adsorbers. 2. Effects of Pesticide and Natural Organic Matter Characteristics on Pesticide Breakthrough Curves. Environmental Science & Technology 36(15), 3432-3438.

Matsui, Y., Knappe, D.R.U. and Takagi, R., 2002b. Pesticide Adsorption by Granular Activated Carbon Adsorbers. 1. Effect of Natural Organic Matter Preloading on Removal Rates and Model Simplification. Environmental Science & Technology 36(15), 3426-3431.

Matsui, Y., Murase, R., Sanogawa, T., Aoki, N., Mima, S., Inoue, T. and Matsushita, T., 2004. Micro-ground powdered activated carbon for effective removal of natural organic matter during water treatment. Water Science & Technology: Water Supply 4(4).

Matsui, Y., Nakano, Y., Hiroshi, H., Ando, N., Matsushita, T. and Ohno, K., 2010. Geosmin and 2-methylisoborneol adsorption on super-powdered activated carbon in the presence of natural organic matter. Water Science & Technology 62(11).

Matsui, Y., Nakao, S., Sakamoto, A., Taniguchi, T., Pan, L., Matsushita, T. and Shirasaki, N., 2015. Adsorption capacities of activated carbons for geosmin and 2-methylisoborneol vary with activated carbon particle size: Effects of adsorbent and adsorbate characteristics. Water Research 85, 95-102.

Matsui, Y., Nakao, S., Taniguchi, T. and Matsushita, T., 2013a. Geosmin and 2-methylisoborneol removal using superfine powdered activated carbon: Shell adsorption and branched-pore kinetic model analysis and optimal particle size. Water research 47(8), 2873-2880.

Matsui, Y., Nakao, S., Yoshida, T., Taniguchi, T. and Matsushita, T., 2013b. Natural organic matter that penetrates or does not penetrate activated carbon and competes or does not compete with geosmin. Separation And Purification Technology 113, 75-82.

Matsui, Y., Sakamoto, A., Nakao, S., Taniguchi, T., Matsushita, T., Shirasaki, N., Sakamoto, N. and Yurimoto, H., 2014. Isotope Microscopy Visualization of the Adsorption Profile of 2-Methylisoborneol and Geosmin in Powdered Activated Carbon. Environmental Science & Technology 48(18), 10897-10903.

Matsui, Y., Yoshida, T., Nakao, S., Knappe, D.R.U. and Matsushita, T., 2012. Characteristics of competitive adsorption between 2-methylisoborneol and natural organic matter on superfine and conventionally sized powdered activated carbons. Water Research 46(15), 4741-4749.

Moreno-Castilla, C., 2004. Adsorption of organic molecules from aqueous solutions on carbon materials. Carbon 42(1), 83-94.

Nakano, Y., Hua, L.Q., Nishijima, W., Shoto, E. and Okada, M., 2000. Biodegradation of trichloroethylene (TCE) adsorbed on granular activated carbon (GAC). Water Research 34(17), 4139-4142.

Newcombe, G., Drikas, M. and Hayes, R., 1997. Influence of characterised natural organic material on activated carbon adsorption: II. Effect on pore volume distribution and adsorption of 2-methylisoborneol. Water Research 31(5), 1065-1073.

Newcombe, G., Morrison, J. and Hepplewhite, C., 2002a. Simultaneous adsorption of MIB and NOM onto activated carbon. I. Characterisation of the system and NOM adsorption. Carbon 40(12), 2135-2146.

Newcombe, G., Morrison, J., Hepplewhite, C. and Knappe, D.R.U., 2002b. Simultaneous adsorption of MIB and NOM onto activated carbon: II. Competitive effects. Carbon 40(12), 2147-2156.

Owen, D.M., 1998. Removal of DBP precursors by GAC adsorption, American Water Works Association.

Pan, L., Matsui, Y., Matsushita, T. and Shirasaki, N., 2016. Superiority of wet-milled over dry-milled superfine powdered activated carbon for adsorptive 2-methylisoborneol removal. Water Research 102, 516-523.

Paune, F., Caixach, J., Espadaler, I., Om, J. and Rivera, J., 1998. Assessment on the removal of organic chemicals from raw and drinking water at a Llobregat river water works plant using GAC. Water Research 32(11), 3313-3324.

Pelekani, C. and Snoeyink, V.L., 2000. Competitive adsorption between atrazine and methylene blue on activated carbon: the importance of pore size distribution. Carbon 38(10), 1423-1436.

Quinlivan, P.A., Li, L. and Knappe, D.R.U., 2005. Effects of activated carbon characteristics on the simultaneous adsorption of aqueous organic micropollutants and natural organic matter. Water Research 39(8), 1663-1673.

Rey-Mafull, C.A., Tacoronte, J.E., Garcia, R., Tobella, J., Llópiz, J.C., Iglesias, A. and Hotza, D., 2014. Comparative study of the adsorption of acetaminophen on activated carbons in simulated gastric fluid. SpringerPlus 3(1), 1.

San Miguel, G., Lambert, S.D. and Graham, N.J.D., 2001. The regeneration of field-spent granular-activated carbons. Water Research 35(11), 2740-2748.

Schmit, K.H. and Wells, M.J.M., 2002. Preferential adsorption of fluorescing fulvic and humic acid components on activated carbon using flow field-flow fractionation analysis. Journal of Environmental Monitoring 4(1), 75-84.

Scholz, M. and Martin, R.J., 1998. Control of bio‐regenerated granular activated carbon by spreadsheet modelling. Journal of Chemical Technology and Biotechnology 71(3), 253-261.

Sontheimer, H., Crittenden, J.C., Summers, R.S., Hubele, C., Roberts, C. and Snoeyink, V.L., 1988. Activated carbon for water treatment, Universitaet Karlsruhe, Karlsruhe.

Summers, R.S., Kim, S.M., Shimabuku, K., Chae, S.-H. and Corwin, C.J., 2013. Granular activated carbon adsorption of MIB in the presence of dissolved organic matter. Water Research 47(10), 3507-3513.

Świetlik, J., Dąbrowska, A., Raczyk-Stanisławiak, U. and Nawrocki, J., 2004. Reactivity of natural organic matter fractions with chlorine dioxide and ozone. Water Research 38(3), 547-558.

Velten, S., Knappe, D.R.U., Traber, J., Kaiser, H.-P., von Gunten, U., Boller, M. and Meylan, S., 2011. Characterization of natural organic matter adsorption in granular activated carbon adsorbers. Water Research 45(13), 3951-3959.

Yu, J., Yang, M., Lin, T.-F., Guo, Z., Zhang, Y., Gu, J. and Zhang, S., 2007. Effects of surface characteristics of activated carbon on the adsorption of 2-methylisobornel (MIB) and geosmin from natural water. Separation and Purification Technology 56(3), 363-370.

Zietzschmann, F., Stützer, C. and Jekel, M., 2016. Granular activated carbon adsorption of organic micro-pollutants in drinking water and treated wastewater – Aligning breakthrough curves and capacities. Water Research 92, 180-187.

(This page is set to be blank.)

Chapter 5. Conclusions

This research investigated the adsorption performance of PAC, SPAC and SSPAC, especially the SPAC and SSPAC produced by micro-milling, with different physiochemical characteristics spotlighting on the particle size, the aggregation extent, the oxidation degree and the impact from preloaded contaminants after several years' service in water treatment.

With the study on the SPACs produced by wet-milling and dry-milling, it is clear that the SPAC got aggregated and oxidized more severely in dry-milling production than in wet-milling production for the similar size reduction extent. These difference between wet-milled SPAC and dry-milled SPAC lead to the superiority of wet-milled SPAC over dry-milled SPAC for MIB removal. It was actually more amenable to disperse the dry-milled SPAC by ultrasonication than the wet-milled SPAC because the former one was more negatively charged after being oxidized during milling process. The improvement of MIB adsorption kinetics was apparent by ultrasonication pretreatment on dry-milled SPAC. However, the oxidation impaired the MIB adsorption capacity of dry-milled SPAC, which made dry-milled SPAC not competitive to wet-milled SPAC on MIB adsorption kinetics even with ultrasonication pretreatment. A model of MIB adsorption, which based on the aggregation extent of SPACs and the MIB equilibrium adsorption isotherms, was simulated successfully to predict the MIB removal rate of PAC and SPACs produced from it by different ways.

The superiority of wet-milled SPAC presents not only in the comparison of MIB adsorption ability with parent PAC and dry-milled PAC, but also in the comparison of MIB adsorption capacity with wet-milled SSPAC. According to previous researches, adsorption capacity increases or un-changes with decreasing carbon particle size and SPAC has similar or higher capacity than PAC. However, this study revealed that the adsorption capacity was lowered with decreasing carbon particle size from 1.5 μm to 150 nm for MIB and some other LMW compounds. The phenomenon was related to oxidization of the carbon during the intensive milling to reduce particle size to around 150 nm, which modify the chemical property, in particular, the hydrophobicity, of carbon, thus reducing adsorptive affinity to hydrophobic compounds, such as MIB. After controlling the carbon oxidation extent during micro-milling manually, the SSPACs produced under less oxidized conditions showed higher MIB adsorption capacity than the ones produced under highly oxidized conditions. Finally, this study revealed that the carbon particle size reduction by milling would enhance the adsorption capacity, but over-milling reduce the capacity for some LMW compounds rather than increase.

Considering the merits of carbon particle size reduction on increasing adsorption kinetics as well as adsorption capacity, the milling technology was brought to reuse of spent GACs which had been used for several years in water treatment plants. SPAC produced from 1-year old GAC and SSPAC from 2-year old GAC showed a similar ability of MIB removal to virgin PAC in the carbon contact time of 30 minutes, which suggested the potential reuse GAC by milling. The potential was due to the increase of equilibrium adsorption capacities by the reduction of carbon particle size as well as improved adsorption kinetics. During the long-term (>1 year) use in GAC bed, pores, in particular for pores with the width of

0.6 to 0.9 nm, in the carbon was significantly reduced. Therefore, the equilibrium adsorption capacities of the compounds having the molecular size of this range could be decreased with increasing the carbon age. Among these compounds, the capacity decrease was prominent for hydrophobic compounds including MIB. For the hydrophobic compounds, however, the equilibrium adsorption capacities increased with the reduction of carbon particle size. Iodine number among other indices was the best correlated to the equilibrium adsorption capacity of MIB, and it would be a useful index to access the remaining MIB adsorption capacity in spent carbon. Spent GAC can be reused as SPAC or SSPAC if it has the iodine number of around 600 mg/g or more.

By clarifying the merits and demerits of micro-milling to produce SPAC and SSPAC in terms of MIB removal, this study attempted to fill up the blank in SPAC research and improve the understanding of adsorption mechanisms. Not only theoretical discussions but also some suggestions for practical SPAC use in water treatment have been put forwards.